Tesis Doctoral

Análisis de retroalimentaciones suelo-atmósfera en América del Sur empleando un nuevo modelo climático regional

Sorensson, Anna Amelia

2010

Universidad de Buenos Aires
Facultad de Ciencias Exactas y Naturales
Departamento de Ciencias de la Atmósfera y los Océanos

Análisis de retroalimentaciones suelo-atmósfera en América del Sur empleando un nuevo modelo climático regional.

Anna Amelia Sörensson

Tesis presentada para optar al título de Doctor de la Universidad de Buenos Aires en el área Ciencias de la Atmósfera y los Océanos

Director de tesis: Dr. Claudio G. Menéndez
Consejero de Estudios: Dra. Carolina Vera

Lugar de trabajo: Centro de Investigaciones del Mar y la Atmósfera (UBA-CONICET)

Buenos Aires, 2010

Volume I: Text

Index Volume I: Text

Resumen

El objetivo principal de la presente tesis es contribuir al entendimiento de la interacción entre la humedad del suelo y la atmósfera durante las fases de desarrollo y madurez del monzón Sudamericano. Con este propósito, se desarrolló y analizó un conjunto de experimentos de regionalización dinámica utilizando el modelo atmosférico regional de Rossby Centre (RCA).

Este objetivo principal lleva asociado un segundo objetivo relacionado con la herramienta empleada para los experimentos, el modelo regional RCA. RCA fue desarrollado por el Rossby Centre de Suecia con el propósito de estudiar el clima europeo y nórdico, y para su implementación sobre Sudamérica la versión RCA3-E fue desarrollada y evaluada.

El tercer objetivo de esta tesis es cuantificar la importancia de las parametrizaciones del clima simulado de Sudamérica.

La implementación del modelo regional sobre Sudamérica es uno de los resultados más importantes de esta tesis. Muchos de los errores de la versión original empleada sobre Europa fueron corregidas cambiando la base de datos de superficie y las parametrizaciones de convección, microfísica y cobertura de nubes.

La presente tesis contribuye además al entendimiento de la interacción entre la humedad del suelo y la atmósfera durante el monzón Sudamericano. Un invierno seco o húmedo puede tener influencias sobre el desarrollo del monzón tanto en la Amazonia como en los subtrópicos como resultado de alteraciones en los vientos continentales, así como también en el reciclaje de evapotranspiración.

El acoplamiento entre la humedad del suelo y la precipitación está conectado al acoplamiento entre la humedad del suelo y la evapotranspiración durante la fase madura del mozón. La Cuenca de la Plata, el Noreste de Brasil y parte de la región del SACZ fueron identificadas como regiones de fuerte acoplamiento entre humedad de suelo y precipitación.

La sensibilidad del modelo a parametrizaciones de superficie es máxima durante la primavera.

Palabras clave: humedad del suelo, interacción superficie continental con la atmósfera, regionalización dinámica, parametrizaciones de superficie, monzón Sudamericano

Analysis of land surface-atmospheric feedbacks in South America using a new regional climate model

Abstract

The primary objective of the present thesis is to contribute to the understanding of the soil moisture – atmosphere interaction during the development and mature phases of the South American monsoon system. A set of dynamical downscaling experiments over the continent are developed and analyzed for this purpose, using the Rossby Centre Atmospheric regional model (RCA).

The primary objective leads directly to secondary objectives related to the tool employed for these experiments, the regional model RCA. RCA was developed at Rossby Centre in Sweden to study European and Nordic climate, and for the implementation of the model over South America the model version employed for the thesis work, RCA3-E, was developed and evaluated.

A third objective is to quantify the importance of the land surface parameterizations for the simulated climate of South America.

The development of the regional model is one of the most important results of this thesis. Many of the biases in the original version employed over Europe (RCA3) could be corrected by changing the surface database and the parameterizatios of convection, microphysics and cloud cover.

This thesis also contributed to the understanding of the interactions between soil moisture and atmosphere during the South American monsoon. The influence of a dry winter on the SAMS can have implications for the development of the monsoon both in the Amazon region and in the subtropics through alternations in the continental winds and by direct evapotranspiration recycling. The coupling between soil moisture and precipitation is connected to the coupling between soil moisture and evapotranspiration during the mature SAMS. The La Plata Basin, North Eastern Brazil and parts of the SACZ region were identified as regions with strong soil moisture – precipitation coupling. The sensitivity of the model to land surface parameterizations was found to have a maximum during spring.

Keywords: Soil moisture, interaction between land surface and atmosphere, dynamic downscaling, land surface parameterizations, South American monsoon system

Acknowledgements

Quisiera agradecer especialmente a Claudio Menéndez quien fue mi director de tesis. Gracias Claudio por aceptar como tesista a una desconocida estudiante sueca, me ayudaste enormemente con las partes prácticas y burocráticas que hicieron posible mi estadía en Argentina. Además, por tu paciencia y valentía de guiar una física sueca en un área de estudio de climatología la cual era nueva incluso para vos. En lo personal, te admiro no solo por tu excelencia científica y capacidad de dirección sino también por ser una excelente persona y por haberme acompañado en los momentos difíciles tanto como en los buenos.

I would like to thank Rossby Centre/SMHI for scientific and financial support. Special thanks to Patrick Samuelsson, Ulf Hansson and Ulrika Willen for your scientifical and technical help with the model RCA and to the directors of Rossby Centre, Markku Rummukainen and Colin Jones for believing in my project.

Thanks to all other financiers that made the realization of this thesis possible; the Swedish foundations: Helge Ax:son Johnson, Eskilsstipendiet, Fredrika Bremer, Petersenska hemmet, Futura, Anna Whitlock, Lars Hjerta, and to the project CLARIS/CLARIS-LBP.

Gracias al Centro de Investigaciones del Mar y la Atmósfera y su director Mario Nuñez por haberme proporcionado el lugar de trabajo. También quiero agradecer a mis profesoras en el Departamento de Ciencias de la Atmósfera y los Océanos, especialmente Carolina Vera, quien fue mi consejera de estudios.

Mamma Lisbeth och Pappa Jan, ni väckte och befrämjade mitt intresse för både naturvetenskap och miljöfrågor. Ni gav mig friheten att välja, men ni är de som känner mig bäst och därför har jag också lyssnat till era råd.

Mamma Lisbeth, systrar Kristin och Amelie: tack for att ni har stött mig från början i mitt beslut att doktorera i Argentina! I början verkade det katastrofalt, långt borta och många år, men karleken har hållit oss nära varandra.

Tack till mina underbara svenska vänner som har stött mig i mitt beslut att flytta från Sverige och som har fortsatt finnas nära. Jag tänker speciellt på Emmy, Vivianne, Karin, Marcus, familjen Bengtsson/Grangärde och Linda.

Manou, sos una persona muy especial para mí. Compartimos el amor por Argentina siendo del "exterior", ja!, tanto como todo lo que bueno y malo que ese amor trae. Gracias ami por ser y por estar!

A mis amig@s Argentin@s, que estuvieron allí compartiendo buenos (y algunos malos) momentos durante estos años. Gracias por acompañarme, Oscar, Nazareno, Maria, Laura, Silvana, Guillermina, Nico, Amalia y Diego.

Gracias a mis compañer@s de oficina y mis compañer@s de doctorado del CIMA, la pase muy bien con ustedes!

Mónica, me mandaste a la Argentina en 2001 y por lo tanto sos la principal culpable de esta tesis. Compartimos no solo la dura tarea de ser científicas, sino además nos tocó el destino de vagabundear por el mundo, siempre cuestionándonos y descubriéndonos. ¡A ver si alguna vez logramos ser vecinas!

Karin, min modell-vetenskapskvinna, var vänskap har utvecklats från Nshima till Bife de Lomo genom dessa år av samboskap, jobb-datar, skatt och analys. Tack for dina vetenskapliga råd, stod och "sharing", men framför allt for din ovetenskapliga vänskap!

Ariel, últimamente me acompañaste en todos los sentidos, hablando de esta tesis, desde las primeras líneas en Norwich hasta las últimas en Lima.

1. Introduction

1.1 South America: General Climatology and Socioeconomic Context

South America, with its diversity of ecosystems, wide range of tropical to extratropical climatic conditions, areas of rapid land use change, and a population vulnerable to climatic variability, will be the region of study in this thesis. The South American continent extends across the equator from about 10°N to 55°S and has unique geographical features, from the world's largest rain forest in Amazonia to the driest desert in northern Chile and a high desert in the Altiplano. The high and sharp Andes Mountains rise along the Pacific coast on the west. The presence of large river basins, such as the Amazon and the La Plata basins, characterizes eastern South America. The La Plata basin region is densely populated, with a 50% of the total population of Argentina, Brazil, Uruguay, Paraguay and Bolivia and contributes with a 70% of the GNP of these countries. Patagonia is the southernmost continental portion, embedded in the Southern Ocean near the circumpolar band of low pressure.

A complex variety of regional and remote factors contribute to define the climate of South America (Nogués-Paegle et al., 2002). The leading modes of variability of the Southern Hemisphere atmosphere; the Southern Annular Mode (SAM) and the Pacific-South America (PSA) teleconnection patterns, modulate the regional variability of the precipitation. In summer, the tropospheric upper levels are characterized by high pressure centered near 15°S, 65°W over the Altiplano (the "Bolivian high") and low pressure over northeast Brazil (the "Nordeste trough"). At low levels, the high Andes mountains to the west effectively block air exchanges with the Pacific Ocean, and a continental-scale gyre transports moisture from the tropical Atlantic Ocean to the Amazon region, and then southward towards extratropical South America, along two preferred paths. The first path is related to the South American low-level jet (SALLJ, e.g. Berbery and Collini, 2000; Salio et al., 2002; Nicolini et al., 2004; Marengo et al., 2004; Saulo et al., 2004), which originates as a regional intensification of the flow channeled along the eastern foothills of the Andes into the Chaco low in northern Argentina. The SALLJ carries a significant quantity of moisture from Amazonia towards Southern South America and although it is strongest during the summer season, it provides moisture to latitudes south of 20°S all around the year

(Berbery and Barros, 2002; Vera et al., 2004) and generates mesoscale convection over the region (Salio et al., 2007). The second path of the tropical moisture is located further to the northeast and is only present when the South Atlantic Convergence Zone is present (SACZ, e.g. Kodama, 1992 and 1993; Figueroa et al., 1995; Nogués-Paegle and Mo, 1997; Liebmann et al., 1999; Seluchi and Marengo, 2000; Robertson and Mechoso, 2000). SACZ is a cloud band that extends from the intense convergence zone of the Amazon basin into the South Atlantic Ocean during the summer season. Liebmann et al. (2004) showed that the SALLJ and the SACZ are modulated by a wave train crossing the Andes from the Pacific Ocean, which directs the moisture to either of the two regions. In tropical and subtropical latitudes a clear warm season precipitation maximum, associated with the South American Monsoon System (SAMS), dominates the mean seasonal cycle of precipitation (Nogués-Paegle et al., 2002; Vera et al., 2006a). Rainfall anomalies over subtropical to extratropical South America are associated with regional feedback processes and interactions between the topography, the SAMS and the midlatitude systems. The timing of the onset and duration of SAMS have important implications for many climate studies and water resources management applications and involves land/sea – atmosphere interactions. The frequency and intensity of daily rainfall have important implications for agriculture, hydroelectric power generation, and for local ecosystems throughout large regions of tropical and subtropical South America. The land surface conditions could have a large impact on the SAMS, and the large-scale land cover changes together with the shift in population to the high density urban areas within the La Plata basin have put supplementary stress on water resources.

1.2 Climate Modeling – Global Climate Models

The most comprehensive tool to study the global general circulation of the atmosphere is the global climate model (GCM). The GCMs integrate the primitive dynamic and termodynamic equations on a grid system in the horizontal and vertical, covering the globe. At the lower boundary the model is coupled to a land surface scheme (LSS) that provides the atmosphere with fluxes of latent- and sensible heat and momentum over land. Over the ocean, an atmospheric GCM can be driven by observed sea surface temperatures (SST), or the model can be coupled to an oceanic general circulation model that provides SST (atmosphere-ocean GCM, AOGCM). A typical

spacing between two grid points in the horizontal for the atmospheric model is around 150 to 400 km. The resolution of the model indicates the upper resolution on which the model can give information. The shortest wave that a model is theoretically able to reproduce is twice its grid spacing, but in practice, to have a realistic representation of the shape and propagation of a wave, waves should be encompassed by a larger amount of grid points. Processes that occur on a smaller spatial scale than the grid size, like convection, can not be resolved by the model and are parameterized.

1.3 Climate Modeling – Regional Climate Models

It is very computational expensive to increase the resolution of AOGCMs since the computational time increases exponentially with resolution. However, for many applications, such as local climate change impact studies, or when model results are used as input to hydrological or ecological models, a much higher resolution than 150-400 km is required (e.g. Mearns et al., 2003). Furthermore, for correct simulation of regions with complex topography or coastline, a higher resolution is necessary. In South America the high and sharp Andes Mountains plays a crucial role for the continental circulation, but are poorly resolved in GCMs. The actual surface elevation of the Andes is lowered by about 2 km in global models (Lenters and Cook, 1995). The results from a global model often need to be downscaled to a scale more appropriate for the purpose of use. This can be done by using statistical relationships between model output and observed in situ data or by dynamical downscaling where output from global models is used as the initial and boundary conditions of a limited area Regional Climate Model (RCM) with higher resolution. In this thesis the dynamical downscaling technique is employed.

Limited area models have been used for prognostic purposes for several decades, and the first use of a regional model for climate simulations started with the work of Dickinson et al. (1989) and Giorgi and Bates (1989) who downscaled month long periods over western U.S. The nesting of the small domain in a GCM is only one-way; the RCM uses the output fields of the GCM but the RCM fields do not feed back on the the GCM. The underlying assumption of regional downscaling is that the GCM provides the correct large scale forcing to the regional model and that the regional model is able to add value to the simulation by resolving smaller scale features. The smaller scale features in a RCM has three sources. Firstly, the regional model has a

more detailed topography and representation of coastlines and lakes, so the surface forcing is more realistic and detailed. This factor is thought to be the main source of added value. Secondly, the nonlinearities in the atmospheric dynamical equations can develop at a smaller scale, for example mesoscale frontogenesis as a response of upperlevel synoptic scale forcing. Thirdly, hydrodynamic instabilities like shear and buoyancy can develop independently of the surface forcing. The fundamental assumption has been debated by the modeling community. An important issue is if the nesting technique presents a source of errors by reflecting or dampening synoptic systems at the borders, thereby creating noise. Most RCMs employ the nesting technique described by Davies (1976), with exponentially decreasing weights and larger buffer zone, as advocated by Giorgi et al. (1993), to provide a smoother transition between the prescribed lateral boundary conditions and the regional climate simulations (Wang et al., 2004). By isolating the effect of the nesting technique in an experiment called "Big Brother", Denis et al. (2002) demonstrated that the effect of nesting did not affect small scale low level and surface features like sea level pressure, and 925 hPa temperature, except over ocean, where there are no surface stationary forcing. However, RCMs have a problem with loss of large scale kinetic energy, which is due to the necessity to increase the diffusion coefficient for smaller scales to maintain numeric stability (Castro et al., 2005). Another issue when changing the scale of a model is the parameterization of sub grid processes, which are scale dependent. Using the same parameterization for both models could be physically inapropriate, although an advantage is that the evaluation of differences between the driving and the regional model will not be dependent on the parameterizations. Another approach is to use different parameterizations for the RCM, physically coherent with the finer scale, with the disadvantage that this could cause noise in the inner part of the RCM domain. For a discussion on the choice of parameterizations for regional models, see Giorgi (1995) and Giorgi and Mearns (1999).

To accurately represent the small scale processes, which are the "added value" of RCMs, it is crucial that the regional model "retains value" in the sense that it does not change the large scale circulation of its driving model and the term "garbage in garbage out" is used by modelers to emphasize the importance of the performance of the GCM for the RCM result. It is important that the global model that is chosen for a regional downscaling represents well the large scale climatology of the region. In the case of South America, this issue is particularly complicated as most global model have

poor performances over the region (for an evaluation of AR4 AOGCMs over South America see Vera et al., 2006b).

Another important issue when setting up a regional model experiment is the choice of model domain size and position. The regional model is governed by the global model to a higher degree close to the boundaries and when using a smaller domain. The issue of domain choice is well studied and discussed by the community (e.g. Giorgi and Mearns, 1999). Seth and Rojas (2003) and Rauscher et al. (2006) focused on domain choice for South America. In general, modelers agree on that the model domain should be large enough to let the RCM develop its own circulation, and the area of interest should not be placed close to the boundaries. Also, the borders should be placed over a region where the driving model gives realistic input values, and are therefore often placed over ocean if possible.

To study historic periods on a regional scale, regional models are most often driven by reanalysis like ERA-40 (from European Center for Medium Range Weather Forecast, Uppala et al., 2005), produced by global models that assimilate observed data. Reanalysis can be viewed as the best comprehensive gridded global dataset for past climate that cover the entire depth of the atmosphere, and are sometimes referred to as observations. To force a RCM by reanalysis also serves to evaluate the RCMs performance, and is useful for model development purposes.

1.3.1 Regional Model Studies over South America

At present, much of the work on regional climate modeling in South America remains at the level of methodological development and preliminary testing (Menéndez et al., 2010). Important processes affecting South America are poorly represented or not included in current climate models (e.g. among the processes particularly important for South America, the feedbacks related with vegetation and aerosol production). Moreover, there is little experience in the use and development of RCMs and downscaling techniques for most of South American regions. The above mentioned problem of global models not providing realistic boundary conditions adds up with the lack of observations. Observational datasets for validation of models and for assimilation in reanalysis are not as reliable as for Northern Hemisphere regions.

Seth and Rojas (2003) and Rojas and Seth (2003), studied the performance of the regional model RegCM driven by reanalysis as well as by a global model. They

focused on the influence of the SST anomalies, the vegetation and soil moisture in the Amazon basin as well as on the domain size for the simulations. Qian et al. (2004) and Seth et al. (2004) studied the effect on periodic reinitialization on RegCM simulation quality. Misra (2005) performed an experiment with the spectral model RSM to study the interannual variation of the SAMS. Collini et al. (2008) studied the influence of initial soil moisture anomalies on the development of the SAMS. Fernandez et al. (2006) assessed the representation of two regional climate models to represent two extreme phases of the ENSO. Roads et al. (2003) presented the first regional model intercomparison study over South America using four regional models forced by NCEP/NCAR reanalysis. Menéndez et al. (2010) presented a coordinated ensemble of six regional models driven by ERA-40 reanalysis, simulating three month-long periods of anomalous climate conditions over southeastern South America. These two last mentioned studies are the only publications up to this date that present results from coordinated regional climate model experiments.

More recently, modeling groups in South America and elsewhere have been able to perform multiyear simulations, essential to study model climatology and interannual variability. Rauscher et al. (2007) studied the timing and characteristics of seasonal precipitation with a four member ensemble of 20 years with RegCM3 driven by NCEP-NCAR reanalysis. Silvestri et al. (2008) performed a 43 years-long simulation with REMO driven by ERA-40 to evaluate the model performance. Solman et al. (2007) presented a ten-year simulation of present day climate with MM5 driven by HadAM3H while Nuñez et al. (2008) continued this work by simulating ten years of future climate using the SRES scenarios B2 and A2. Marengo (2007) analyzed the challenges for regional climate projections over South America. Sörensson et al. (2009) simulated present and future climate with the regional model RCA3 with boundaries from ECHAM5/MPI-OM.

1.4 Soil moisture – atmosphere interaction

This section gives a brief introduction to the importance of land surface for the climate, and on how the land surface – atmosphere interaction is represented in the climate models. For the purpose of this thesis, more details are given on soil moisture – atmosphere feedbacks and on land surface investigation over South America, and in particular on the South American Monsoon System.

1.4.1 Land in the climate system

The continental land surface is, together with the oceans, the lower boundary of the climate system and affects the lowest layers of the atmosphere through exchange of heat, moisture and momentum. The atmosphere in its turn, affects the land surface through rain- and snowfall, winds and radiation. The feedback processes occur on a wide range of spatial- and time scales. At short time scales, the land surface decreases the atmospheric momentum due to its roughness and exchange heat and moisture. The partitioning of the sensible and latent heat fluxes influences on the near surface temperature and moisture and on the daily boundary layer development as well as on the soil moisture development. The soil moisture content is a low frequency modulator of climate that influences on near surface variables through its influence on the partitioning of heat fluxes. The total energy available for heat fluxes is determined by the radiation budget that depends on e.g. cloud cover, solar constant, and also on land surface parameters as albedo and emissivity. Pitman and Zhao (2000) made a comparative study between the effect of CO_2 increase and changes in land use with an AOGCM and found that on local scales land use changes can affect the near surface temperature with 50-100% of the effect of CO_2 increase from 250 to 355 ppmv.

The coupled land – atmosphere system is very complex and difficult to implement in climate models, especially since it is difficult to validate each component of the coupled system. Purely observational studies are scarce, and are carried out on a small time-spatial scale in comparison to the scales used by both global and regional climate models. Studies carried out with reanalysis are helpful to learn about physical processes. Taking advantage of the natural variability of the atmosphere it is possible to draw conclusions about land – climate interactions (van den Hurk et al., 2000; Li and Fu, 2004; Seneviratne et al., 2004; Betts and Viterbo, 2005) that can be used for land surface scheme improvement. RCMs can represent the land surface heterogeneity like topography, vegetation and soil heterogeneity, lakes and coast lines, at a higher resolution than GCM, and this is probably one of the most important factor that make RCMs add value to any coarser resolution simulation. At the early stages of land surface scheme development, land surface studies focalized on parameters like albedo and roughness length (see e.g. the review by Garratt, 1993). The first LSS often didn't include vegetation, and consequently did not take into account the complex processes of

evapotransporation, rainwater that intercepts on leafs and the cooling effect of a deep forest in comparison to a savannah or desert. The vegetation was represented only by larger roughness lengths for higher vegetation. For soil moisture storage, the so called bucket model was employed, with only one reservoir of water storage and the evaporation was modeled as a fraction of potential evaporation, sometimes even independent on soil moisture availability. The LSS are nowadays more complex. Some schemes account for biophysical processes, like distribution of leafs in different vegetation types to calculate diurnal albedo, evaporation of water intercepted on leafs and throughfall. To calculate evapotranspiration from canopy, the stomatal resistance is calculated from a number of factors, including CO_2 concentration. Since satellite information became available, global high resolution datasets of vegetation and soil types have been developed. Parameters that are vegetation/soil dependent like albedo, leaf area index and roughness length can be incorporated in the model by the land use given by the database. High resolution (1 km) global land use data bases are available today. The RCMs, with a resolution of 25-80 km, use the more detailed information from the surface database either by averaging the parameters in each grid box before calculating surface fluxes or by using the tile approach (van den Hurk et al., 2000), where the surface fluxes are calculated for each sub grid tile and then averaged to the lowest atmosphere level. The most recent challenge to the community is to incorporate dynamic vegetation in the fully coupled Earth System Models (see e.g. http://www.quest-esm.ac.uk/). One of the most challenging tasks in this process will be how to model the human future influence on land use.

1.4.2 Soil moisture

Soil moisture is one of the land surface properties that have received most attention in recent literature. Soil moisture affects the surface fluxes partitioning directly, and have a large influence on near surface temperature and humidity, important for human activity and ecosystems. For example, several authors attribute the 2003 European summer heat wave to anomalously low levels of spring soil moisture (Fischer, 2007; Vautard, 2007). Positive biases of near surface temperature in regional models can sometimes be related to unrealistically low soil moisture (e.g. due to too small water reservoirs, van den Hurk et al., 2005). While the connection between soil moisture and

temperature and evaporation is quite direct, the influence of soil moisture anomalies on precipitation is a more complex issue.

Observational studies on soil moisture anomalies influence on the atmosphere are scarce for the whole globe and, are even rarer for South America. This is due to both lack of observational datasets and the difficulty of quantifying the relative importance of observed soil moisture on the atmosphere. For example, it is straightforward that positive precipitation anomalies cause positive soil moisture anomalies, and this effect is difficult to separate from the other way around interaction where soil moisture anomalies causes precipitation anomalies. A few observational studies suggest that soil moisture – precipitation feedback exists on regional scales. Findell and Eltahir (2003) found a possible positive feedback between soil moisture and moist convection in the eastern US. Taylor et al. (2007) found that soil moisture from recent rainfall induce mesoscale circulations inducing convection in the Sahel.

However, most knowledge about soil moisture – atmosphere interaction relies on either studies using natural variability from reanalysis data or on model studies. Schär et al. (1999) found three possible processes for the soil moisture to influence on precipitation in their RCM study: i) Wet soils with small Bowen ratios can lead to the build up of a relatively shallow boundary layer, capping the surface heat and moisture fluxes in a comparatively small volume of air, and building up high low-level moist entropy to provide a source of convective instability, ii) Wet soils contribute to the lowering of the level of free convection and iii) Wet soils decrease thermal emission, increase cloud backscatter, and increase water vapor greenhouse effect to reduce the net shortwave absorption at the surface, further increasing the moist entropy flux into the boundary layer. These three processes interact to increase the potential for convective activity.

1.4.3 Land – atmosphere interaction studies over South America

Global warming would expand the area suitable for forests as equilibrium vegetation types. However, it is unlikely that tropical forests will occupy increased areas since the intensity of contemporary human alterations of the Earths land surface is unprecedented. Land use and land cover change are among the most significant of these human influences. In Brazil, Bolivia, Paraguay, and Argentina, soybean production is the major cause of deforestation of millions of hectares of seasonally dry forests. At the

same time, rural-urban migration is leaving marginal grazing and agricultural lands abandoned. Abandoned rural areas help to ecosystem recovery in forested (e.g., Patagonia, northwest Argentina and Ecuador) and nonforested ecosystems (e.g., mountain deserts and Andean tundra ecosystems of Bolivia, Argentina and Peru). Although the potential for wide-scale recovery is encouraging, the land-use history of many areas has caused severe degradation, and recovery can be slow when invasive species, such as African grasses, dominate recently abandoned pastures or agricultural fields (Aide and Grau, 2004)

The first studies that addressed the land surface influence in the Amazon region were deforestation experiments performed with general circulation model GCMs (Dickinson and Henderson-Sellers, 1988; Lean and Warrilow, 1989; Shukla et al., 1990; Nobre et al., 1991). These authors found that precipitation decreased as a result of decreased evapotranspiration and/or moisture convergence. More recent GCM studies (e.g. Fennessy and Shukla, 1999; Costa and Foley, 2000; Roy and Avissar, 2002; Avissar and Werth, 2005) have identified the sensitivity of rainfall to changes in vegetation and soil moisture conditions in the region. According to the majority of modeling studies on the effects of large-scale deforestation in Amazonia, deforestation results in hydrological cycle weakening: precipitation, evapotranspiration and moisture convergence would decrease in the tropical forest. However, assessments also indicate that this effect may be modified by changes in atmospheric moisture convergence, that there are significantly different responses to similar land use changes in different tropical regions (e.g. Voldoire and Royer, 2004; Feddema et al., 2005). Similarly, large-scale desertification in northeast Brazil (a large semi-arid area covered by xeromorphic vegetation) leads to precipitation decrease and weakening of the hydrological cycle (Oyama and Nobre, 2004). Mesoscale models have also been employed to investigate the impact of deforestation in Amazonia (Roy and Avissar, 2002). Misra et al. (2002) conducted a moisture budget over South America using a regional model. Their results indicate that both surface evaporation and surface moisture flux convergence are critical in determining the interannual variability of precipitation over southern South America, while over Amazonia the moisture flux convergence determines most of the interannual variability of precipitation. Dirmeyer and Brubaker (2007) used a back-trajectory methodology to determine precipitation recycling rates for the whole globe, and they identified northern Amazon basin as a region with weak precipitation recycling while la Plata Basin had a relatively high recycling rate.

1.4.4 Land Surface Influence on SAMS

The land-ocean thermal contrast and the continental latent heat flux release contribute to the determination of the onset, the intensity and spatial distributions of monsoons (Webster et al., 1998). It is not clear how these two processes contribute to the different phases of the South American monsoon. The soil moisture memory contributes to atmospheric variability and seasonal predictability and could potentially affect the development of the SAMS through its influence on the partitioning in sensible and latent heat flux. On the one hand, if the main source of moisture is provided by the trade winds (as in e.g Ropelewski and Halpert, 1989), a dryer soil can lead to higher air column temperatures because evapotranspiration (latent heat flux) decreases and, therefore, a larger portion of outgoing energy will be in the form of warm air rising (sensible heat flux). This increases the thermal gradient between the continent and the ocean which can produce stronger inflow of the Atlantic trade winds over the continent, bringing moisture to the monsoon region and producing an early onset of the monsoon. On the other hand, some studies have shown that destabilization of the atmosphere through latent heat flux influences the large-scale circulation by triggering the inflow of trade winds during the monsoon onset phase. A dry disturbance resulting in weaker latent heat fluxes may, therefore, lead to a later onset of the monsoon (e.g. Li and Fu, 2004). The soil moisture–precipitation feedback processes during the SAMS is the central issue of this thesis, and a more detailed review on the subject will be given in the introduction to chapter 6.

1.5 The context of CLARIS / CLARIS LPB

This thesis work was partly developed within the framework of two European Union financed projects: CLARIS (2004-2007) and its succesor CLARIS LPB (2009-2012).

The two projects aim at strengthening the collaboration between European and South American institutes and to assess climate change, variability and extremes as well as impacts and adaptation to climate change over South America. Dynamic downscaling is one of the central work packages in the two projects, providing climate change scenarios for impact studies with a focus on the hydrological cycle in the La Plata Basin (central and northern Argentina, Uruguay, Paraguay and southern Brazil).

CLARIS 1 was a multidisciplinary pilot project mainly aiming at strengthening the collaboration between institutions from Europe and South America and creating common research strategies (Boulanger et al., 2009). The dynamic downscaling work package aimed at setting up a methodology for model intercomparison and validation of regional climate model performance over South America (Menéndez et al., 2010 and 2009).

The CLARIS LPB dynamic downscaling work package aims at generating climate change scenarios for near and far future with a focus on hydro climate over the La Plata Basin. The methodology for intercomparison between regional models follows projects like PRUDENCE and ENSEMBLES, although comprising a smaller ensemble of models.

Participation in the coordinated dynamical downscaling experiments formed an important part of the thesis work and made possible the evaluation of the regional model employed for this thesis (RCA3-E) not only to reanalysis and observational datasets, but also to other regional models. At the starting point of the project there was little experience in the use and development of RCMs and downscaling techniques for most of the South American regions. Nevertheless, downscaled multi-year simulations and climate change projections are starting to become available for this region and a great part of the effort is being channeled within the CLARIS LPB framework. Multi-year simulations were recently accomplished and first results are being independently analyzed by the different groups within the project (e.g. Solman et al., 2007; Nuñez et al., 2008; Silvestre et al., 2008; Sörensson et al., 2009).

1.6 The CIMA - Rossby Centre collaboration

The regional model that was employed for this work, Rossby Centre regional atmospheric model (RCA) is from the Rossby Centre at the Swedish Meteorological and Hydrological Institute (SMHI). The model was available through the colloboration project “Regional simulations of climate change and variability in South America: analysis of land surface-atmospheric feedbacks” between Centro de Investigaciones del Mar y la Atmósfera (CIMA) and Rossby Centre. RCA had not been used over South America before, and during the thesis work the model was developed, adapted and evaluated in cooperation with Rossby Centre. The collaboration also made possible the realization of multiannual integrations that were run at the Swedish National

Supercomputer Center, and the technical assistance with the design of some of the experiments.

1.7 Objectives of this Thesis

The primary interest of this thesis is to contribute to the knowledge on the soil moisture – atmosphere interaction during the onset and mature phases of the South American monsoon. The approach is to study this on a seasonal to daily scale through a set of experiments with a regional climate model.

Since the model had not been used for tropical regions before, it was necessary to change model parameterizations and land surface database for the South American continent. This was done in collaboration with the research institute Rossby Centre/SMHI. Furthermore, an extensive part of the thesis work was dedicated to the evaluation of the model performance, focalizing on timescales, periods and processes important for the primary objective. The development and evaluation of RCA over South America is therefore a secondary objective of the thesis.

A third objective was to quantify the importance of the land surface parameterizations for the simulated climate of South America.

The present thesis should be interpreted as a contribution towards the understanding of the interactions between land-surface hydrology and the regional climate of South America.

2. Methodology

In this chapter, the regional climate model RCA3 is described (section 2.1). The rest of the chapter gives the reader an overview of the logic behind the planning and realization of the investigation (sections 2.2 – 2.8). The detailed methodology of each experiment is found in the respective chapter.

2.1 The Rossby Centre regional Atmospheric model, RCA3

The Rossby Centre regional Atmospheric model, RCA, is a hydrostatic, primitive equation grid-point limited area model. At an initial stage of this thesis work, the most recent official version of RCA, RCA3 (Kjellström et al., 2005), was employed for test simulations over South America. The analysis of these simulations showed that to be able to perform the work proposed for the thesis it was necessary to modify the model to get a better representation of the climate of the region. The modified version was called RCA3-E and a description of the differences between RCA3-E and RCA3 is found in chapter 3 (Model development, section 3.2). In the following two sub sections, the general features of the official version RCA3 will be described.

2.1.1 General model description

RCA3 is an atmospheric model that interacts with a land surface model and with the lake model PROBE (Ljungemyr et al., 1996). The radiation scheme, which was originally developed for numerical weather prediction purposes by Savijärvi (1990) and Sass et al. (1994), is a simplified scheme that only includes one wavelength band for longwave and one for shortwave radiation which makes it computationally fast. The scheme has been modified by Räisänen et al. (2000) to include CO_2 absorption. The cloud emmissivity and albedo are linked to the cloud water and ice amounts and to a diagnosed effective radius (Wyser et al., 1999). In the microphysics and radiation calculations, the cloud droplet concentration depends on the surface type (land, sea etc.). The turbulence scheme in RCA3 is based on prognostic turbulent kinetic energy combined with a diagnostic length scale (Cuxart et al., 2000) with updates (Lenderink and de Rooy, 2000; Lenderink and Holtslag, 2004) to have a smoother transition between stable and unstable conditions and to be more numerically stable. The clouds

are separated in explicit clouds and sub grid clouds. The resolved, large and mesoscale cloud description follows Rasch and Kristjánsson (1998). The sub grid convective cloud description follows the Kain and Fritsch (1993) entraining and detraining plume model. The RCA3 convective Kain and Fritsch scheme assumes that shallow convection does not precipitate, but can be detrained into the environment and evaporated depending on the grid box relative humidity. The remaining cloud water resides in a diagnosed shallow cumulus cloud fraction (Albrecht, 1981). The microphysic conversions used for shallow convective cloud water to precipitation is the same as for large scale clouds. The impact of this change to the original Kain and Fritsch is reduced precipitation from shallow convective clouds, and a larger reflectance (Jones and Sanchez, 2002). Earlier versions of RCA had too frequent weak precipitation, and modifications to the large scale precipitation microphysics were made to RCA3 to reduce this phenomenon.

In all experiments in this thesis, a domain that covers the South American continent and parts of adjacent oceans (Figure 2.1) is used. To reduce the number of gridpoints and to make the grid point spacing more uniform, the grid used for the integration is rotated. The horizontal resolution is 0.5° x 0.5° with 24 sigma levels in the vertical.

2.1.2 Land surface scheme

The land surface scheme of RCA3 (Samuelsson et al., 2006) employs the tile approach (van den Hurk et al., 2000) for calculation of surface fluxes. The surface of each grid box is decomposed in tiles according to the sub grid vegetation cover and the surface fluxes are calculated separately for each tile. The main tiles are open land and forest, the open land tile being divided in a vegetated and a bare soil sub tile while the forest tile is divided in forest canopy and forest floor. RCA3 uses two types of forest: deciduous and coniferous forest and one type of open land vegetation. These three types of vegetation differ in parameters such as albedo, Leaf Area Index (LAI) and roughness length. Snow is treated separately in both open land and forest. The individual fluxes of heat and moisture from the tiles are weighted due to fractional coverage of grid to grid-averaged values at the lowest atmospheric layer. To calculate the surface water balance, processes such as interception of rain, throughfall and canopy transpiration controlled by photosynthesis, are considered. The soil moisture is supposed to be independent of surface cover in RCA3 and has two prognostic soil moisture storages, the top layer

which has a depth of 7 centimeters, and the deep layer which has a depth of 2.2 meters for all regions but mountainous regions where a depth of 0.5 meters is used.

In the version of RCA used in this thesis, RCA3-E, the original physiography was replaced by the Ecoclimap database (Masson et al., 2003; Champeaux et al., 2005) in order to initialize and drive its soil–vegetation–atmosphere transfer scheme. Ecoclimap is a complete and coherent surface dataset based on a very high-resolution classification of a large number of homogeneous ecosystems. The database contains all the necessary surface parameters (e.g., roughness length, vegetation fraction, leaf area index, albedo and rooting depth) and will be described, together with the implementation process, in section 3.2.1.

2.2 Transfering RCA3 from Europe to South America – Model development

The Rossby Centre regional Atmospheric model was developed at the Rossby Centre at the Swedish Meteorological and Hydrological Institute, with the original main purpose to downscale European climate and in particular Swedish and Nordic climate. It is natural that models that are developed in Europe are tested against European mid latitude to polar climate, and therefore the parameterizations of processes common for the region will probably be more tested and developed than processes that are unlikely to occur in the region. A related issue is that the forcing datasets, for example databases of land use, that are employed to drive the model could be more accurate for the region of models' origin than for other regions. By the time that this thesis was begun (August 2005), the RCA model had been developed for Europe, and was participating in the regional climate change project PRUDENCE (Christensen et al., 2002). RCA had a satisfying performance over Europe, while simulations had not been carried out over other regions, except for North America.

The capacity of a model, developed for some special region, to represent the climate also for other regions is usually called transferability of the model (see e.g. Takle et al., 2007). The first simulations over South America with the original version of RCA3 showed that it would not make sense to transfer the model to South America for investigation purposes without making adjustment to the models' parameterizations (these kind of adjustments are called tunings) and without changing the surface database. The Ecoclimap database was therefore incorporated in the model.

Furthermore, tunings of various parameterizations, like convection and microphysics were implemented, and tests of varying land-surface parameters like albedo, soil depth and leaf area index were performed.

2.3 Evaluation of the model internal variability

The primary objective of this thesis is to evaluate the influence of soil moisture on atmospheric processes for RCA, in other words, to study the sensitivity of the model to anomalous soil moisture. When testing sensitivity of a model to some change in the forcing, it is necessary to have a measure of model responses that should be considered as significant. Since climate models are highly non linear systems, there is no straightforward way to obtain such a measure, but a common way to estimate the significance of model sensitivity is to test the internal variability of the model. Internal variability will here be defined as the variability of the model output that is a result of the models non linearity and is independent on external forcing. In the case of a regional model, the external forcing are the lateral boundaries, provided by reanalysis or a global model; SST, which is provided from either an observed dataset or from a global model; and the continental surface forcing, which are determined by the land surface scheme. A common method to test the internal variability was employed for this purpose. An ensemble was created by initializing RCA3 on different days, thereby running the model with the same forcing fields but with different initial conditions.

2.4 Evaluation of model climatology

The model development for South America was carried out by performing multiple ensembles of different model versions of the length of two years, which was considered to be a reasonably long period to detect differences among ensemble members without being too time- and computer resource demanding. However, to evaluate the models' climatology, longer simulations are necessary to evaluate the representation of the climate, and in particular of its interannual variability. A 22 years long (1979-2000) simulation was made with the objective of model evaluation, using "perfect" boundary forcing from ERA-40. The 20-year period 1980-99 was evaluated against CRU observational gridded data (New et al., 1999 and 2000) and ERA-40 fields. The period 1991-2000 had been chosen as a common period for model evaluation within the context of CLARIS (section 1.5). Three regional models (RCA3,

REMO and PROMES) and a stretched grid global model (LMDZ) participated in these coordinated simulations. This multi model ensemble experiment made it possible not only to evaluate the regional model against observed data, but also compare its results to other regional models in an organized and coherent manner.

Due to the lack of observations, the model could not be evaluated against observational data on surface fluxes, which is of great importance when studying land-atmosphere interactions, which is the main objective of this thesis. It is therefore assumed that RCA3-E represents the latent and sensible fluxes well in the following chapters, although this assumption needs to be confirmed by comparison to observational data when those are available.

2.5 The Monsoon Development with anomalously winter Soil Moisture Initial Conditions

The main characteristics of the South American Monsoon System were described in section 1.1. The ongoing deforestation of Amazonia and other parts of South America could modify the soil moisture of parts of the continent. This could potentially modify the monsoon rainfall. Studies using either observational data or global / regional climate models of deforestation and modified soil moisture have shown quite opposite results on the influence of the surface in the development of the monsoon (section 1.4.4 and 6.1.2). In this study, this phenomenon was investigated through an ensemble simulating the spring and summer climate over South America initialized in late winter of 1992 with both anomalously dry and wet conditions.

2.6 Rooting depth influence on SAMS

In this experiment, the importance of rooting depth for the development of the SAMS is examined. In general RCMs are developed for mid- and high latitudes and use 1-2 meters as soil depth depending on vegetation type (Boone et al., 2004). However, in Amazonia, observational studies show that the rooting depth is substantially deeper (Nepstad et al., 1994). In RCA, the maximum rooting depth is equal to the soil depth, so the water storage also increases when employing deeper roots in the model.

The interest in focusing on the soil depth is motivated by two factors: (i), the soil depth in RCA3 is set to a constant value of 2.2 meters (0.5 meters in mountainous regions), while in Ecoclimap it is spatially variable. This is important for South America

in particular, since the soil depth of tropical forest that cover large areas of northern South America are increased to 8 meters with the incorporation of Ecoclimap in the model, and (ii) previous works suggest the importance of soil depth and deep rooted vegetation on the climate system (Kleidon and Heimann, 2000; Van den Hurk et al., 2005; Swenson and Milly, 2006)

2.7 The Soil Moisture – Atmosphere coupling during the SAMS

In this experiment, the coupling strength between soil moisture, evapotranspiration and precipitation is examined, as another methodology of estimating the influence of the soil moisture on the South American Monsoon. Coupling strength is defined as the degree to which some prescribed boundary condition affects some atmospheric quantity and is still largely unknown for South America and is a very uncertain aspect of regional modeling. The importance of soil moisture anomalies for the near surface climate is strongly model dependent because of the models different surface and boundary layer parameterizations, and it is therefore important to define zones with high coupling strength for a model used for investigation of hydrological processes.

2.8 Land surface parameterization ensemble

There are several studies that confirm the importance of surface fluxes, and their partitioning, on atmospheric variables like cloud-base, cloud field and short- and long-wave radiation, vertical motion and precipitable water for tropical and sub-tropical South America (see section 1.4.3). Surface fluxes are highly dependent on the surface parameterization scheme and on parameters such as soil depth, leaf area index, albedo and emissitivity. An ensemble of land surface physics parameterizations is examined to quantify the importance of surface forcing for model performance over South America. The ensemble is constructed by varying parameters like rooting depth, leaf area index and root distribution to study the influence of each component to simulated climate. For this study, both RCA3-E and a newer model version RCA3.5 (Jones et al, 2009) are employed.

3. Model Development

3.1 Introduction and motivation

Until recently most regional climate model development has, for natural reasons, been focusing on the regions of the models' origin. Only during the last few years, South American countries have acquired capacity to perform RCM simulations longer than a few months and are starting to get more involved in the climate modeling community. As an example of this tendency, the present thesis was partly developed within the framework of the European founded projects CLARIS and CLARIS LPB (section 1.5).

In many cases, models that originally were developed for Europe or North America are being run over the South American continent and modeling groups are becoming aware of the problems related to transferring these models to South America. Few RCM studies have been published up to this date, and results from multi model ensemble experiments are virtually absent in the literature. In general the models, although driven by reanalysis, show very large biases for variables like precipitation and near surface temperature at a seasonal scale (Menéndez et al., 2009, see also chapter 5 of the present thesis). An ensemble of models have less bias than individual models in some cases, as a result of cancellation of large errors, while in other cases errors are similar among models. When driven by atmosphere-ocean general circulation models (AOGCM), regional models inherit their erroneous representation of the Intertropical and South Atlantic convergence zones (Vera et al., 2006b; Sörensson et al., 2009). For realistic climate change assessments including potential land use changes it is essential that both RCMs and AOGCMs develop their performance over the South American continent.

When RCA3 was implemented over South America, the model simulated a very erroneous climate, with up to around 10°C biases of 2 meter temperature (t2m) and several hundred percent of precipitation bias on seasonal scales for some regions. The objective of the present chapter is to achieve a model version with more coherent results over South America by changing the physics parameterizations and the land surface database. The result of this model development is the version that was used for this thesis, RCA3-E. As will be discussed in chapter 5, the severest problems of RCA3-E in the context of this thesis, is the large dry bias of precipitation in the LPB region that dry

out the soil and produces too hot near surface temperatures. However the original RCA3 had even stronger biases over South America and the modifications that were implemented improved the model substantially. In chapter 9, a newer version of the model that mitigates most of the biases discussed in this chapter will be evaluated. However, this version was only available from 2009, when most of the thesis work had been accomplished.

3.2 Differences between RCA3 and RCA3-E

3.2.1 The surface database Ecoclimap and its implementation in RCA3

The original version of RCA3 used HIRLAM climate fields for surface forcing. In these climate fields, the fraction of forest was based on a Max Planck Institute database (Hagemann et al., 1999) which in turn was based on the database USGS EROS Data Centre. RCA uses two types of forest, deciduous and coniferous forest and two types of open land: bare or vegetated. In RCA3, the fraction of deciduous forest was a function of latitude and longitude, and this was not applicable for South America. The leaf area index (LAI) was set to 4.0 for coniferous forest, while for deciduous forest and open land vegetation, LAI was a function of soil temperature (Hagemann et al., 1999) and varied between 0.4-4.0 and 0.4-2.3 respectively. In RCA soil depth is equal to rooting depth, and RCA3 used a constant soil depth of 2.2 meters for all regions but mountainous regions which had the soil depth 0.5 meters.

The database Ecoclimap (Masson et al., 2003; Champeaux et al., 2005) was implemented in RCA3 to obtain a more accurate description of the land surface. Ecoclimap is a global and complete surface database with 1 km resolution and supports tiled land surface schemes. Ecoclimap identifies 215 ecosystems that are derived from combining satellite data (Hansen et al., 2000; Loveland and Belward, 1997) with a map of climate types of the world (Koeppe and Delong 1958). Topography and soil type data is from FAO 1998 and are independent of the surface cover. Vegetation parameters like LAI, albedo, roughness length and rooting depth depend on the vegetation. LAI vary along the year for many ecosystems, and is specified using maximum and minimum values for each vegetation class. For bare soil, the albedo is specified depending on the

soil type, and the vegetation albedo is retrieved from look-up tables for each vegetation class.

Since RCA has three vegetation classes, the 215 ecosystems were grouped in these three classes. However, monthly fields of vegetation related parameters like LAI and albedo from Ecoclimap are employed and are therefore not dependent on the RCA land cover. The rooting depth was tiled in open land, deciduous and coniferous forest. Each grid cell will normally contain tiles of all these land cover types. For the forest tile, the rooting depth is weighted to one forest depth for each grid cell.

3.2.2 Tunings of convection and microphysics

To adapt RCA3 to tropical climate, the convection scheme and the microphysics were modified. In RCA3, the Kain and Fritsch (1993) approach for convective clouds is used with modifications as described in section 2.1.1. In RCA3-E, the convection has been modified with a trigger function from Rogers and Fritsch (1996) and in the Convective Available Potencial Energy (CAPE) closure a dilute updraft profile is used instead of an undilute one (Kain, 2004) and the entrainment and detrainment factors are hardcoded to 0.5 each. With respect to the microphysics, the conversion of liquid water to rain was changed. In RCA3 the parameterization of Chen and Cotton (1987) was used, in which the threshold for autoconversion (q_{crit}) is parameterized as a function of the effective radius of the droplets (r_{eff}), the density of air and the mean cloud droplet concentration, which differs for maritime and continental air and the height above the surface. The radius for which the autoconversion become efficient is set to $1{,}1*10^{-5}$ m. In RCA3-E, the autoconversion follows Khairoutdinov and Kogan (2000) that used an explicit drop size model to simulate drop size distributions that are incorporated in the bulk model. The autoconversion becomes a function of cloud water content and drop concentration and no critical droplet radius is used.

3.2.3 Summary of main differences between RCA3 and RCA3-E

Albedo: In RCA3, the albedo for open land was set to the constant value 0.28, while in RCA3-E (i.e. Ecoclimap) the albedo for open land is spatially varying and in general lower than 0.28 in South America. The albedo in Amazonia is around 0.13 in Ecoclimap while in RCA3 it was around 0.18.

Leaf Area Index (LAI): Ecoclimap has a larger spatial variability of LAI than RCA3, for example larger values in the tropical forest region and smaller values in Patagonia and the Andes. Ecoclimap also has larger annual cycle amplitude in regions out of the evergreen forests.

Soil/rooting depth: In RCA3 the depth of the deep soil moisture layer was 2.2 m for all areas with an exception for mountainous regions where it is set to 0.5 m. In RCA3-E, the Ecoclimap soil depth is employed, which is a function of vegetation type. The largest change is in the Amazon region where the rooting depth is 8 m.

Convection: In RCA3-E, the convection scheme was modified by adding the trigger function of Rogers and Fritsch, the CAPE closure was modified and the entrainment and detrainment factors are hardcoded to 0.5 each.

Microphysics: In RCA3 the autoconversion from liquid water to rain follows Chen and Cotton (1987), and in RCA3-E it follows Khairoutdinov and Kogan (2000).

3.3 Methodology

A 12 member ensemble of 2-year long simulations differing in physics parameterizations was performed. The years 2000 and 2001 were chosen since for this period satellite data and in situ measurements of surface fluxes for two sites in Amazonia, Manaus and Santarem were available (in situ measurements provided by the project Inter-Continental Transferability Study, Takle et al., 2007). The different model versions are listed in table 3.1. The simulations 1-6 were designed to explore the differences between the RCA3 and the RCA3-E versions to get ideas of how the differences in the land-surface parameters introduced by Ecoclimap as well as the modified convection and microphysics in RCA3-E influence on the performance on seasonal and monthly scales. The differences between these 6 simulations are explained in table 3.1 and in section 3.2. Simulations 7-12 were based on a working model version called RCA3.1 which include Ecoclimap but differ from RCA3 in convection scheme and microphysics as well as treatment of radiation in forest and emissivity and the lake model FLake is used (Mironov, 2008; Samuelsson et al., 2009).

Eight regions, shown in figure 3.1, were selected for calculation of annual cycles.

	1	2	3	4	5	6	7	8	9	10	11	12
ECOCLIMAP	No	Yes	Yes	yes	yes	yes	yes	yes	yes	yes	yes	yes
Albedo for open land	0,28	ECOC	ECOC	ECOC	ECOC	ECOC	ECOC +0,04	ECOC +0,04	ECOC	ECOC	ECOC	ECOC
Depth of deep soil moisture layer	2,2m	Weight	Weight	2,2m	2,2m	weight	weight	weight	max	max	max	max
Leaf Area Index	RCA3	ECOC	ECOC	ECOC	RCA3	RCA3	ECOC	ECOC	ECOC	ECOC	ECOC	ECOC
Maximum snow cover fraction	0,95	0,95	0,95	0,95	0,95	0,95	0,985	0,985	0,985	0,985	0,985	0,985
emissivity of water	0,97	0,97	0,97	0,97	0,97	0,97	0,94	0,94	0,94	0,94	0,94	0,94
emissivity of snow	0,99	0,99	0,99	0,99	0,99	0,99	0,85	0,85	0,85	0,85	0,85	0,85
Distinction between direct and diffuse radiation in forest	not split	not split	not split	not split	not split	not split	split	split	split	split	split	split
Flake lake model	No	no	No	no	no	no	yes	yes	yes	yes	yes	yes
Rate of collection of ice by snow	R&K98	R&K98	R&K98	R&K98	R&K98	R&K98	Lin83	Lin83	Lin83	Lin83	Lin83	Lin83
Rate of autoconversion of ice to snow	R&K98	R&K98	R&K98	R&K98	R&K98	R&K98	Lin83	Lin83	Lin83	Lin83	Lin83	Lin83
conversion of liquid water to rain	C&C87	C&C87	K&K00	K&K00	K&K00	K&K00	C&C87	K&K00	C&C87	C&C87	C&C87	K&K00
radius at which autoconversion become efficient	1,1E-05	1,1E-05	not used by K&K00	not used by K&K00	not used by K&K00	not used by K&K00	5E-06	not used by K&K00	1,1E-05	1,1E-05	not used by K&K00	not used by K&K00
Convection	orig. RCA3	orig. RCA3	Modified	modified	modified	modified	orig. RCA3	modified	orig. RCA3	modified	orig. RCA3	orig. RCA3
Cloud fraction	Slingo	Slingo	Slingo	Slingo	Slingo	Slingo	Slingo	Slingo	Xu-Randall	Xu-Randall	Xu-Randall	Xu-Randall

Table 3.1: The 12 ensemble members, R&K98 - Rasch and Kristjánsson (1998), Lin83 – Lin et al. (1983), C&C87 - Chen and Cotton (1987), K&K00 - Khairoutdinov and Kogan (2000), Slingo – Slingo (1987), Xu-Randall – Xu and Randall (1996).

3.4 Results

The sensitivity to physics parameterizations in the 12-members ensemble depends on the variable, region and season. The spread between ensemble members is high in the Amazon region, while the southern Andes are practically not affected, as would be expected since the Amazon is highly influenced by land surface and convection, while the western side of the Andes is governed by synoptic systems coming in from the Pacific Ocean. The RCA3-E was the version chosen for further South American investigation for two reasons: i) it was one of the versions of best performance ii) some of the ensemble members of table 3.1 gave very similar results, but out of those, the RCA3-E version was considered to be the most physically correct.

In this section the results will be presented only for RCA3-E (in table 3.1 no 3) as compared to RCA3 (no 1) and RCA3 with Ecoclimap, but without other modifications (no 2, in the following called RCA3_ECO). In chapter 9 the importance of land surface parameterizations will be assessed through the development of a systematic ensemble.

Figure 3.2 shows the annual bias of total precipitation relative to CRU precipitation for the three model versions, and figure 3.3 shows the annual cycles for the regions in figure 3.1. RCA3 has a dry annual bias of more than 50% in central Brazil and in northern La Plata Basin. When using land surface data from Ecoclimap, this bias is mitigated, but in the northeast a wet bias appears, due to too heavy rains during May through July (figure 3.3, tropical region TR). In RCA3-E the positive bias in TR is eliminated. The annual cycles shows that the original model version is failing, not only in the rain amount, but also in some regions in the timing of maximum and minimum rainfall. In most regions the representation of both shape and amplitude are improved in RCA3_ECO and RCA3-E. However, RCA3-E does not capture the local winter precipitation maximum over the La Plata regions.

The annual biases and annual cycles for t2m are shown in figures 3.4 and 3.5 respectively. The warm spring biases over the Amazon, central Brazil and La Plata Basin in RCA3 are induced partly by the dry biases over the same regions during winter and amounts to up to around 10 degrees for October (SAmz, figure 3.5). This warm bias is also related to a drying out of the soil that does not only depend on deficient rainfall, but also on the shallow soil in RCA3. In general RCA3_ECO and RCA3-E mitigate these biases as well as the cold JJA biases in the regions NeB and EB. The cold bias in the Amazon region in RCA3-E is possibly related to the fact that the t2m is calculated within the forest in the model, while CRU observation sites are located at open land spots. The three model versions have a negative annual bias, in comparison the satellite data from International Satellite Cloud Climatology Project (ISCCP) of cloud cover over the regions of warm bias (figure 3.6), but the bias is mitigated in the RCA3 with Ecoclimap and in RCA3-E. This is probably a result of a positive feedback between the land surface and the atmosphere, contributing to the hot land surface.

3.4 Summary and Conclusions

The model version RCA3, which was developed for simulations over Europe, had a very poor performance over South America and did not convince for studies of

soil moisture – atmosphere interaction as had been proposed for this thesis. The surface database was not realistic for the South American continent, and was therefore changed to the database Ecoclimap, which resulted in a more realistic overall performance of the model. Tunings of the convection and microphysics parameterizations corrected the model performance further. The resulting model version, RCA3-E, was employed for the following chapters. RCA3-E does not represent all the important features of South American climate, however, to be able to continue with the proposed plan for the present thesis, it was necesary to finish the model development process at some point. RCA3-E will be evaluated in detail in chapter 5.

4. Model internal variability

4.1 Introduction

Internal variability of GCMs is known as the fact that models, due to the nonlinear nature of the climate system, are sensitive to different initial conditions. A global model initialized with slightly different initial fields will after some days of simulation differ considerably on short time scales, that is, in their day to day simulation of weather. However, the climatologic statistics for long time periods, like interannual variability, should not be affected by initial conditions. For a recent discussion on the different types of nonlinearities of the climate system, and the mechanisms that generate them, the reader is referred to Rial et al. (2004).

In the context of regional models, driven by external forcing at the boundaries, internal variability has been defined as sensitivity to either different initial conditions (IC, e.g. Giorgi and Bi, 2000; Alexandru et al., 2007) or to different lateral boundary conditions (LBC, e.g. Giorgi and Bi, 2000; Wu et al., 2005). In the case of sensitivity to different ICs, the internal variability of the RCM can be interpreted as the models ability to find different solutions to equal driving boundary fields (von Storch, 2005). The different solutions can in principle be decomposed in two parts: one reproducible, equal among ensemble members of different ICs, and one depending on internal variability that differs among ensemble members (Ji and Vernekar, 1997). The internal variability can modulate and mask physically forced signals, and several authors have suggested that assessment of the internal variability of the RCM is important for experiment design as well as for analysis and interpretation of results (Weisse et al., 2000; Giorgi and Bi, 2000; Christensen et al., 2001; Wu et al., 2005; Alexandru et al., 2007). As an illustrating example, Weisse et al. (2000) found that the sensitivity of the sea state-dependent roughness on the atmospheric circulation was only detectable during periods for which the internal variability was small, while for periods when it was large, the response to the changed parameterization was concealed by the model "noise". These results indicate that when estimating the sensitivity of a model to e.g. different land surface parameterizations, convection schemes or soil moisture initial state, the internal variability of the season studied should be taken into account as a measure for the significance of the response.

Christensen et al. (2001) made ensembles of different ICs with two RCMs and one GCM and found that the magnitude of internal variability of the RCMs and the GCM differed among variables. The internal variability of surface temperature was much lower for the RCMs than for the GCM, while that of precipitation showed similar values for the three models. This suggests that the evolution of some variables is stronger LBC dependent, while others are more dependent on the parameterizations of the RCM. Several authors have found that the internal variability increases with domain size, since the regional model has more freedom to develop its own climate far from the driving borders (Seth and Giorgi, 1998; Lucas-Picher et al., 2004; Vannitsem and Chomé, 2005; Alexandru et al., 2007). Therefore the internal variability should be evaluated in particular when the area of interest is much smaller than the model domain. Internal variability can differ during the year, and most authors agree on higher internal variability during summer than during winter (Giorgi and Bi, 2000; Christiensen et al., 2001; Caya and Biner, 2004), although Lucas-Picher et al. (2004) found that internal variability were higher during winter for eastern North America. The impact of initial conditions decreases with the simulation length (Wu et al., 2005), but can vary during the simulation due to different types of synoptic event (Giorgi and Bi, 2000; Alexandru et al., 2007). Considering that each specific experiment set up (domain, season, analyzed variables e.g.) has an unique impact on internal variability it can be concluded that to be used as a benchmark for e.g. sensitivity study outcomes, it should be estimated for each specific experiment set up. The objective of evaluating the internal variability of RCA3 is to find useful measures that can be used for comparison with other model sensitivities and variability.

4.2 Methodology

The internal variability was calculated for austral summer, which is the season that this thesis focuses on. The period that was used for the three experiments that focuses on soil moisture during the SAMS that will be presented in the chapters (6-8) is August 1992 to February 1993, and therefore the internal variability was calculated for four of the SAMS months for this period: November 1992 to February 1993. RCA3-E was driven by ERA-40 over the same domain that was presented in chapter 3 and that will be used for the studies in chapters 5-8. Internal variability was defined as sensitivity to different ICs, initializing the model on different dates. The soil moisture was

initialized in equilibrium with the model atmosphere, as will be described in section 5.2.2.

The size of the ensemble influences clearly on the internal variability. Alexandru et al. (2007) estimated the ensemble size for calculating the sensitivity to initial conditions and found a good agreement in the internal variability for large ensembles of 10, 15 and 20 members. Due to computational restrictions the lower end of this estimate was chosen. The ensemble consists of 10 simulations with the common integration period November 1992 – February 1993, and members differ only in the initialization dates which are 1, 4, 7, 10, 13, 16, 19, 21, 24 and 26 of October. When using different initial dates, the ensemble members also differ in atmospheric spin up period (see section 5.2.2), which could potentially have an influence on the November results. The difference in atmospheric spin up period could have been limited by using consequent days, but 2-3 days difference between the initialization dates was chosen to avoid synoptic similar days. It should be noticed that the spin up period is inevitably different when testing the sensitivity to different IC with a RCM.

In the literature, different measures for internal variability are found. In this thesis, most analyses are based on monthly or seasonal means, and is focusing on precipitation and temperature, so an appropriate measure should be on the same time scale using these variables. The internal variability was calculated by taking the monthly means for each ensemble member and calculating the grid point by grid point ensemble maximum value minus the minimum value. This approach gives a spatial distribution of the monthly ensemble spread and can be considered as an upper limit internal variability. This methodology was also chosen because it is comparable to a similar RCA study that had been realized over Europe (Claus Wyser, personal communication 2005), although his study only employed 5 ensemble members. It should be noticed that small spatial location differences in precipitation maximum gives very large values of internal variability using this approach.

To obtain one single value that estimates the internal variability for the whole South American domain that can be compared to the results for Europe, the 95th percentile of the ensemble spread was also calculated.

4.3 Results

Internal variability of 2 meter temperature and precipitation together with their corresponding ensemble means for the four months November'92 to February'93 are displayed in figures 4.1 and 4.2. The temperature internal variability is highest at locations where the model has positive biases, as for example for November in northeastern Brazil and for all months in northern Argentina / La Plata basin. As will be discussed in chapter 5, the bias in the La Plata region has to do with a dry soil bias for these months, and a negative bias in cloud cover, which could both influence on the temperature variability. The values of internal variability are however very high for some regions considering that the calculations are based on monthly means.

The precipitation internal variability is highest in regions where the precipitation is governed by convection and, naturally, the variability is higher in regions with high precipitation values (comparare figure 4.1). In November, the convective activity is located more to the north, while for the consequent months it migrates down to the La Plata region, in accordance with the evolution of the monsoon. A comparison of the internal variability to the ensemble mean shows that for some grid points (e.g. December at around 15°S, 55°W) the difference between the highest and the lowest ensemble monthly mean is higher than the ensemble mean, which indicates that the ensembles differ in the positioning of precipitation maximum.

When calculating the 95^{th} percentile of the internal variability, all domain land was included except for the Andes, since both temperature and precipitation over the elevated terrain are difficult to assess due to sparse observational data and complex physiographic details. In figure 4.3 the temperature and precipitation distributions for November are shown as examples. In figure 4.4, the accumulated temperature and precipitation distributions for all four months are displayed. In 4.4 a), the black arrows show the 95^{th} percentile of November temperature spread, indicating how ΔT and ΔP are calculated. Table 4.1 shows ΔT and ΔP for all months compared to the boreal summer month July ΔT and ΔP over Europe.

	ΔT (°C)	ΔP (mm/day)
November	2,76	10,82
December	2,69	13,33
January	3,23	10,05
February	3,69	13,09
July (Europe)*	0,64	1,27

Table 4.1: ΔT and ΔP (95th percentile values) for the four months over South America, and for July over the European domain. * These values are from a five member's ensemble.

The ΔP exceeds 10 mm/day for all months over South America. The value for Europe is lower probably due to various reasons. The ensemble used for the calculation of internal variability over Europe had only 5 members, and the model domain is smaller than for South America (102x111 as compared to 220x170 grid points), potentially giving the regional model more freedom in the inner part of the South American domain. Furthermore, the largest part of the South American continent has a tropical climate with precipitation governed by convection, while the European domain has its lowest latitude at 35°N. The months November – December are months of highest monthy preciptation for many regions (see figures 3.3, 5.2 and 5.3), which introduces more variability, as calculated here, in absolute values.

ΔT is also substantially higher for South America than for Europe. This is probably not related to the ΔP, as figure 4.1b) and 4.2b) shows that the regions of high internal variability in temperature and in precipitation do not coincide. Possibly this has to do with the erroneous soil dryness, as will be discussed in the following chapters. A dry surface responds more rapidly to e.g. small diferences among the ensemble members in radiation and cloudiness, than a humid surface. The ΔT is higher for the two last months than for the two first months of the simulation, but since the simulation is short it is difficult to attribute this to a trend in ΔT over time, and could also be due to seasonality of the internal variability.

4.4 Conclusions and importance for the interpretation of RCA3 results in further work

The internal variability of RCA3 was evaluated for four months of the monsoon season. The internal variability was calculated by taking the monthly means for each ensemble member and calculating the grid point by grid point ensemble maximum

value minus the minimum value, and the 95th percentiles were calculated as a general upper limit for the whole continent. The measure for internal variability used here is quite extreme in comparison to other definitions (e.g. standard deviation). The 95th percentile values will not be used for further analysis in this thesis, since the spatial differences are very high over the continent, and were calculated for comparison with the corresponding results over Europe. It was found that for summer the internal variability is much larger over South America than over Europe, and this was attributed to the fact that South America is a tropical region with convective precipitation regimes, larger precipitation values than for Europe, and also to the soil dryness in some regions. The European domain is also smaller and a smaller ensemble size was employed. Although the 95th percentile values are very high, there are large regions with quite small internal variability.

In the following chapters, where e.g. sensitivity to soil water content or to rooting depth are assessed, the spatial distribution of internal variability will be useful to evaluate the significance of the sensitivity. However, to assure statistical significance, in the following chapters, either ensembles or multiyear simulations are employed. The results obtained in this chapter serve to qualitatively identify regions with high internal variability, that is, the values of internal variability are not to be seen as lower limits for evaluating if the model response is quantitatively significant or not.

5. Model Evaluation

5.1 Introduction

The RCA3-E performance over South America is evaluated using a 22-years simulation with ERA-40 reanalysis as initial and boundary conditions. A multi-year evaluation of the performance of the model driven by perfect boundary conditions is necessary since the model was used over South America for the first time for the purpose of this thesis. The evaluation will help to interpret the results of the experiments in the following chapters. The model is evaluated in comparison to observational datasets and to the driving reanalysis. Furthermore, a ten-year sub-period is compared to the results of three regional climate models. Giorgi and Mearns (1999) recommended that coordinated RCM intercomparison experiments should be carried out since each model has its unique formulation and non linear feedback loops. Through these kind of experiments, processes that are simulated systematically well or poorly can be identified, both rising confidence about the RCMs performance over the region of interest, and to identify model formulations that needs improvement. Several regions of the world have been studied in such a framework, e.g. over Asia (Fu et al., 2005), United States (Takle et al., 1999; Anderson et al., 2003) and Europe (Christensen et al., 2002; Hewitt, 2005). Over South America an intercomparison experiment has been carried out by Roads et al. (2003), with 4 RCMs spanning 2 years, and within the context of CLARIS (Menendez et al., 2009a) with 6 RCMs spanning 3 periods of two months each. The intercomparison experiment presented here includes 3 RCMs and one stretched grid global model and spans a 10-year period. Since regional modeling is still in its development phase over South America, this intercomparison between models is useful to learn more about similarities and differences between models and their possible causes.

5.2 Methodology

5.2.1 Simulations

A simulation of 22 years (1979-2000) was carried out. The 20-year period 1980-1999 (in the following called RCAERA) is evaluated in comparison to CRU data and to

the driving reanalysis, considering the first year as a spin up period. For an analysis of the model interannual variability, ideally a longer simulation would have been required, but since the ERA-40 reanalysis is improved substantially for the Southern Hemisphere from year 1979 due to the inclusion of satellite data, a shorter period was chosen to have more uniform and reliable boundary conditions.

The CLARIS ensemble consists of regional simulations performed with three RCMs models (RCA3, REMO and PROMES) and one global stretched grid model (LMDZ) for the period 1991-2000. The domains are somewhat different from model to model but include most of South America. The domain of analysis covers from 50°S to the equator and from 85°W to 35°W. The four models are described in table 5.1.

	RCA3	LMDZ	PROMES	REMO
Reference	Kjellström et al. (2005)	Hourdin et al. (2006)	Castro et al. (1993)	Jacob (2001)
Grid resolution	50 km	0.5° to 0.7°	50 km	0.5°
Grid (lat*lon)	155x134	100x97	139x145	121x145
Vertical levels	24	19	28	31
Convection	Kain and Fritsch (1993); Jones and Sanchez (2002)	Emanuel (1993)	Kain and Fritsch (1993)	Tiedtke (1989), modifications after Nordeng (1994)
Microphysics	Rasch and Kristjansson (1998)	Bony and Emanuel (2001)	Hsie et al. (1984)	Sundquist (1978)
Radiation	Savijärvi (1990); Sass et al. (1994); Räisänen et al. (2000)	Morcrette (1991)	Stephens (1978); Garand (1983)	Morcrette et al. (1986); Giorgetta and Wild (1995)
Land surface	Samuelsson et al. (2006); Champeaux et al. (2005)	Krinner et al. (2005)	Ducoudre et al. (1993)	Dümeniel and Todini (1992)
Soil thermal layers	5	11	7	5
Soil moisture layers	2	2	2	1

Table 5.1: Details on the models participating in the CLARIS coordinated simulations.

5.2.2 Spin up and soil moisture initialization

An important internal property of a model is the spin up time. Since the RCM is initialized using all initial fields from another model, ERA-40, the properties of the initial fields will not be in equilibrium with the RCM dynamics and this will cause noise

during a period of adjustment. The spin up time is referred to as the time, from the moment of initialization that the model needs to reach a dynamical equilibrium between lateral boundary forcing and internal model forcing (Anthes et al., 1989). In the case of the atmospheric processes, there are several studies that consider that the spin up time is 2-10 days, depending on the model, the forcing model and the nudging method, but also on model domain size (e.g. Seth and Giorgi, 1998). Since this is a well studied subject, the atmospheric spin up time is not investigated in this thesis, and instead the analyses of the results are started at least one month after initialization. However, as was explained in section 1.4.2, soil moisture processes are much slower than atmospheric processes and a study was made to estimate the spin up time of soil moisture, which is defined as the time the model soil moisture takes to reach equilibrium with the model atmosphere. To have a practical criterion for this, the spin up time was defined as the time that any linear trend can be seen in the soil moisture. It was estimated that 2 years can be seen as an upper limit for the Tropical (TR) region (figure 3.1), while the rest of the continent showed a faster spin up, from one month to a year. It was concluded that at least one year of spin up of soil moisture should be employed.

As examples of regions with different soil moisture spin-up time and time evolution, the soil moisture evolution for TR, SAmz, NeB and LPB are shown from January 1979 to 1999 in figure 5.1 (regions employed for the analysis are the same as in chapter 3, figure 3.1).

The experiments in the present chapter, as well as in the following 7, 8 and 9 are carried out with soil moisture in equilibrium with the atmosphere, which has been demonstrated by Rodell et al. (2004) to be the most efficient way of soil moisture initialization. This was achieved for multi-year-runs by using a one year spin-up time, or in the case of short simulations, by initializing the simulations with saved soil moisture from a longer simulation.

5.3 Results from the 20-years RCA3-E integration

The seasonal means of precipitation of CRU and RCAERA are found in figure 5.2. RCAERA has a reasonable representation of the large scale patterns for all seasons, although in tropical regions as well as in the Southern Andes, the maximum intensities are overestimated. The JJA local maximum in south eastern South America is underestimated, which is a common bias of both reanalysis driven RCMs (Menéndez et

al., 2010) and AOGCMs (e.g. Vera et al., 2006). The precipitation over the central Andes is overestimated in the regional model but is difficult to assess due to the complex topography of the sharp Andes and the sparse observational data used for the CRU compilation in this region (New et al., 1999). The model simulates reasonably well the 20-years monthly interannual variability, although with a tendency to overestimate the amplitude for regions and months where the model does not have a dry bias (figure 5.3). When extreme dry biases occur, the model interannual variability is naturally smaller than the CRU variability, (see JJA for NLPB and LPB). The time series of the 20-year annual means are shown in figure 5.4, and the 20 years total means together with the standard deviation are presented in table 5.2. The model represents well the year-to-year variability for most regions, with "offset" positive or negative biases.

Region	RCA mean	CRU mean	Bias (mm/day)	Bias (%)	RCA std	CRU std
TR	5,4	6,3	-0,8	-13	0,98	0,57
SAmz	7,1	5,5	1,6	28	0,68	0,37
NeB	3,0	2,6	0,5	18	0,92	0,60
EB	4,0	3,8	0,3	7	0,43	0,44
NWASB	4,8	2,4	2,4	101	0,55	0,35
NLPB	3,6	4,3	-0,7	-16	0,37	0,53
LPB	2,2	3,2	-1,0	-31	0,36	0,36
SA	4,5	3,3	1,2	38	0,57	0,46

Table 5.2: The RCA and CRU 1980-1999 annual means of precipitation (mm/day). The absolute bias and the bias in percent of total rain amount and the 20-year standard deviation of the model and of CRU respectively.

These systematic biases of rainfall during 20 years of simulation create soil moisture anomalies that possibly feed back on the climate through an erroneous surface climate. Since the season that will be studied in chapters 6-8, is the monsoon season, the temporal evolution of land precipitation during the initial and mature phases of the SAMS averaged between 60°W- 40°W was plotted in figure 5.5. The model simulates an early migration of the monsoon rains to higher latitudes in comparison with CRU, and the maximum precipitation in January – March is overestimated.

The seasonal means of 2 meter temperature (t2m) of CRU and the difference between RCAERA and CRU is shown in figure 5.6. RCA3-E shows large positive biases over central eastern Argentina for the DJF and SON seasons, probably associated with a drying of the soil in this region as described above. During SON, northern Brazil shows a warm bias as well as Northern Argentina during JJA. The MAM season is

relatively well represented. The Andes negative biases in all seasons are difficult to assess for the same reasons as for precipitation. The biases of the annual cycle of t2m (figure 5.7) can in many cases be related to the precipitation biases, anomalous wet (dry) climate generating a cold (warm) bias. This effect can have a lag of a month to a season, due to a delay feedback between precipitation and deep soil moisture; note especially the two La Plata regions where the dry winter bias could contribute to the warm spring biases. Table 5.3 shows that the monthly t2m biases are highly correlated to deep soil moisture for the regions SAmz, NeB, NLPB and LPB.

Region	Correlation t2m biases - deep soil moisture
TR	-0,38
SAmz	-0,89
NeB	-0,82
EB	-0,67
NWASB	-0,59
NLPB	-0,71
LPB	-0,75
SA	-0,29

Table 5.3: Correlations between monthly t2m biases and level of deep soil moisture for 1980-1999. All correlations are statistically significant with 95% confidence.

The monthly interannual variability, defined here as the standard deviation is also diplayed in figure 5.7. In general RCA3-E tends to overestimate rather than underestimate the interannual monthly variability, although for many regions/months it is close to observations. As for precipitation, the model represents well the interannual t2m temporal oscillations (figure 5.8), although with offset biases, and in all cases, an overestimation of the interannual variability (table 5.4).

Region	RCA mean	CRU mean	Bias	RCA std	CRU std
TR	25,3	25,9	-0,58	0,43	0,27
SAmz	26,4	26,0	0,31	0,53	0,32
NeB	26,2	25,8	0,35	0,60	0,31
EB	22,4	23,3	-0,84	0,55	0,34
NWASB	20,2	20,9	-0,78	0,53	0,33
NLPB	22,5	21,4	1,09	0,50	0,33
LPB	19,2	17,4	1,85	0,54	0,32
SA	10,2	9,0	1,22	0,31	0,22

Table 5.4: The RCA and CRU 1980-1999 annual means of t2m (°C). The absolute bias and the bias in percent of total ran amount and the models' and the CRU 20-year standard deviation.

Since the model has some problems representing the precipitation pattern over South America, the total column water is shown in figure 5.9. Due to lack of observational data, this variable is compared to ERA-40. The precipitable water "biases", that is RCAERA – ERA-40 and the precipitation differences between RCA3-E and CRU (see figure 5.2a and b) are not directly linked during DJF and MAM, although the RCA3-E precipitation excess over the Amazonia delta in comparison to CRU in DJF coincides with an "excess" of precipitable water. This suggests that the precipitation biases are linked to other processes like microphysics parameterizations or triggering of convection. On the other hand, the dry (wet) JJA and SON differences are in agreement with an excess (lack) of precipitable water.

The seasonal averaged winds of ERA-40 and the model wind biases are displayed in figure 5.10a and b respectively. The South American low level jet carries moisture to latitudes south of 20°S during the whole year (see section 1.1). Weak low level winds in the regional model is therefore another possible reason for the dry biases of The La Plata basin in winter, and for the northern part of the basin also during fall (figure 5.3). During all seasons, the south/south eastern flow to the northern La Plata Basin region is weaker in RCA than in ERA, consistent with the lower precipitation in the model in comparison with CRU (figure 5.2). During the DJF season however, the flow is also weaker to the whole basin, but the precipitation is well represented.

5.4 Results from the coordinated 10-years RCM integration

Figure 5.11 shows the seasonal precipitation distribution over South America for the period 1991-2000 for CRU, the ensemble and the four regional models. To a first approximation, the annual cycle of precipitation tends to follow that of insolation, although there are marked west-east asymmetries. The wet and dry seasons have clear differences. The monsoon season DJF is the wettest three-month period, with largest values over southern Amazonia and towards the South Atlantic Convergence Zone region. All models tend to overestimate rainfall over the northern part of the domain. The ensemble mean represents the precipitation pattern quite well, although PROMES places the SACZ too far south, and in LMDZ the Brazilian coast is too wet. The largest values are in the north and northwest during winter while large areas further south in the continent are quite dry. The ensemble captures relatively well this distribution. The secondary maximum over La Plata Basin is underestimated by RCA3, and (to a less

extent) by REMO. Over northern South America, rainfall during fall (MAM) is heavier and more evenly distributed in longitude than in spring (SON). This is relatively well captured by the ensemble mean, but with stronger rainfall maximum. In southern South America, the ensemble seems to capture the observed rainfall, although some models do not simulate the regional distribution (e.g. the marked west-east variations in SON is absent in RCA3). PROMES and LMDZ tend to overestimate precipitation in parts of La Plata Basin in spring.

While the models have some similar problems and virtues in simulating the precipitation, they show large differences in seasonal temperature, and the ensemble mean is closer to observations than any individual model. The ensemble tends to be warmer than the observations (figure 5.12), with largest biases in SON (but also with large biases during DJF over La Plata Basin). There is a large intermodel spread, suggesting different problems in the simulated surface heat budget of each model.

5.5 Conclusions and implications for interpretations of further RCA3 results

A 20-year long simulation driven by ERA-40 was evaluated against CRU and ERA-40 data. The model represents the main pattern of seasonal precipitation quite well. However the model does not capture the local precipitation maximum over La Plata Basin in JJA and overestimates rainfall in the precipitation maximum in the central and northern part of the continent. The low level winds that carry moisture to the La Plata Region are underestimated in all seasons, probably contributing to the winter dryness. The land surface is too hot in many regions, in particular about a month after negative rainfall anomalies have occurred.

The comparison with two other regional models (REMO and PROMES) and a global stretched grid model (LMDZ) for the period 1991-2000 showed that the models have similar problems in representing seasonal rainfall, in particular they overestimate the rainfall in the northern part of the domain. The ensemble performance for each season is better than the worse model, but not necessarily better than the model that represent that particular season best. With respect to temperature, RCA3-E, REMO and PROMES have problems with hot biases over the whole continent except for Patagonia, while LMDZ shows negative biases over most part of the continent all around the year.

The ensemble mean are therefore improved with respect to any individual model, due to cancellation of errors.

Within the context of CLARIS/CLARIS-LPB, the regions of interest are the La Plata Basin regions, and the precipitation was found to be best represented for spring and summer for these regions. The following three chapters will focalize on the interaction between soil moisture and precipitation during the monsoon season (spring and summer) through three independent experiments. For the interpretation of the results, the present chapter is fundamental. Soil moisture is a model dependent variable, and even if there would be datasets of soil moisture for comparison to model results, the comparison would only serve as a qualitative measure. The soil interaction with the atmosphere through its influence on Bowen Ratio, is not only dependent on the soil moisture content, but fundamentally on each models' parameterization scheme of transpiration and runoff, and also depends on parameters such as leaf area index (LAI) and soil type. Therefore, when in the following text reference is made to low or high soil moisture content, what is meant is soil moisture that produces an erroneous model surface climate. In this chapter it was found that the t2m biases are strongly correlated with soil moisture content for Southern Amazonia and the La Plata Basin regions, which are regions of high interest for this thesis. The results of the model evaluation suggest that the positive biases of t2m during spring and summer in these regions indicate that the deep soil moisture is too low, due to previous precipitation dry biases. Although the following chapters studies the monsoon season, where precipitation biases are not as pronounced as for the winter season, the winter negative precipitation biases are of great importance through the generation of erroneous soil moisture for this season.

An important caution to this chapter, is that the model, due to the lack of observations, could not be evaluated against observational data on surface fluxes, which is of great importance when studying the land-atmosphere interactions. Therefore, in the following chapters 7-8, it is assumed that RCA3-E represents the latent and sensible fluxes well, although this assumption needs to be confirmed by comparison to observational data when those are available.

6. Anomalously winter Soil Moisture influence on the SAMS

6.1 Introduction

The onset and intensity of the South American Monsoon System have important implications for many climate studies and water resources management applications for agriculture and hydroelectricity. Liebmann and Marengo (2001) found that the onset date of the monsoon is more important for the total seasonal contribution to total rainfall than the intensity of the rainfall during the wet season.

The recent review paper on the SAMS, Vera et al. (2006a), identified land surface processes like topography, soil moisture and vegetation cover, and their relative role in the development of the SAMS as a mayor research question to achieve a better understanding of the monsoon system. In this chapter the impact of anomalously dry and wet winter surface conditions on the development will be studied as an approach to understanding the soil moisture influence on the monsoon.

A summary on how land surface processes can influence in the development of SAMS was given in section 1.4.4. In the following section, the main characteristics of SAMS are described, and the monsoon processes related to atmosphere interactions with land surface, and in particular with soil moisture, are revised in more detail.

6.1.1 The South American Monsoon System, main features

Monsoons develop as a response to seasonal changes in the thermal gradient between continent and ocean in low latitudes. Since most of South America is situated in the tropics, the annual temperature amplitude is smaller than for other monsoon regions, and easterly winds dominate all through the year. The characteristics of SAMS are therefore different than those of other monsoon systems, and the SAMS became recognized as a monsoon only about a decade ago when Zhou and Lau (1998) demonstrated that a reverse in the low-level circulation monthly anomalies becomes evident when the annual mean is removed from winter and summer composites.

The beginning of the SAMS is characterized by convective activity intensification over northwestern Amazonia that then progresses to southeastern South America (Kousky, 1988; Marengo et al., 2001; Liebmann and Marengo, 2001; Gan et

al., 2004; Vera et al., 2006a). The onset of the monsoon has been defined by some authors (Kousky, 1988; Marengo et al., 2001; Li and Fu, 2004) as the dates when precipitation reaches a threshold of five days mean of around 6mm/day. The onset date typically occurs in early November, but can vary between late August to late December (Li and Fu, 2004). The monthly development of rainfall over the SAMS region from 20 years of CRU data averaged between 40°W-60°W was shown in figure 5.5a. The onset is preceded by a north-south cross-equatorial flow over South America (e.g. Marengo et al., 2001) which starts in the equatorial Amazon and spreads rapidly to the east and to the SACZ zone (southeast). The precipitation is associated with the Bolivian high, a high air pressure system centered over the Bolivian plateau at upper atmospheric levels (e.g. Lenters and Cook, 1997). Another important circulation characteristic is the surface thermal low over Paraguay and northern Argentina, known as the Chaco low (e.g., Satyamurty et al., 1990; Gan et al., 2004). The Andes plays a crucial role in blocking the air masses coming in from the Atlantic. The continental-scale low level gyre that transports moisture from the tropical Atlantic to lower latitudes was illustrated by the DJF 1980-1999 winds from ERA-40 at 850hPa in figure 5.10a. On shorter time scales, the moist air is channeled either towards the SACZ region or through the SALLJ reaching Southeastern South America.

The mature phase typically occurs between late November and late February and is characterized by deep convection over central Brazil, extending eastwards, southeastwards, and to the Altiplano Plateau, while heavy rainfall is absent in eastern Amazonia and northeastern Brazil. The monsoon begins to decay during March, with decreased precipitation and migration northwestwards.

6.1.2 Land surface processes linked to the SAMS onset

The land-ocean thermal contrast and the continental latent heat flux release contribute to the determination of the onset, the intensity and spatial distributions of monsoons (Webster et al., 1998). How these two processes contribute to the different phases of the South American monsoon has been debated during decades.

Rao and Erdogan (1989) suggested that the land surface fluxes are the main contributors of moisture in the wet season and that they also control the wet-season circulation pattern over South America, such as the Bolivian High. Other authors (Moura and Shukla, 1981; Aceituno, 1988; Ropelewski and Halpert, 1989; Fu et al.,

2001) have suggested that the main source of moisture during the wet season is the transport from the Atlantic, by direct thermal circulation from the Atlantic as well as through the influence of Rossby waves propagating from the extratropical South Pacific to subtropical South America. Fu at al. (1999) studied the onset phase of the monsoon through satellite, radiosonde and assimilation data and concluded that the moistening of the boundary layer, leading to lower convective inhibition energy, controls the large scale circulation and the onset of the monsoon. Their results suggested that both adjacent SSTs and land surface forcing could be important for the onset.

One hypothesis is that land surface conditions are more important at the initial stage of the monsoon, with humid land surface and latent heat flux triggering convection over Amazonia. These conditions would influence on the large scale circulation, such as the Bolivian high, and once these conditions are established, the moisture transport from the Atlantic Ocean is a main contributor to the precipitation. In a study using ERA15 data, Fu and Li (2004) and Li and Fu (2004) found that the continental surface conditions seem to control the onset date of the monsoon. An increase of surface evapotranspiration and local water recycling is necessary for initiating the onset, while at the developing and mature phases, both water fluxes and the moisture transport from the Atlantic are important. In particular, an anomalously dry land surface during the dry season could delay the onset of SAMS with as much as two months while wet conditions do not influence as much on the onset date. Collini et al. (2008) showed similarly that October precipitation was more responsive to reductions than to increases in initial soil moisture using a regional mesoscale model. They found that reductions in initial soil moisture produced almost linear reductions in precipitation over the monsoon region, principally because of the more stable boundary layer that results from the increase of the Bowen ratio.

Grimm et al. (2007) studied the link between precipitation and soil moisture conditions during November and January over central eastern Brazil using both observational data and regional model experiments. In their study, dry (wet) conditions during spring enhanced (reduced) the moisture flux to the region and produced more (less) rainfall during the mature monsoon phase. These results are limited to precipitation and soil moisture anomalies over central eastern Brazil, and are not directly comparable with the aforementioned studies by Collini et al. (2008), that reduced soil moisture for the entire continent; or to Li and Fu (2004) that studied the surface conditions for Southern Amazonia. However it is interesting to notice that in

Grimm et al. (2007) reduced spring soil moisture induces changed circulation patterns that enhance precipitation during the mature phase, while the other studies came to the opposite conclusion.

Xue et al. (2006) analyzed the role of vegetation biophysical processes in the structure and evolution of SAMS through (GCM) experiments with different land surface parameterizations. The inclusion of an explicit representation of vegetation processes modified the Bowen Ratio and led to a more realistic simulation of precipitation amount, but also of the spatial and temporal evolution of the monsoon since the division of the surface fluxes influence the continental scale circulation.

6.2 Methodology

The influence of anomalous soil moisture initial conditions in late austral winter on the intraseasonal development of the SAMS is explored through simulations initialized with highly idealized and extreme anomalous soil moisture conditions. The study covers the monsoon of 1992-93, which was chosen since it is a neutral ENSO period. Some authors have suggested that the surface and dynamical processes of the SAMS act independently of the large-scale conditions. Fu et al. (1999) found that the forcing that control the onset of the monsoon are the same for El Niño and La Niña event. Collini et al. (2008) draw similar conclusions in a regional climate model study of several October months.

Two ensembles with anomalously dry and wet land surface initial conditions over the whole domain were created. Each ensemble has five members initialized on different dates, all members including the period 1 August 1992 – 31 March 1993. The ensembles will in the following be called “DRY” and “WET”. The initial soil water availability (SWA) for the two simulations was modified from the SWA of the driving reanalysis of the corresponding initialization dates ($SWA_{ERA\text{-}40}$). To generate dry conditions, $SWA_{ERA\text{-}40}$ was multiplied by a factor 0.2, and to generate wet conditions without allowing super saturation the formula $SWA_{WET}=SWA_{ERA\text{-}40} + (1- SWA_{ERA\text{-}40})*0.8$ was used. These modifications create highly anomalous initial SWA fields that are shown in figure 6.1.

6.3 Results

The soil moisture initial condition has a strong influence on spring and summer rainfall over the continental convective monsoon regions. The precipitation of the two ensembles is displayed as maps of two-month means (figure 6.2) and the temporal evolution of the monsoon between 60°W and 40°W is dispalyed in figure 6.3. The SAMS is a complex system with land surface–atmosphere interactions depending on numerous factors. During the first two months of simulation, August and September, the difference between the DRY and WET ensemble in the partitioning of surface fluxes induced a large difference between the ensembles in air column temperature over the central part of Amazonia. In ensemble DRY, the continental air temperature was higher and brought in stronger Atlantic trade winds over the northern part of the continent that were blocked and turned anti-clockwise to the south by the Andes Mountains (figure 6.4 a-c). Moisture convergence in ensemble DRY was larger than in ensemble WET east of the northern Andes and in southern Amazonia, producing more rainfall over these regions (figure 6.2 a-c). The WET ensemble produced more rainfall over the La Plata Basin, possibly a consequence of both higher moisture transport with the low level jet to this region and of higher local water recycling than in DRY. The different soil moisture content also affected the precipitation over ocean due to the impact of land–atmosphere interaction on circulation; in the WET ensemble the ITCZ is stronger than in the DRY, similar to Sato et al. (1989) and Xue et al. (2006). This is consistent with recent studies on tropical deforestation in the Amazon Basin suggesting that land surface conditions can amplify teleconnections through compensating subsidence (Avissar and Werth, 2005; Feddema et al., 2005; Voldoire and Royer, 2005).

The evaporative fraction (latent heat flux fraction of total heat flux) is displayed in figure 6.5 and the soil moisture development in figure 6.6. The difference DRY-WET in evaporative fraction of August-September (figure 6.5 a-c) is influenced by the stronger rainfall over the region east of the northern Andes and in southern Amazonia in DRY, feeding back on the consequent evolution of column temperatures and moisture convergence for October-November (figure 6.4 d-f). Similar to August-September precipitation pattern, during these months of initial monsoon development, the ensemble WET also increases precipitation along the ITCZ and compensating subsidence produce large areas of decreased precipitation further south in tropical South America (figure 6.2 d-f).

In December-January, the initial soil moisture difference between the ensembles are only persistent over the northern part of the continent (figure 6.6 g-i), and during this mature phase of the monsoon, precipitation is stronger in WET than in the DRY in central Amazonia (figure 6.2 g-i). Since no difference of moisture convergence DRY-WET is observed in this region (figure 6.4 g-i), an explanation could be local precipitation recycling, since the region remained wetter during the whole simulation period. The band of stronger rainfall in the DRY ensemble around 20°S is a consequence of higher moisture convergence in this region.

In February-March the initial soil moisture anomaly prevails over central-eastern northern Amazonia creating differences in flux partitioning only over this region (figures 6.5 and 6.6 j-l). The rainfall differences over the central part of the continent (figure 6.2 j-l), is 1-6 mm/day and could be a consequence of the difference in circulation pattern and moisture transport. The higher rainfall in central Amazonia in WET could be connected to the higher evaporative fraction further north, providing moisture to the atmosphere that is transported southwards.

The daily precipitation frequency gives a more detailed picture of the model's sensitivity than the bi-monthly mean values. Figure 6.7 shows the histograms of daily rainfall on different intensity classes for SAmz for October and December. The graphs are constructed by counting for each grid point, the total number of days within each interval representing dry days (0-0.5 mm/day) and light (0.5–6 mm/day), moderate (6–15 mm/day), strong (15–30 mm/day) and heavy (> 30 mm/day) precipitation days. The effect of soil moisture late winter initial conditions on the precipitation regime are considerable, especially during December. In October, SAmz received less precipitation total in ensemble WET, due to the above discussed inflow of moist air from the Atlantic. The precipitation regime differs in that WET has more dry days and less days of light to strong precipitation. In December the intense convective rainstorms (strong and heavy rainfall days) are more frequent in the WET than in the DRY. This supports the possibility that the December rainfall processes in SAmz are related to local precipitation recycling, since deep convective cumulus are more likely to develop over a wet land surface (e.g. Pielke, 2001).

6.4 Conclusions and Discussion

The impact of soil moisture initial conditions on the SAMS development was studied in this chapter. In this case, two simulations of the period 1 August 1992 – 31 March 1993 with modified initial soil moisture have been compared. Studying the impact of soil moisture initial conditions constitutes a limited approach as part of the difficulty for understanding and simulating the hydrologic cycle in this region. In this simple and qualitative assessment of the soil–precipitation feedback, simulations with opposite soil moisture initial conditions have been employed in order to represent two highly idealized and extreme anomalous surface conditions during the late austral winter. The differences in precipitation between the two ensembles are explained by dynamical and physical mechanisms interacting. The results suggest that the initial winter soil moisture conditions feed back upon the SAMS during the warm months, not only over Amazonia but in subtropical South America as well. This is related with different mechanisms, e.g.: (i) Dry conditions during August and September lowered the evaporative fraction and the air column temperature increased. This brought in strong winds from the Atlantic that produced strong precipitation in the east of the northern Andes and in southern Amazonia. The mechanism is similar to the Grimm et al. (2007) results for central eastern Brasil. (ii) In La Plata Basin, the stronger rainfall in the WET ensemble could be related to the transport of atmospheric moisture associated with the low-level jet (as in Collini et al., 2008) (iii) Local precipitation recycling created stronger rainfall in Amazonia during the mature monsoon (January and February); and (iv) Changes in convection patterns can affect the Hadley Circulation and thus propagate climate perturbations into the subtropics (as suggested e.g. in Branstator, 1983; Sadershmukh and Hoskins, 1985; Figueroa et al., 1995).

7. Rooting depth Influence on SAMS

7.1 Introduction

The amount of water that is available in the soil for evaporation back into the atmosphere depends, among other factors, on the soil and rooting depth. Land surface parameterizations in RCMs generally use values of 1-2 meters for soil/rooting depth, depending on vegetation type or topography (Boone et al., 2004). RCA3 employed a constant soil and rooting depth of 2.2 m for all regions but mountain regions where it was set to 0.5 m. This is in contrast to observational data over South America, for example in the Amazon basin deep roots of several meters was found by Nepstad et al. (1994).

The interest in focusing on the soil/rooting depth is motivated by two factors: (i) the soil depth of tropical forest that cover large areas of northern South America are increased to 8 m with the incorporation of Ecoclimap in the model, and (ii) previous works suggest the importance of soil depth and deep rooted vegetation on the climate system.

Van den Hurk et al. (2005) analyzed the soil hydrological memory in the Rhine basin using large scale analyses of atmospheric water convergence and river discharge. They concluded that the depth of the hydrological soil reservoir in RCMs is indicative for the strength of the hydrological response of the whole river basin to a global temperature increase, and that a proper specification of this depth is an important factor. Kleidon and Heimann (2000) investigated this aspect in the context of the climatic effects of large-scale deforestation in Amazonia. They found that most of the regional and remote changes could be attributed to the removal of deep roots. Swenson and Milly (2006) examined GRACE satellite data of monthly changes in continental water storage and compared the results with five AR4 models at regional scales. GRACE data shows that the Amazon basin has the largest annual amplitude of water storage in the world. While the high latitude water storage was represented quite well in the models, the storage in tropical regions was poorly represented. The reason for this can be due to many reasons such as erroneous precipitation or erroneous soil water storage capacity, and was not investigated in the study.

Regional simulations with deficient representation in parameters of the underlying physical environment such as soil depth possibly include associated errors in

the computation of the hydrological cycle. Here the influence of a shallow soil depth of 2 m in RCA3-E is examined during the spring and summer of 1992-93.

7.2. Methodology

In order to estimate the impact of introducing a spatially varying soil depth in the model on the development of the SAMS, two ensembles of five members with different initialization date were created, each one of the members including the period September 1st 1992 through March 31st 1993. An analysis of the time evolution of the soil moisture of a multi-year integration with RCA3-E initialized and forced by ERA-40 showed that the soil moisture spin-up time can be up to 2 years for regions with deep rooting depth as Amazonia. To initialize the regional model with the atmosphere-soil moisture in equilibrium without a long spin-up time, the soil moisture initial conditions (meter of water per meter of soil) are set to the soil moisture fields of corresponding initial date from a RCA3-E/ERA-40 integration initialized 1st September 1990. Ensemble CTL was run with soil depth from the new Ecoclimap database while ensemble CON with the constant soil depth (2.2 m) employed by RCA3. Figure 7.1 shows the soil/rooting depth of RCA3-E.

7.3 Results

Figure 7.2 compares the CRU precipitation climatology for the spring and summer 1992-93 with the simulated ensemble means for the CON and CTL. The bias for ensemble CON (figure 7.2 c) during the onset phase of the monsoon (SON) is around +3-6 mm/day over the rainy central-western Amazonia down to the SACZ region, and the SACZ is shifted southwards. Over the northern La Plata Basin there is a negative bias of 1-3 mm/day. The inclusion of a spatially varying soil depth (figure 7.2 e) tends to reduce the bias in northwestern Amazonia, while to the south, over tropical regions, the positive precipitation bias was increased in CTL, likely due to an enhanced southward transport of atmospheric moisture associated with the SALLJ. During the mature phase of the monsoon, the CON ensemble is too dry in northwestern Amazonia (1-6 mm/day) and positively biased in the Amazon basin (>9 mm/day). The difference between both ensembles is largest over Brazil where CON tends to decrease the precipitation over the region affected by the SACZ (figure 7.2 f).

The differences between the two ensembles are however very small on a seasonal scale compared to the large bias of the model (figures 7.2 c and d). In chapter 6, the differences between the ensembles DRY and WET were larger and did not have the "noisy" character that was seen in this experiment. The differences between DRY and WET precipitation could also be explained by evaluation of e.g. the moisture transport and heat fluxes of the two ensembles, and the significance of the results was not discussed. For the present experiment, the significance of the differences will be evaluated with help from the results obtained in chapter 4. Since the evaluation of internal variability was made on a monthly scale, the monthly differences between CTL and CON of the November -92 to February -93 are displayed in figure 7.3. In the comparison between this figure and figure 4.2, it should be considered that in this chapter the difference is between two ensembles of five members each, and not between individual simulations, increasing the significance of the results.

The positive difference between the ensembles in the western Amazon in November, a region with low internal variability for November, can be considered as significant. The CTL ensemble is wetter than the CON ensemble, and this is probably related to local precipitation recycling. CTL has a larger water reservoir in this region, and on the third month from initialization it is likely that the CON ensemble has a drier soil. Another difference CTL-CON that is likely significant is in January, in the SACZ region, where the model has a relatively low internal variability. The CON ensemble is wetter here, which could be due to an altered preferred path for the moisture transport to the SACZ region due to differences in soil moisture between the ensembles.

However, on a monthly scale, the differences between the ensembles are quite small and spatially noisy. On a seasonal scale the differences are cancelled to a high degree and do not alter the main features of the simulated rainfall.

7.4 Conclusions and Discussion

An ensemble of simulations which includes spatially varying soil depth was compared to an ensemble with a constant soil depth of 2 m. The role of the soil depth depiction was relatively less critical than expected, with both beneficial and detrimental effects on the simulation of the seasonal mean rainfall. However, it should be considered that the simulations were initialized in late winter, extending only throughout spring and summer. Kleidon and Heimann (2000) suggest that the

incorporation of deep roots into a climate model would be important especially during the dry season (i.e. austral winter in South America), since during the wet season the soil moisture content is near field capacity due to heavy rains and the evapotranspiration is not limited by soil moisture. During the dry season though, the ever-green forest would be capable of transpiring considerable amounts of water throughout the dry season if deep soil depth and deep roots are included in the model. According to Kleidon and Heimann (2000), in that case, evapotranspiration and the associated latent heat flux are considerably increased and the enhanced atmospheric moisture is transported towards the main convection areas in the inner tropical convergence zone where it supplies more energy to convection thus intensifying the tropical circulation patterns. This effect still needs to be verified with RCA3-E, but is out of scope for this thesis work which focalizes on soil processes during the SAMS.

8. Soil Moisture - Atmosphere Coupling during the SAMS

8.1 Introduction

The feedback processes between soil moisture and precipitation are difficult to assess for various reasons. Because of the lack of soil moisture observational data there are very few observational studies. The results of both observational and model studies are difficult to interpret in terms of causality due to the many complex feedbacks between the components of the system, such as radiation budget, boundary layer development and land surface fluxes. In this chapter, the influence of soil moisture on evapotranspiration and precipitation is studied through an experimental design that isolates this connection from the direct and strong impact of precipitation anomalies on soil moisture anomalies. The quantified influence of soil moisture on evapotranspiration or precipitation is called coupling strength (CS). In general terms, CS is defined as the degree to which some prescribed boundary condition, for example SST or soil moisture, affects some atmospheric quantity in a climate model. Several recent studies focus on the coupling strength between soil moisture and precipitation and/or surface variables such as temperature and evaporation (Koster et al. 2003, Koster et al. 2004, Dirmeyer et al. 2006, Koster et al. 2006, Guo et al. 2006, Seneviratne et al. 2006, Wang et al. 2007, Yamada et al. 2007). These authors use somewhat different approaches but all aim to quantify the fraction of atmospheric variability that can be ascribed to soil moisture anomalies.

The CS between soil moisture and precipitation should not only be thought of as a result of local water recycling, in the sense that the precipitation at each grid cell originates from the same grid cell trough evapotransporation (as in Elthair and Bras 1994, 1996, Trenberth 1999). This process contributes to the CS, but is not identified separately here. Instead the CS should be understood as how the soil moisture field influences on the fields of evapotranspiration and precipitation. This is a result of non-linear interactions within a climate model, including components such as moisture transport, parameterizations of evapotranspiration, moist convection and boundary layer development. The water vapor that rains out does not necessarily come from the grid box where it evaporated, but can as well be advected from its origin to a grid box of highly favorable conditions for rainfall.

The effect of soil moisture on the surface fluxes and consequently on the Bowen ratio can lead to changes in precipitation (e.g., Betts and Viterbo 2005; Taylor and Ellis, 2006). Collini et al. (2008) discuss the local effects that soil moisture anomalies have on the overlying atmosphere during the early stages of development of the SAMS. Reduction of the soil moisture gives rise to changes in the boundary layer structure and thermodynamic stability: the increased sensible heat flux and reduction of latent heat flux (evapotranspiration) favor mixing and a warmer, deeper and drier boundary layer. These changes affect the convective instability: the convective available potential energy (CAPE) is reduced while the convective inhibition (CIN) is increased slightly (resistance to convection). These effects are dependent on numerous factors including the time of day (effects described in Collini et al. (2008) are most apparent during daytime), the time of year (Silva and Berbery, 2006) found little relation between the monsoon precipitation and CAPE during the austral summer months when the SAMS is already established), the spatial-scale of convective systems (Taylor and Ellis, 2006) and the land cover types (Juang et al., 2007).

Within the GLACE project (e.g. Koster et al. 2003, 2004 and 2006, Guo et al. 2006); the CS between soil moisture and atmosphere for 16 global atmospheric models was explored over the northern hemisphere for boreal summer, a season where soil moisture – atmosphere coupling could be comparable or even stronger than sea surface temperature (SST) – atmosphere coupling for midlatitudes (e.g. Dirmeyer 2003). They showed that global models vary substantially in CS, both in global averages and in spatial distribution. This implies that e.g. sensitivity to soil moisture anomalies is highly model dependent. To evaluate a climate models' CS and identify regions with high CS ("hot spots") is one way to understand the model processes. Some authors have investigated the causes of different components of the CS. One of the models of lowest soil moisture – precipitation CS in the GLACE project was the HadAM3. Lawrence and Slingo (2005) studied the influence of increased soil moisture – evaporation CS on soil moisture – precipitation CS for HadAM3 and found that it remained at a low level. This indicates that the evaporation – precipitation coupling is low. Wang et al. (2007) investigated the CS dependence on changes in surface water budget due to increased throughfall with the global atmospheric model CAM3-CLM and found that coupling increased.

The motivation of the present study is the interest in documenting the degree to which the precipitation responds to soil moisture anomalies during the SAMS in RCA3-

E and to identify hot spots. Coupling strength is still largely unknown for South America and is a very uncertain aspect of regional modeling. The ensemble experiments, which will be described in detail in the next section, were performed with the regional model for the season DJF of 1992-93. Two different indices of CS were calculated and the analysis focalize on the link between soil moisture evapotranspiration coupling and precipitation coupling, the relation betwen the CS and the predictability and the importance for extreme precipitation events.

8.2 Methodology

8.2.1 General experiment set up

The methodology has been adapted to regional modeling following Koster et al. (2006), with the differences that 10 ensemble members were employed instead of 16 and the models were forced with both top and deep soil moisture instead of only by deep soil moisture.

Two ensembles (called W and S) of ten members each were created, starting from different initial dates. Each member includes the 120-days-period from November 1st 1992 to March 31 1993. The soil moisture was initialized in equilibrium with the model atmosphere using the same method that was described in section 7.2. All other initial and boundary conditions are from ERA-40.

Ensemble W: Model with a fully land surface – atmosphere interaction. The soil moisture is calculated by the model at each time step and the only difference between members is the initialization date.

Ensemble S: The ensemble members are forced, at each time step, to maintain the same space-time varying series of top and deep soil moisture. The series is obtained from a previous simulation of the same period from which top and deep soil moisture had been saved every 30 minutes (model time step). Consequently, between the soil moisture and other components of the system, and in particular the water budget, there is only a one way interaction. The soil moisture influence on variables like precipitation, evapotranspiration and surface temperature, but these variables do not feed back upon soil moisture.

Since the initial dates and the lateral boundary forcings as well as the SST are the same for the two ensembles, the only difference between ensemble W and S is that

in W, there is fully interaction between soil moisture and the atmosphere, while in S, the soil moisture is a boundary condition and e.g. a day of heavy precipitation will not increase the soil water content.

8.2.2 Time period and time scales

Our study covers only the monsoon cycle of 1992–93. Previous studies (Fu et al. 1999; Collini et al. 2008) have suggested that the surface and dynamical processes of the SAMS act in the monsoon region independently of the large-scale conditions. However, the interannual variability modulates the frequency and intensity of synoptic systems and also the patterns of soil moisture anomalies (i.e. ideally this experiment should be repeated with different boundary forcing).

To examine the CS on a subseasonal but supra-synoptic scale, 6-days means were calculated for the period December 1 to February 28 for each ensemble. This gives a time series of 15 steps for each ensemble member from which CS was calculated for precipitation and evapotranspiration. It should be noticed that other choices of mean period (as 3,4,5 and 9 days) gave similar results in the location of hot spots.

The period DJF was chosen to be able to compare the results from other studies, such as Koster et al. (2006) that calculated CS for boreal summer (JJA) and Wang et al. (2007) that calculated CS for both boreal and austral summer. To reduce noise from high precipitation values, the CS was calculated from the natural logarithm of precipitation.

8.2.3 The ΔΩ index

The GLACE project defined CS as the difference between the similarity among the members of the ensembles S and W. The similarity of the variable X, Ω_X, is a measure of how similar the time series of the ensemble are. It represents the relative contribution of all boundary conditions on the variability of X. A strict mathematical interpretation of Ω can be found in Yamada et al. (2007).

The Ω index for any atmospheric variable X is:

$$\Omega_X = \frac{m\sigma_{X^\wedge}^2 - \sigma_X^2}{(m-1)\sigma_X^2} \qquad \text{Eq. 8.1}$$

where $\sigma^2_{X^\wedge}$ is the variance of the mean time series of all members of one ensemble, σ^2_X is the ensemble intermember variance which is obtained by calculating the variance among all time steps and ensemble members and *m* is the number of ensemble members. Ω_X is interpreted as the fraction of the variance of X that is explained by boundary conditions (the total variance depends on internal variability of the model and on boundary conditions). The similarity of X is 0 if there is no correlation among ensemble members and 1 if the time series of X are identical for all ensemble members. From this interpretation and from the fact that ensemble S is driven by prescribed soil moisture, it is expected that Ω will be larger for ensemble S in regions were the soil moisture explains some of the variance of the variable X. The CS ($\Delta\Omega_X$) between soil moisture and X is defined as the difference between the similarities of the two ensembles:

$$\mathbf{\Delta\Omega}_X = \mathbf{\Omega}_X(S) - \mathbf{\Omega}_X(W) \qquad \text{Eq. 8.2}$$

$\mathbf{\Delta\Omega}_X$ isolates the soil moisture boundary condition influence on the phase, amplitude and mean value of the timeseries of the variable X (Yamada et. al 2007).

8.2.4 The ΔΘ index

The ΔΘ index was proposed by Wang et al. (2007), using the same experimental design as described in 8.2.1, as an index that can be more useful for seasonal predictions, using soil moisture as a predictor. That is, the index should depend less on phase similarity than the ΔΩ index, and more on predictability of mean seasonal precipitation. The interpretation of predictability that will be used here is that regions with high $\Delta\Theta_X$ will show less seasonal mean spread of the variable X among the members of ensemble S than among members of ensemble W, since the members of S are forced by the same soil moisture field. The ΔΘ index is based on the intraensemble relative variance averaged across time:

$$\mathbf{\Theta}_X = \frac{1}{15}\sum_{j=1}^{15}\left\{\frac{1}{X_j^2}\left[\frac{1}{10}\sum_{i=1}^{10}(X_{ij} - \bar{X}_j)^2\right]\right\} \qquad \text{Eq. 8.3}$$

where the outer summation is over time steps of the period of study (in our case 15), and the inner summation is over number of ensemble members (in our case 10). $\bar{X}_j$ corresponds to the ensemble averaged value of X for time step j and X_{ij} corresponds to the value of ensemble member number i at time step j.

In regions of coupling between soil moisture and X, the variance should be higher for the W ensemble than for ensemble S. The fraction of the W interensemble variance that is explained by soil moisture – X coupling is the ΔΘ index:

$$\Delta\Theta_X = \frac{\Theta_X^W - \Theta_X^S}{\Theta_X^W} \qquad \text{Eq. 8.4}$$

8.3 Results

8.3.1 The chain soil moisture – evapotranspiration – precipitation using the ΔΩ index

Regions where the precipitation is governed highly by the boundary conditions have a high Ω_P. The influence of the SST and lateral boundary conditions results in high Ω_P(S) in the ITCZ region (The ITCZ is located between the equatorial Andes and the mouth of the Amazon River near the equator, figure 8.1) and in centraleastern Argentina where synoptic systems governs precipitation variance. In regions with low Ω_P, the precipitation variance is governed by model internal variability. In regions where soil moisture does not influence on rainfall, Ω_P(W) is almost equal to Ω_P(S) and $\Delta\Omega_P$ is close to zero. Only when Ω_P(S) is in part governed by soil moisture, $\Delta\Omega_P$ is positive (figure 8.2). The high values around the La Plata Basin, are a result of a high percentage of the boundary forcing coming from the soil moisture conditions. In the figure, negative values are masked with grey. Negative values occur in regions where the soil moisture does not influence on the precipitation and the similarity of the W ensemble is slightly higher than for the S ensemble.

High $\Delta\Omega_P$ can be a result of the feedback chain that connects soil moisture with precipitation through evapotranspiration. This feedback can be a local land surface influence on precipitation, when a soil moisture anomaly at one gridpoint generates an evapotranspiration anomaly that in its turn generates a rainfall anomaly. In this case, the

coupling between soil moisture and evapotranspiration ($\Delta\Omega_E$), is high at this gridpoint. It can also be a remote influence, when the moisture in the boundary layer is provided mainly by transport from upstream. In the calculations of CS, which are made grid point by grid point, it is impossible to separate these two processes.

A necessary, but not sufficient, condition for the local chain soil moisture – evapotranspiration – precipitation not to be "broken" is not only a high $\Delta\Omega_E$, but also a high variance of evapotranspiration (σ_E). This is because without a high variance of evapotranspiration, the evapotranspiration changes induced by soil moisture anomalies will not be sufficiently high to generate precipitation through direct processes (Guo et al. 2006). The CS between soil moisture and evapotranspiration, $\Delta\Omega_E$, and the product $\Delta\Omega_E*\sigma_E$ are shown in figures 8.3 and 8.4 respectively. The product is related to the soil moisture content. In figure 8.5 the product is binned by soil water availability (SWA), which is a variable that is calculated on basis of amount of top and deep soil moisture and on the soil properties, and has values between 0 (wilting point) and 1 (field capacity). $\Delta\Omega_E*\sigma_E$ has maximum values for small to intermediate values of SWA (0.2 – 0.4). For dry regions with low SWA, $\Delta\Omega_E$ is high since the atmosphere is dry and the evapotranspiration is not limited by high atmospheric moisture content. However, the σ_E is small, since the amounts of precipitation are small. For wet soils, the coupling between soil moisture and evapotranspiration is weak, since the evapotranspiration is limited by the high near surface humidity, and consequently the product $\Delta\Omega_E*\sigma_E$ is low.

Comparing the figures 8.3 and 8.4, the central La Plata Basin and northeastern Brazil have both high $\Delta\Omega_P$ and high $\Delta\Omega_E*\sigma_E$. In regions where $\Delta\Omega_P$ is low although the $\Delta\Omega_E*\sigma_E$ is high, as for example in Northwestern Argentina, the coupling between evapotranspiration and precipitation is low. This coupling can not be quantified directly through the experiments in the present study, but could only be calculated through performing two ensembles employing evapotranspiration (instead of soil moisture) as boundary conditions. However, through the present experiments, it is possible to identify grid points with low evapotranspiration – precipitation coupling roughly as points with high $\Delta\Omega_E*\sigma_E$ and low $\Delta\Omega_P$.

Conversely, there are areas with a weak coupling between soil moisture and evapotranspiration and high values of $\Delta\Omega_P$. This can be explained by the fact that evapotranspiration is a variable of a much higher local character than precipitation. As highlighted in the introduction, the coupling strength at each grid point is a result of the boundary forcing from the entire soil moisture field. Since the evapotranspiration at a

grid point, “A”, is a local process, the relative influence of the soil moisture of the surrounding area on evapotranspiration will be small in comparison to the influence of the soil moisture at A. In the case of precipitation, the contribution of the soil moisture of grid points around A could have a much higher influence through advection of moisture to A. One region where this happens is the hot spot of $\Delta\Omega_P$ around 20°S, 50°W, which is a region within the South Atlantic Convergence Zone (SACZ), where $\Delta\Omega_E * \sigma_E$ is low. This is a region of strong convergence of moisture, and the moisture could origin from soil moisture anomalies upstream.

8.3.2 The Θ index

The geographical distribution of the CS soil moisture – evapotranspiration calculated with the ΔΘ index ($\Delta\Theta_E$, figure 8.6) is similar to the $\Delta\Omega_E$ index. According to Wang et al. (2007) the advantage of the ΔΘ index compared to the ΔΩ index is that it expresses seasonal predictability to a higher degree than the ΔΩ index, while the ΔΩ index depends to a higher degree on phase similarity. Here, seasonal predictability is understood as small spread of the seasonal ensemble mean evapotranspiration, (the spread is measured by the standard deviation of the ensemble means, $\sigma_{DJF}(E)$). In a region with high $\Delta\Omega_E$, $\sigma_{DJF}(E)$ of ensemble S should be lower than for ensemble W, since the soil moisture in S is equal for all ensemble members. This definition of seasonal predictability is motivated by the practical use that knowledge of soil moisture could have for seasonal predictions over regions with large soil moisture – atmosphere coupling. The difference between $\sigma_{DJF}(E)$ of the two ensembles is displayed in figure 8.7. From a visual comparison of this figure with $\Delta\Theta_E$ (figure 8.6) and $\Delta\Omega_E$ (figure 8.3), it is clear that the ensemble W has a higher seasonal spread than S in regions with high $\Delta\Theta_E$ and $\Delta\Omega_E$, in this experiment, both indices indicate seasonal predictability.

The soil moisture – precipitation coupling, $\Delta\Theta_P$, in figure 8.8, shows a very different pattern than the $\Delta\Omega_P$, and is highly noisy. Furthermore, most grid points show negative values of $\Delta\Theta_P$. From Eq. 8.4, negative $\Delta\Theta_P$ is a consequence of Θ^S being larger than Θ^W. Examining Eq. 3, $\Theta^S > \Theta^W$ can imply that the variance of S is larger than the variance of W, as can occur as a result of internal variability at grid points where precipitation is not influenced by the forcing soil moisture field of ensemble S. Another situation that produces a negative $\Delta\Theta_P$ is when the $\bar{X}_j$:s of ensemble S are of less

magnitude than the $\bar{X}_j$:s of ensemble W. Since the $\bar{X}_j$:s correspond to the ensemble averaged value of X for time step j, this would indicate that the seasonal mean of ensemble S is of less magnitude than for ensemble W. Another property of the $\Delta\Theta$ index worth noting is that for grid points with negative (positive) $\Theta^W - \Theta^S$, the absolute values of $\Delta\Theta_E$ are higher (smaller) as a consequence of dividing with a smaller (higher) Θ^W. To give an illustration of how the temporal behavior of the precipitation can be at at grid points with different values of $\Delta\Theta_P$ and $\Delta\Omega_P$, one point with positive and one with negative $\Delta\Theta_P$ were randomly selected (35.5°S, 67°W with $\Delta\Theta_P$= 0.51 and 16.5°S, 55°W with $\Delta\Theta_P$= -0.52). Both grid points have low but positive $\Delta\Omega_P$ ($\Delta\Omega_P$= 0.066 and 0.086, respectively). The time series of both ensemble 6-days averaged precipitation are displayed in figure 8.9. In the case of the grid point of positive $\Delta\Theta_P$, and low but positive $\Delta\Omega_P$, there is not much difference between the phase correlation of the S and W time series. The maximum amplitude difference is higher in ensemble S, but on the other hand, only for a few of the members and for two out of fifteen time steps. The seasonal ensemble mean of S ($SEM_P(S)$) is slightly higher than $SEM_P(W)$ (2.37 and 2.22 respectively). In the case of the second grid point, it is more directly visible why $\Delta\Omega_P$ is positive – the time series of S is clearly more both phase and amplitude correlated than the W series. However, it seems like $\Delta\Theta_P$ is negative because of the lower $SEM_P(S)$ ($SEM_P(S)$= 6.50 and $SEM_P(W)$= 7.91). To confirm this, in figure 8.10a, $\Delta\Theta_P$ of all grid points are binned by $SEM_P(S) - SEM_P(W)$. The $\Delta\Theta_P$ index clearly depends on small seasonal mean precipitation differences between the ensembles. This could be seen as a deficiency of the $\Delta\Theta_P$ index of the present experiment, since small differences in seasonal mean precipitation between the two ensembles should not be important for the CS. For comparance, $\Delta\Omega_P$ is binned by $SEM_p(S) - SEM_p(W)$ in figure 8.10b, and it is clear that $\Delta\Omega_P$ is not sensitive to small differences in the seasonal mean precipitation. In this experiment the number of ensemble members was limited to 10, and it is possible that employing larger ensembles smooth out the differences in seasonal mean between ensemble S and W. For the present experiment with a limited ensemble, the $\Delta\Omega_P$ index was considered to be more appropriate to estimate the CS soil moisture – precipitation, and since its properties can be explained physically the index seems to be a useful measure.

8.3.3 Relationship between precipitation regime and Ω index

The interest in focusing on a possible relationship between land surface processes and extreme precipitation events is motivated by the following factors: (i) The strongest convective storms are often found over land in semiarid regions (Zipser et al. 2006); (ii) Analysis of the global models within the GLACE project by Guo et al. (2006) revealed that the coupling soil moisture – convective precipitation was higher than the coupling soil moisture – total precipitation; and (iii) Our results suggest a hot spot of strong coupling between soil moisture and both evapotranspiration and precipitation in southern La Plata Basin, a region characterized by high rainfall extremes associated with mesoscale convection (Velasco and Fritsch, 1987).

Here, $\Delta\Omega_E$ and $\Delta\Omega_P$ will be compared to the fraction of precipitation due to heavy precipitation events. The fraction is measured by calculating the 95th percentile of the wet days precipitation divided by the total seasonal precipitation. This extreme precipitation index (EPI, displayed for ensemble W in figure 8.11) is a measure of how important the severe precipitation events are in comparison to the total seasonal mean and contains some information on the precipitation regime. Severe rainfall, as represented by this index, has a rather different geographical distribution than mean total precipitation or conventional measures of convective activity (e.g. average outgoing longwave radiation). The rainiest parts of the regional monsoon in central South America have numerous events of strong rains but relatively few severe storms (i.e., EPI displays a minimum over this region). The main regions with high EPI are southeastern South America (southern La Plata Basin) and northwestern South America (Colombia and Venezuela). Interestingly, the first region coincides with the high coupling strength area for evapotranspiration (see $\Delta\Omega_E$ in figure 8.3). In contrast, the coupling strength over Colombia and Venezuela is very low (similarly, the arid South American west coast and centraleastern Argentina show up as regions with high EPI and low $\Delta\Omega_E$). This suggests that extreme precipitation events in northern South America are not influenced by feedbacks from the ground, but that heavy rainfall around the Rio de la Plata may be partly related to these processes.

In order to further explore the possible relation between soil moisture feedbacks and extreme precipitation, the extreme index calculated from ensembles S and W are compared (figure 8.12). Both ensembles give very similar results over most regions, except over areas of high EPI. Parts of northern South America and Centraleastern Argentina and the Pacific coast are characterized by a non-uniform and patchy

distribution of EPI(S) – EPI(W), further confirming that soil moisture feedbacks are not connected to extreme events in these regions.

Southeastern South America is a region with a well defined pattern of EPI(S) – EPI(W). The EPI is higher in ensemble W over the Uruguay's hot spot, an area with high $\Delta\Omega_P$ due to local evapotranspiration recycling. On the other hand, this index is higher in ensemble S over large areas of northern and central Argentina, a region with high $\Delta\Omega_E$ but low $\Delta\Omega_P$.

A fundamental question is whether we can understand conceptually why EPI(W) > EPI(S) over Uruguay and why EPI(W) < EPI(S) over parts of Argentina. Two main contrasting physical mechanisms may be invoked to explain such a difference. The feedback between soil moisture and the subsequent occurrence of convective rainfall may be either positive or negative (Taylor and Ellis, 2006; Alfieri et al., 2008). A positive feedback has been suggested by Eltahir (1998): high soil moisture values induce a decrease in the albedo and the Bowen ratio, thus favoring energy inflow from the soil surface and convective instability, and hence the triggering of convective rain. The fact that ensemble W, which has a complete soil moisture – atmosphere coupling, presents higher EPI at the hot spot suggests that a positive feedback is dominant over Uruguay. In contrast, a negative feedback has been proposed in Taylor and Ellis (2006) and Cook et al. (2006): surface fluxes from wet soils are associated with surface cooling and the possible stabilization of the planetary boundary layer, thereby leading to subsidence. In this case, convective initiation occurs preferentially over dry soils. This mechanism is plausible to be dominant over parts of Argentina where $\Delta\Omega_P$ coupling is weak but $\Delta\Omega_E$ coupling is high.

Both mechanisms may occur during the warm season leading to a complex local climatology in which the feedback between soil moisture and subsequent heavy precipitation occurrence is difficult to detect (Alfieri et al., 2008). Moreover, the sensitivity of convective initiation to soil moisture depends not only on surface processes. The stability of the layer into which the boundary layer is growing is considered to be important for determining the sign of the feedback (Ek and Mahrt, 1994). Other mechanisms for enhancement of mesoscale convective precipitation (Ruane and Roads, 2007) include (i) Land's evaporative potential and heat capacity allow for fast variations in atmospheric stability and convective available potential energy affecting mesoscale convection; and (ii) Sharp horizontal gradients in land

characteristics lead to more rapid intensifications and moderation of existing lower-frequency storms as they pass over the region.

These results only provide a first approach to the hypothesized relation between soil moisture and intense rainfall in southern La Plata Basin. Further diagnostics (e.g. diurnal cycle) with a larger sample size and using different models are required to confirm our results.

8.4 Conclusions

Process-based studies of regional scale features driving the climate system is an important component for interpreting climate models results and assessing the strengths and weaknesses of dynamical downscaling. However, the comprehension of the physical basis of simulated variability and changes is not always readily apparent given the complexity of the processes involved. Precipitation is generated through interactions of dynamical atmospheric advection, convergence, and lifting mechanisms, as well as thermodynamic processes such as moisture availability and thermal stability. Land surface conditions feed back on atmospheric conditions and in particular on precipitation through the partitioning of surface fluxes. In some geographic areas these feedbacks could be similar or stronger than other processes.

With this in mind, the impact of soil moisture conditions on rainfall generation was examinated through calculating the coupling strength between soil moisture and evapotranspiration and precipitation with a regional climate model over South America for the austral summer season. The study isolates the aspects related to the locally forced component of evapotranspiration and precipitation (that is, climate variability arising from the interactions with the continental surface) and constitutes a contribution towards process-based understanding of features driving the climate system at the regional scale.

The geographical distribution of precipitation coupling strength, $\Delta\Omega_P$, for South America reveals large regions with relatively weak or non-uniform random values while some main hot spots – regions with high $\Delta\Omega_P$ - could be identified. The main hot spot of strong coupling between land and both evapotranspiration and precipitation is located near the Rio de la Plata in South Eastern South America. The breakdown of the coupling mechanism into two segments—the link between soil moisture and evapotranspiration and the link between evapotranspiration and

precipitation—helps to identify some of the reasons for the geographical distribution of the hot spots. Evapotranspiration rates are sensitive to soil moisture in dry climates but not in wet climates where it is partially controlled by atmospheric demand. However, a strong coupling with precipitation benefits from high atmospheric moisture variability as found in wet climates but not in dry climates. In consequence, in transition zones between wet and dry conditions (like in parts of La Plata Basin), where evapotranspiration variations are suitably high but are still sensitive to soil moisture, the land states tend to have relatively strong impacts on precipitation. A part of the SACZ region was also found to be a mayor hot spot, however, this region has low evapotranspiration variation and a low $\Delta\Omega_E$ and could not be attributed to local recycling. Since this is a region of strong moisture convergence, the high $\Delta\Omega_P$ could be a result of moisture advection originated from soil moisture anomalies upstream. The magnitude of the $\Delta\Omega_P$ and $\Delta\Omega_E$ is comparable with the results of Koster et. al (2006) and Guo et. al (2006) for boreal summer using global models. Wang et. al (2007) calculated CS with a global model for DJF and their hot spots of $\Delta\Omega_P$ coincides with two hot spots found in this study, the La Plata Basin and Norteastern Brazil.

Another concern of this research was to relate the influence of the land–atmosphere coupling on the occurrence of extreme precipitation. For this purpose, an extreme precipitation index (EPI) is used, defined as the fraction of the total seasonal precipitation that is due to the 95th percentile of daily precipitation (similar to R95t in Frich et al., 2002). The regional spatial patterns of EPI are well correlated with the regions of strong coupling between soil moisture and evapotranspiration (as characterized by the diagnostic product $\Delta\Omega_E*\sigma_E$) over large areas of South Eastern South America. However, the feedback between soil moisture and subsequent heavy precipitation occurrence may be either positive or negative. Comparing the EPI for the S ensemble with that for the W ensemble, the latter is noticeably stronger over Uruguay, a region approximately coincident with the main hot spot area in southern La Plata Basin. The fact that extreme precipitation is enhanced in the hot spot if the model includes a complete land surface-atmosphere interaction suggests that a positive feedback is dominant over regions of high $\Delta\Omega_P$. On the contrary, extreme precipitation events tend to be favored when soil moisture is prescribed in the model (ensemble S) over parts of Argentina where $\Delta\Omega_E*\sigma_E$ coupling is high but $\Delta\Omega_P$ coupling is weak suggesting a negative feedback. The fact that the extreme rainfall events prefer regions of strong land-evapotranspiration coupling corroborates the previously noted connections

between convective precipitation and land surface moisture variations (Emori 1998, Guo et al. 2006).

Provided the existence of relatively strong soil-evapotranspiration-precipitation feedbacks in summer over areas of La Plata Basin some conclusion can be drawn concerning seasonal prediction and regional climate change assessment. First, initial soil moisture conditions provide "memory" to climate system's predictability and are more important than the initial atmospheric conditions at seasonal prediction time scales (e.g. Lawford et al., 2007). This needs to be especially recognized for the hot spots areas. Second, since not all land-atmosphere interactions are currently fully resolved in models and considering the non-linearities in the climate system, it is difficult to assess how these feedbacks may alter the downscaled climate projection for regions with high CS.

RCMs suffer relatively low skill in reproducing the daily precipitation intensity distributions over South Eastern South America (Menéndez et al., 2010). In general, precipitation falls too frequently but intensities are too light. The frequency of strong and heavy precipitation events is underestimated by models (including RCA3-E). This deficiency seems related to uncertainties in physics parameterizations. For example, convective parameterizations being too strongly dependent on non local driving mechanisms, lead to reduced mesoscale activity but longer periods of light precipitation (Ruane and Roads, 2007). As southern La Plata Basin is a region with relatively high CS, a realistic representation of the land-atmosphere interaction would be particularly critical. A complex combination of several factors is required for improving models' performance including proper land surface characterization, high resolution (both horizontal and vertical, the number of soil layers influence on the soil moisture memory which in turn affects the precipitation variability; Ruane and Roads, 2007) and the use of good-quality database for initializing and driving surface parameters (e.g., roughness length, vegetation fraction, leaf area index, albedo, rooting depth; Masson et al. 2003). These aspects affect models' feedbacks and deserve further assessment and development so that the land-precipitation coupling and the daily intensity distribution of precipitation can be simulated realistically in La Plata Basin. Such a skill is important to give confidence of the model-simulated climate sensitivity or climate change scenarios.

Finally some caveats on this study are as follows: We must caution against generalizing the results of this chapter as the experiments have been restricted to one

single regional model and one single season. The CS patterns for the NH evaluated with global models were very different among different models (Koster et al. 2004, 2006), suggesting that repeating our experiment with other RCMs could lead to different patterns over Southern America as well. Probably part of the intermodel variability in coupling patterns derived from global models was due to limited sampling of only one single season, which is also the case in this study. In order to address the realism of RCA3-E's coupling strength more simulations under different seasons are needed and, in addition, it would be useful to determine how it compares with other RCMs in this region.

9. Land surface parameterization ensemble

9.1 Introduction

There are several studies that confirm the importance of surface fluxes, and their partitioning, on atmospheric variables like cloud-base, cloud field and short- and long-wave radiation, vertical motion and precipitable water for tropical and sub-tropical South America (see section 1.4.3). Surface fluxes are highly dependent on the surface parameterization scheme and on parameters such as soil depth, leaf area index, albedo and emissitivity.

Erroneous surface forcing could be an important contribution to the poor results over South America, considering that the surface schemes of RCMs in general, and the surface scheme of RCA in particular, were developed for higher latitudes. In this chapter, an ensemble of surface parameterizations is developed and analyzed to quantify the importance of surface forcing for the climate.

The ensemble is partially based on the experience from replacing the land surface data employed by the original RCA3 version used over Europe, to data from Ecoclimap. By implementing Ecoclimap in RCA3, more realistic results of near surface temperature and monsoon precipitation were achieved (chapter 3) and in this ensemble, some of the changes introduced by Ecoclimap are isolated. Other ensemble members are based on the differences between the land surface scheme in RCA3-E and a newer version of RCA, RCA3.5. RCA3.5 was developed by Rossby Centre after the RCA3-E had been employed for this thesis and includes important changes in both the atmosphere and in the land surface scheme (Jones et al., 2009). Furthermore, the tests of soil depth and leaf area index are based on common values of these parameters employed by the regional models within CLARIS.

9.2 Methodology

For this study, ERA-Interim data were employed as initial and boundary conditions (Simmons et al. 2006). It was considered that 5 years simulations that included both phases of ENSO would be sufficient to capture major differences between ensemble members. The selection of period was based on observational and satellite data availability, as well as by the ERA-Interim period. Considering these restrictions,

the period January 1997 to December 2001 was chosen, with one year (1996) of spin up.

As a preparatory study, the sensitivities to model version, vertical levels and model domain were examined. This study has two motivations: a) to employ the model set up with best performance for the sensitivity studies, having in mind that more computational resources are needed for more vertical levels and for larger domains, and b) to compare these sensitivities to the sensitivity to surface physical parameterizations.

To evaluate the near surface temperature, the open land 2m temperature was employed instead of the total grid average 2m temperature. The motivation for this approach is that in forest areas, RCA simulates the 2m temperature within the forest, where the temperature is lower than for open land. Since observational data from CRU are from open land sites, the RCA open land temperature was considered to be more comparable to CRU data. To be able to realize this comparison RCA is forced to have at least 1% of open land in each grid box, overriding in some cases the vegetation data from Ecoclimap.

The results are presented on monthly and seasonal time scales and are compared to gridded observational data (CRU) and to the driving reanalysis data. The regions that were selected for analysis of annual cycles are the same that have been employed in previous chapters.

9.2.1 Sensitivity to model version and vertical levels

The model versions RCA3-E and RCA3.5 were compared. RCA3.5 was ran with standard 24 levels (used for this thesis work, see chapter 2) and with 40 levels. The motivation for testing sensitivity to vertical levels is that most precipitation in the tropical regions is convective and a higher vertical resolution could improve the triggering of convection (Druyan et al. 2006).

9.2.2 Sensitivity to domain

The standard model domain employed for this thesis work covers the whole South American continent, but to save computational resources, it does not include much of the adjacent Pacific and Atlantic oceans. Domain choice could be an important factor for simulated climate of the South American continent (e.g. Raucher et al. 2006). As has been pointed out earlier in this thesis, the inflow of trade winds from the Atlantic

is important for the climate of the tropical and subtropical regions of South America, and therefore a domain that extends over the Atlantic was chosen. To simulate the Hadley and Walker circulations over the Pacific with the regional model, a domain that extends over the Pacific was also selected. In figure 9.1 the standard domain, as well as the two new domains are shown. As will be shown in section 9.3.1, RCA3.5 with 40 vertical levels gave significantly better results than RCA3-E and RCA3.5 with 24 levels. Therefore this version was used for the domain tests.

9.2.3 Sensitivity to land surface parameterizations

The model set up for these experiments was based on the results of the previous tests. It was considered that RCA3.5 with 40 levels had an enough better performance than RCA3.5 with 24 levels to employ the 40 levels version in spite of longer integration time. The choice of domain was found to be insignificant and therefore the standard, smaller domain was chosen. In a previous study (chapter 3), an ensemble of atmospheric and surface parameterizations had been created with RCA3-E. One of the parameterization tests presented here was performed also with RCA3-E, to compare its influence on climate to the RCA3.5 version.

Standard versions of models

RCA3-E was presented in the previous chapters 2 and 3. For a description of RCA3.5 the reader is referred to (Jones et al. 2009). The characteristics of the land surface scheme of RCA3.5 important for this chapter are described in the following description of the ensemble members.

Rooting depth (2mSD)

The soil depth is set to a constant value of 2 meters over the whole continent, except for mountainous regions were it is set to 0.5 meters. The motivation for this ensemble member has been discussed in chapter 7.

Leaf Area Index dependent on Tsoil (LAI_T), high (LAI_H) and low (LAI_L)

In the standard version of RCA3.5 as well as in RCA3-E, the Leaf Area Index is given by a monthly database from Ecoclimap. In the ensemble member LAI_T, the LAI

from Ecoclimap is modulated by the soil temperature of the 4th soil layer (RCA employs 5 soil layers with respect to temperature).

Previous experience with RCA3-E has shown that the surface fluxes and the near surface temperature are sensitive to LAI in the Amazon region. The value of LAI in Amazonia in Ecoclimap is around 6 for all seasons. To create the ensemble members LAI high and low, the LAI of the CLARIS LPB regional models were examined. The model WRF had the lowest value of around 3.5 and PROMES the highest value of 9. Over the rest of the continent the examined models (RCA3, WRF, REMO and PROMES) coincide more or less. The two ensembles LAI_H and LAI_L are constructed by replacing the LAI values in the Amazon region with 9 and 3.5 respectively.

noFLake

The lake model FLake (Mironov, 2008, Samuelsson et al. 2009) has been incorporated in the RCA3.5 and RCA3-E versions. All inland water (natural lakes, manmade reservoirs and rivers) are modeled by FLake. For South America, a continent with sparse density of lakes in comparison to Euroasia, this should have largest effects for the two big river basins Amazon and La Plata. The ensemble member called noFLake replaces all continental water with land.

Root distribution percentual (PERC)

In this ensemble member a root distribution that is proportional to each soil moisture layers' contribution in percent to total depth was used. This distribution was used in RCA3-E, where the land surface scheme had two soil moisture layers, the top one being 7 cm deep and the deep one was determined by Ecoclimap at each grid point. RCA3.5 employs three layers with respect to soil moisture, the first (top) layer is 7 cm thick, the second one 21 cm, and the third deep layer is determined by the soil depth given by Ecoclimap.

Root distribution exponential without compensation for upper level dryness (NO_comp)

In RCA3.5 the root distribution is exponential, declining with depth. This is more realistic than a percentual root distribution due to observational studies (Henderson-Sellers and McGuffie 1987). When three layers of soil moisture together with exponential root distribution was employed, it was found that the upper soil layers

dried out fast and that during dry periods, the evapotranspiration was very low although the lowest soil moisture layer had a high soil water content. Observational studies show that when upper layers dry out, the plants increase their demand of water from deeper roots (Henderson-Sellers and McGuffie 1987). Therefore, the water demand of deep roots was implemented as a function of soil water content in upper layers. In this ensemble member, the root distribution is exponential but the water demand function of deep roots is desactivated.

Root distribution exponential with linear compensation for upper level dryness (comp_LIN)

RCA3.5 uses a parabolic function to control the water demand of deep roots by the soil water content of upper layers. In this ensemble member a linear function is applied, which makes the connection between upper level dryness and deep root water demand stronger.

Direct and diffuse forest radiation treated equally (FR)

In the RCA3-E, as well as in this ensemble member, no distinction is made between how short- and long-wave radiation penetrates through the forest canopy layer. In RCA3.5 the fraction of diffuse/direct solar radiation is described as a function of sun elevation. This is combined with cloud cover and separate formulas for the sky view factor for short- and long-wave radiation, $\chi_{LW} = \exp(-0.5 * LAI)$, $\chi_{SW} = \exp(-0.5\ LAI(4-3\cos))$.

Table 9.1 shows the 12 members of the ensemble.

Parameterization	Short name	RCA3-E	RCA3.5 40 levels
Standard version	SV	X	X
Rooting depth set to 2 meters	2mSD	X	X
Leaf Area Index dependent on Tsoil	LAI_T		X
Leaf Area Index high	LAI_H		X
Leaf Area Index low	LAI_L		X
Without the lake model FLake	noFLake		X
Root distribution percentual	PERC		X
Root distribution exponential without compensation for top soil dryness	NO_comp		X
Root distribution exponential with linear compensation for top soil dryness	comp_LIN		X
Direct and diffuse forest radiation treated equally	FR		X

Table 9.1: Summary of sensitivity experiments

9.3 Results

9.3.1 Sensitivity to model version, vertical levels and domain

The results of these experiments will not be presented in detail, since their main purpose was to select the model set up with best performance for the surface physics parameterization ensemble. The differences between the performance of RCA3-E and RCA3.5 are very large both in near surface temperature and in precipitation. All the selected regions except the Southern Andes region have problems with large negative or positive temperature biases during different seasons of the year in RCA3-E. These biases are mitigated or eliminated with the new model version. In some cases the two RCA3.5 simulations with different numbers of vertical levels are very similar, but in some cases the 40-levels version has a better representation of the annual cycle (figure 9.2). To further illustrate the differences between the three simulations, the temperature

biases of the SON season, for which RCA3-E have the largest biases, are displayed as maps in figure 9.3.

With respect to precipitation, RCA3-E has problems with dry biases for many regions, in particular in Southern Amazonia and the northern La Plata region where the bias is present all through the year and in the La Plata basin region for the winter season. Figure 9.4 shows the difference between the simulations: the biases are corrected in Southern Amazon region with the RCA3.5 version, but in the two La Plata regions a large winter bias is still present. Precipitation during summer and spring are better represented in the 40 levels version. This is probably due to a more realistic spatial and temporal triggering of the convection since the thermal and moist profiles are better resolved.

The different domain size did not have any significant effect on the results and figures will not be displayed here.

As a conclusion of these experiments, the RCA3.5 version with 40 vertical levels and the standard domain were chosen for the physics parameterizations studies.

9.3.2 Sensitivity to land surface parameterizations

It was found that the model was not sensitive to the parameterization changes in the members LAI_T, noFLake and FR. The results of these three members will therefore not be displayed here, since they are not significantly different from the standard RCA3.5 member.

The two RCA3-E ensemble members are easily distinguished in figure 9.5 of open land temperature annual cycles. Comparing the RCA3-E and RCA3-E/2mSD with the RCA3.5 and RCA3.5/2mSD, it is evident that RCA3-E is more sensitive to the soil depth than RCA3.5. This is probably in greatest part because of the differences in the land surface schemes explained above, although differences in the two models' atmospheres, such as the cloud cover and convection parameterizations could enhance the differences through feedbacks with the surface.

In the RCA3.5 ensemble, the spread of monthly open land temperature differs among regions and months, but all regions except for NeB and SA have a maximum spread of temperature of 1 – 1,5 degrees. The spring season shows the largest spread in most of the regions and seasonal maps of biases of open land temperature for all individual ensemble members during SON are therefore shown in figure 9.6. The

members 2mSD, LAI_L and NO_comp show larger warm biases than the standard version. In 2mSD and NO_comp this is due to dryer soil. In 2mSD the soil is shallower and dries out faster in the Amazon region. In NO_comp, the top soil layers dries out and the water from the lower layer does not reach the atmosphere. In the case of LAI_L, the warm bias is due to the lower transpiration capacity of the leaves with LAI=3,5 instead of 6. In all three members a smaller part of the surface energy is converted to latent heat flux and a larger part to sensible heat flux, generating a higher temperature. As an example of this, the sensible heat flux and the soil water availability for the SAmz region is presented in figure 9.7. In 2mSD, the SWA is lower than for all other RCA3.5 members, while for LAI_L and NO_comp it is slightly higher, since the water is not available for evapotranspiration. This generates larger sensible heat fluxes for the three members. The other three RCA3.5 members mitigate the RCA3.5 positive bias during SON. In all these members this is due to a higher capacity of the vegetation to transpire. In LAI_H because of the higher area of the leaves, in PERC, the deepest soil layer has more roots that can extract deep soil water, and in comp_LIN, the vegetation demands more water from the lowest soil moisture layer when the top soil layers are dried out. The soil water availability is therefore lower for these three members than in the reference member RCA3.5 (figure 9.7 b)

The annual cycles of precipitation are shown in figure 9.8. The two RCA3-E members distinguish by producing dry biases for many regions and seasons. This bias is, as was also shown in section 9.3.1 mitigated or absent in the RCA3.5 version. The spread among the RCA3.5 members is largest in the rainy seasons, for TR in JJA and for SAmz, EB, NWASB, NLPB during the monsoon (November to March), and in LPB in JFM. Particularly for the TR region, it is clear that the members with lower evapotranspiration and higher open land temperature are dryer than the members with higher evapotranspiration during JJA. This indicates a coupling between the evapotranspiration and the precipitation. As have been mentioned in chapter 8, this can be due to both local evaporation recycling and to boundary layer processes, since a wetter boundary layer is more unstable and convection is facilitated.

In figure 9.7 b, the soil water availability in the RCA3-E and RCA3.5 ensemble members are shown for the SAmz region. In this region, the precipitation is higher all year around in RCA3.5 and it is therefore not surprising that the SWA is higher in RCA3.5. However, in the La Plata region (annual cycle of SWA shown in figure 9.9) the winter precipitation bias prevails in the RCA3.5 version, and the reason for the

higher soil moisture can therefore not only be higher precipitation, but the evapotranspiration is also lower in RCA3.5 than in RCA3-E (figure 9.10). An important implication of the soil maintaining more humidity is the mitigation of the warm biases in these regions, especially during spring (see figures 9.5 and 9.9). One of the reasons for the higher soil water content is the changes in the soil and root parameterizations from the RCA3-E to the RCA3.5 version. The land surface scheme with three layers for soil moisture and an exponential root distribution maintains the moisture in the ground. Furthermore, in the RCA3.5 version, another parameterization for cloud cover is used, that implicates a cloud cover fraction that is higher and closer to satellite data (International Satellite Cloud Climatology Project, ISCCP) and to CRU data over this region. The cloud cover annual biases with respect to ISCCP and CRU in RCA3-E and RCA3.5 are shown in figure 9.11. The larger fraction of the sky covered by clouds in RCA3.5 restricts the land surface evaporation.

9.4 Conclusions and discussion

The improved performance of RCA3.5 in comparison to RCA3-E has been demonstrated. Both the atmosphere and the land surface scheme are substantially different for the two model versions, and are out of scope of this chapter to explain. However some conclusions could be drawn from the results of the land surface parameterization ensemble. The mitigated open land temperature bias in the La Plata region has to do with both a higher capacity of the land surface scheme of RCA3.5 to retain soil moisture, and to the changed cloud cover parameterization. Over other regions the more realistic open land temperature can be attributed to a better precipitation annual cycle. The exponential instead of percentual root distribution in RCA3.5 generated a dryer top soil layer due to more roots in the upper layer. This is compensated with a function that links the soil water content in the upper layer to the plant water demand in the lowers soil layer.

The model performance is improved, especially over the Amazon region, when the vertical levels are increased from 24 to 40. This is probably related to a more realistic spatial and temporal triggering of convection, due to a better resolved thermal and humidity vertical profile.

The model is not sensitive to changes in lateral borders location over ocean. Although one of the objectives of this thesis is to improve the RCA climate

characteristics over South America, this result is encouraging for two reasons. If the location of borders over oceans would produce large differences in the model performance, this would implicate a more unstable model and be a motivation to try to optimize the location of the borders. Furthermore, for computational resources reasons, this result implicates that the smaller domain can be used for future RCA experiments over South America, such as computational costly climate change experiments.

The land surface parameterization ensemble showed that RCA3-E is more sensitive to changes in soil depth than RCA3.5. Other studies with changed LAI e.g. indicates that RCA3-E is more sensitive to land surface parameterizations in general (results were not shown here). A possible reason for this is that the soil is much dryer in RCA3-E, while in RCA3.5 the moisture content is close to saturation (as an example of this, see figures 9.7 b and 9.10), and the evapotranspiration is closer to the potential evapotranspration in all ensemble members.

The RCA3.5 ensemble shows a maximum monthly scale sensitivity of open land temperature of 1 – 1,5 degrees. The sensitivity of precipitation to the ensemble is more region dependent, and can be up to 20% of total rain for the TR region during the rainy season, while for other regions like the SA and the La Plata regions, where the precipitation is more governed by incoming moisture from ocean and by synoptic variability, the model is much less sensitive. Some regions, and in particular the TR region, show a possible relation between the evaporation sensitivity and the precipitation sensitivity.

The three ensemble members that showed mitigated temperature biases in comparison to the standard RCA3.5 version were LAI_H, PERC and comp_LIN. This is explained by the fact that all these three ensemble members allow a higher evapotranspiration through different mechanisms; LAI_H because of the higher area of the leaves, PERC because the deepest soil layer has more roots that can extract deep soil water, and comp_LIN because the vegetation demands more water from the lowest soil moisture layer when the top soil layers are dried out. The PERC member is less physically correct than the standard RCA3.5 version, but the LAI_H and comp_LIN parameterizations could be considered for further experiments with RCA over South America.

10. Summary and Outlook

10.1 Summary of main conclusions

The principal objective of this thesis was to contribute to the understanding of the interactions between the soil moisture and the atmosphere during the South American monsoon. The tool for studying these interactions was a regional climate model, RCA, which was employed for South America for the first time for the purpose of this thesis. Therefore, an important part of the thesis was to improve the model performance over the continent as well as evaluating the model climate. The chapters 3-5 are dedicated to this preparatory work. In chapter 3, the model development that was carried out before going on with further work was presented. The official version of RCA, RCA3, developed for European high latitudes, had a very poor performance over South America over large parts of the continent. The surface database Ecoclimap was incorporated in the model and tunings were made to the convection and microphysics scheme. A 12-members ensemble of two years with different parameterizations was carried out, and on basis of the evaluation of the ensemble, the version used for further thesis work was selected, called RCA3-E.

In chapter 4, the internal variability was evaluated with the purpose of having a qualitative measure of the significance of the following sensitivity experiments. The methodology for calculating the internal variability was adapted from a previous study on the internal variability of RCA3 over Europe for comparison. This method was based on monthly means of an ensemble of simulations, which suited the following analysis of monthly – to – seasonal means of the thesis well. The internal variability was found to be very high in comparison to the results for Europe, which is probably the consequence of i) the model domain was larger over South America, ii) 10 ensemble members were employed over South America, and 5 over Europe, iii) the precipitation in large parts of South America is governed by convection and the high precipitation values, iv) the soil dryness in some regions of South America could increase varibility since a dry surface responds more rapidly to e.g. small diferences among the ensemble members in radiation and cloudiness, than a humid surface.

The evaluation of a 20-year long simulation with RCA3-E forced and initialized by ERA-40 was presented in chapter 5. The soil moisture spin up was examined to have a benchmark for this and the following chapters. The seasonal

precipitation patterns are quite well represented by the model, but the intensities are overestimated in regions/seasons of heavy rainfall. The winter dry biases over La Plata Region is related to deficient moisture transport to the region, and causes important soil dryness which produces positive biases of near surface temperature, especially during spring. Soil moisture content and temperature anomalies are highly (negatively) correlated for most regions. The conclusions of this chapter are very useful when evaluating the results of the following chapters. For example, the soil moisture anomalies that are introduced in Amazonia and La Plata Basin during winter persist during the onset phase of the monsoon. This chapter also presents some results from a coordinated experiment within the context of CLARIS, where the period 1991-2000 was simulated by three regional models (RCA3-E included) and one stretched grid global model. The models have quite similar seasonal mean simulated precipitation and the ensemble not representing the climate better than the best individual model, while the ensemble temperature is closer to observations than any individual model, due to models having opposite biases. An important caution is that the model, due to the lack of observations, could not be evaluated against observational data on surface fluxes, which is of great importance when studying the land-atmosphere interactions. Therefore, in the following chapters, it is assumed that RCA3-E represents the latent and sensible fluxes well, although this assumption needs to be confirmed by comparison to observational data when those are available.

The following three chapters are dedicated to three different approaches to study the interaction soil moisture – atmosphere during the SAMS. In chapter 6, the influence of an anomalously dry or wet land surface in late winter on the SAMS development is discussed through the results of two 5-member ensembles initialized in late July. During the first months of simulation, the difference in evaporative fraction of the total heat flux between the ensembles (DRY has a larger fraction of sensible heat flux, and WET a larger fraction of latent heat flux), produces large differences in air column temperature over central Amazonia. In ensemble DRY, this temperature difference brought in stronger Atlantic trade winds over the northern part of the continent that were blocked and turned anti-clockwise to the south by the Andes Mountains. Moisture convergence for dry initial conditions was therefore larger than for wet east of the northern Andes and in southern Amazonia, producing more rainfall over these regions during spring. During the mature phase of the monsoon, precipitation was stronger in the wet ensemble than in the dry one in central Amazonia. Because no difference was observed

in moisture convergence in this region among the two ensembles, and since the initial soil moisture anomaly persists in this region, this is attributed to local precipitation recycling. This was further confirmed by an analysis of daily precipitation frequency distributions. The results suggest that the initial winter soil moisture conditions feed back upon the SAMS during the warm months, not only over Amazonia but in subtropical South America as well.

An ensemble of simulations which includes spatially varying soil depth was compared to an ensemble with a constant soil depth of 2 m in chapter 7. The spring and summer seasons were studied, including the onset and mature phases of the monsoon. The study was motivated by that fact that the soil depth of tropical forest that cover large areas of northern South America are increased to 8 m with the incorporation of Ecoclimap in the model, and that previous works suggest the importance of soil depth and deep rooted vegetation on the climate system. In general, the role of soil depth was less critical than expected, and did not have any mayor impacts on seasonal precipitation. However, on a monthly scale the analysis showed that in some regions the alteration of precipitation due to a shallow soil is significant.

In chapter 8, the coupling strength (CS) between soil moisture and precipitation and evapotranspiration during the mature SAMS is examined with a methodology that isolates the soil moisture influence on these variables from the strong impact of precipitation anomalies on soil moisture anomalies. Two ensembles of ten members each were compiled; the ensemble W has full soil moisture – atmosphere coupling, while in the ensembe S soil moisture is a boundary condition. Two indices designed to measure the CS were calculated, called the $\Delta\Omega$ and the $\Delta\Theta$ indices. Regions of intermediate values of soil water content are most likely to have strong soil moisture – evapotranspiration CS ($\Delta\Omega_E$, or $\Delta\Theta_E$) since the evapotranspiration are not limited by the near surface atmospheric moisture content. To have strong soil moisture – precipitation CS $\Delta\Omega_P$ it is also favorable with high evapotranspiration variability (σ_E). The coupling between soil moisture and evapotranspiration ($\Delta\Omega_E$) was found to be connected to the coupling between soil moisture and precipitation ($\Delta\Omega_P$) in some regions where the product $\Delta\Omega_E*\sigma_E$ is high, as a result of direct evapotranspiration recycling. Through this mechanism, parts of the La Plata Basin and northeastern Brazil have a strong $\Delta\Omega_P$. However, the condition high $\Delta\Omega_E*\sigma_E$ is not always necessary, since atmospheric moisture can be advected to the region where it precipitates, while the $\Delta\Omega_E$ is due to much more local process. Part of the SACZ region was identified as a region where the

$\Delta\Omega_E*\sigma_E$ is low and the $\Delta\Omega_P$ is high, and this was attributed to advective mechanisms. Finally, points with high $\Delta\Omega_E*\sigma_E$ but low $\Delta\Omega_P$ are explained by the fact that the evapotranspiration – precipitation coupling is weak in these regions. The $\Delta\Theta_E$ was found to be similar to the $\Delta\Omega_E$, and the product $\Delta\Theta_E*\sigma_E$ has a similar relation to soil water availability as the product $\Delta\Omega_E*\sigma_E$. However, the soil moisture - precipitation coupling $\Delta\Theta_P$ was found to be highly noisy and the continental field showed large regions of negative coupling. Through an examination of the equations to calculate $\Delta\Theta$, it was concluded that for this particular experiment, the index has a strong dependence on the seasonal ensemble precipitation mean difference between the two ensembles S and W. The other index, $\Delta\Omega_P$ is independent on this difference, and it was concluded that the $\Delta\Omega_P$ index is therefore a more appropriate measure of coupling strength in these experiments.

Another concern was to relate the influence of the land–atmosphere coupling on the occurrence of extreme precipitation. For this purpose, an extreme precipitation index (EPI) is used, defined as the fraction of the total seasonal precipitation that is due to the 95^{th} percentile of daily precipitation. The regional spatial patterns of EPI are well correlated with the regions of strong coupling between soil moisture and evapotranspiration (as characterized by the diagnostic product $\Delta\Omega_E*\sigma_E$) over large areas of South Eastern South America. However, the feedback between soil moisture and subsequent heavy precipitation occurrence may be either positive or negative. Comparing the EPI for the S ensemble with that for the W ensemble, the latter is noticeably stronger over Uruguay, a region approximately coincident with the main hot spot area in southern La Plata Basin. The fact that extreme precipitation is enhanced in the hot spot if the model includes a complete land surface-atmosphere interaction suggests that a positive feedback is dominant over regions of high $\Delta\Omega_P$. On the contrary, extreme precipitation events tend to be favored when soil moisture is prescribed in the model (ensemble S) over parts of Argentina where $\Delta\Omega_E*\sigma_E$ coupling is high but $\Delta\Omega_P$ coupling is weak suggesting a negative feedback. The fact that the extreme rainfall events prefer regions of strong land-evapotranspiration coupling corroborates the previously noted connections between convective precipitation and land surface moisture variations (Emori 1998, Guo et al. 2006).

Finally, in chapter 9, the influence of land surface parameterizations on simulated climate was examined through an ensemble of 12 members. This experiment was carried out in 2009, when an updated version of RCA3 – RCA3.5 was available.

The first part of the chapter discusses the differences between RCA3-E and RCA3.5 as well as the difference between RCA3.5 with 24 or 40 vertical levels, concluding that RCA3.5 with 40 levels is substantially more coherent in its representation of the South American climate than the RCA3-E version. Although some important biases persists in RCA3.5, such as the negative precipitation bias in the La Plata Basin, this bias does not produce warm spring biases since the soil in RCA3.5 does not dry out. This has to do with both a higher capacity of the land surface scheme of RCA3.5 to retain soil moisture, and to the changed cloud cover parameterization. Over other regions the more realistic open land temperature can be attributed to a better precipitation annual cycle. The influence of using larger domains – one extending over the Atlantic while the other extending over the Pacific – was also examined, and it was concluded that the domain size did not affect the simulated climate. The sensitivity to land surface parameterizations of RCA3.5 was found to have a maximum in SON, with a spread among members of around 1.5°C. It is important to note here that the land surface parameterizations that were chosen for this study are based on values of parameters that are in use for regional climate models within CLARIS. The ensemble was less sensitive to precipitation, although the tropical region was sensitive during JJA, which was attributed to a coupling between evapotranspiration and precipitation. Three of the ensemble members showed mitigated temperature biases in comparison to the standard RCA3.5 version. This is explained by the fact that all these three ensemble members allow a higher evapotranspiration, through different mechanisms. One of the ensemble members was considered as physically incorrect, but the other two could be used for further work with RCA over South America.

RCMs suffer relatively low skill in reproducing the daily precipitation intensity distributions over South Eastern South America (Menéndez et al, 2010). In general, precipitation falls too frequently but intensities are too light. The frequency of strong and heavy precipitation events is underestimated by models (including RCA3-E). This deficiency seems related to uncertainties in physics parameterizations. For example, convective parameterizations being too strongly dependent on non local driving mechanisms, lead to reduced mesoscale activity but longer periods of light precipitation (Ruane and Roads, 2007). As southern La Plata Basin is a region with relatively high CS, a simulation of the regional energy and water cycles would also be particularly critical to a realistic representation of the land-atmosphere interaction. A complex combination of several factors is required for improving models' performance including

proper land surface characterization, high resolution (both horizontal and vertical, the number of soil layers influence on the soil moisture memory which in turn affects the precipitation variability (Ruane and Roads, 2007), and the use of good-quality database for initializing and driving surface parameters (e.g., roughness length, vegetation fraction, leaf area index, albedo, rooting depth; Masson et al. 2003). These aspects influence on models' feedbacks and deserve further assessment and development so that the land-precipitation coupling and the daily intensity distribution of precipitation can be simulated realistically in La Plata Basin. Such a skill is important to give confidence of the model-simulated climate sensitivity or climate change scenarios.

10.2 Outlook and further work

During this thesis work, the Swedish Rossby Centre Regional Atmospheric model was evaluated and developed in collaboration with Rossby Centre. The latest model version RCA3.5 has a substantially more satisfactory representation of the characteristics of the South American climate in comparison to both the version available at the beginning of the collaboration (RCA3) and to the version employed for this thesis (RCA3-E). Through the collaboration, Rossby Centre is a partner of CLARIS LPB, and will participate in the coordinated downscaling of South American present and future climate (www-claris-eu.org). These experiments focus on the hydroclimate of the La Plata Basin and experiments to identify regions of strong land surface – atmosphere coupling for the region will also be realized.

This thesis focalized on the soil moisture –atmosphere coupling during the SAMS, and in particular during its mature phase (DJF). This season was chosen for the reasons: i) the availability of results for the northern hemisphere for the boreal summer and for austral summer, and ii) the performance of RCA3-E precipitation over the La Plata Basin was reasonably good for this season.

However, recent studies (see references in chapter 6) have proposed that the land surface interactions are more important for the developing phase of the monsoon (SON) than for the mature phase, when large scale circulation is relatively more important for the monsoon precipitation.

Since the model version RCA3.5 has a more realistic land surface scheme and better surface climate for SON than RCA3-E, it would be interesting to employ RCA3.5 to identify hot spots of soil moisture – precipitation coupling during austral spring for

the la Plata Basin. It would also be important to analyze the present and future climate simulations projected within CLARIS with focus on the identified regions of high coupling.

References

Aceituno, P., 1988: On the functioning of the Southern Oscillation in the South American sector. Part I: Surface climate. Mon. Wea. Rev., 116, 505–524.

Aide T.M., H. R. Grau, 2004: Globalization, Migration, and Latin American Ecosystems. Science, 305, 1915-1916.

Albrecht, B.A., 1981. Parameterization of trade-cumulus cloud amounts. J. Atmos. Sci., 38, 97-105.

Alexandru A., R. de Elia, R. Laprise 2007: Internal Variability in Regional Climate Downscaling at the Seasonal Scale. Mon. Wea. Rev., 135: 3221–3238.

Alfieri, L., P. Claps, P. D'Odorico, F. Laio, and T.M. Over, 2008: An analysis of the soil moisture feedback on convective and stratiform precipitation. J. Hydrometeor., 8, 280-291.

Anderson C. J., R. W. Arritt, E. S. Takle, Z. Pan, W. J. Gutowski Jr., F. O. Otieno, R. da Silva, D. Caya, J. H. Christensen, D. Lüthi, M.l A. Gaertner, C. Gallardo, F. Giorgi, S.-Y. Hong, C. Jones, H.-M. H. Juang, J. J. Katzfey, W. M. Lapenta, R. Laprise, J. W. Larson, G. E. Liston, J. L. McGregor, R. A. Pielke Sr., J. O. Roads, and J. A. Taylor, 2003: Hydrological Processes in Regional Climate Model Simulations of the Central United States Flood of June–July 1993. ***J. of Hydromet.,*** 4, 584–598.

Anthes, R. A., Y. H. Kuo, E. Y. Hsie, S. Low-Nam, and T. W. Bettge, 1989: Estimation of episodic and climatological skill and uncertaintly in regional numerical models. Quart. J. Roy. Meteor. Soc., 115, 763–806.

Avissar R., D. Werth, 2005: Global hydroclimatological teleconnections resulting from tropical deforestation. ***J. of Hydromet.,*** 6: 134–145.

Berbery, E. H., and E. Collini, 2000: Springtime precipitation and water vapor flux convergence over Southeastern South America. Mon. Wea. Rev., 128, 1328–1346.

Berbery, E. H. and V. R. Barros, 2002: The hydrologic cycle of the La Plata basin in South America *J. Hydromet.,* **3**, 630-645

Betts, A. K., and P. Viterbo, 2005: Land-surface, boundary layer, and cloud-field coupling over the southwestern Amazon in ERA-40, J. Geophys. Res., 110, D14108, doi:10.1029/2004JD005702.

Bony S, Emanuel KA (2001) A parameterization of the cloudiness associated with cumulus convection; evaluation using TOGA-COARE data. J Atmos Sci 58(21):3158–3183.

Boone A., F. Habets, J. Noilhan, D. Clark, P. Dirmeyer, S. Fox, Y. Gusev, I. Haddeland, R. Koster, D. Lohmann, S. Mahanama, K. Mitchell, O. Nasonova, G.-Y. Niu, A. Pitman, J. Polcher, A. B. Shmakin, K. Tanaka, B. van den Hurk, S. Vérant, D. Verseghy, P. Viterbo, and Z.-L. Yang, 2004: The Rhône-Aggregation Land Surface Scheme Intercomparison Project: An Overview. J. Clim., 17: 187–208

Boulanger J.-P., G. Brasseur, A. Carril, M. Castro, N. Degallier, C. Ereño, H. Le Treut, J. Marengo, C. Menéndez, M. Nuñez, O. Penalba, A. Rolla, M. Rusticucci, R. Terra, 2009: The

European CLARIS Project: A Europe-South America Network for Climate Change Assessment and Impact Studies. Accepted for publication in Climatic Change.

Branstator, G., 1983: Horizontal energy propagation in a barotropic atmosphere with meridional and zonal structure, J. Atmos. Sci.,40, 1689-1708.

Castro C. L., R. A. Pielke Sr., and G. Leoncini, 2005: Dynamical downscaling: Assessment of value retained and added using the Regional Atmospheric Modeling System (RAMS). J. Geophys. Res., 110, D05108, doi:10.1029/2004JD004721

Caya, D., and S. Biner, 2004: Internal variability of RCM simulations over an annual cycle. Climate Dyn., 22, 33–46.

Champeaux J.L., V. Masson, F. Chauvin, 2005: ECOCLIMAP: a global database of land surface parameters at 1 km resolution. Met. Appl., 12, 29-32.

Chen C., W.R., Cotton, 1987: The Physics of the Marine Stratocumulus-Capped Mixed Layer, J. Atmos. Sci,. 44, 2951–2977.

Christensen, O. B., M. A. Gaertner, J. A. Prego, and J. Polcher, 2001: Internal variability of regional climate models. Climate Dyn., 17, 875–887.

Christensen, J.H., T. Carter, F. Giorgi, 2002: PRUDENCE Employs New Methods to Assess European Climate Change, EOS, Vol. 83, p. 147.

Christensen, J.H., Carter, T.R., Rummukainen M., and Amanatidis, G. 2007. Evaluating the performance and utility of climate models: the PRUDENCE project. Climatic Change, Vol 81. doi:10.1007/s10584-006-9211-6.

Collini E.A., E.H. Berbery, V.R. Barros, M.E. Pyle, 2008: How does Soil Moisture Influence the Early Stages of the South American Monsoon? J. Clim., 2, 195–213

Cook, B. I., G. Bonan, and S. Levis, 2006: Soil moisture feedbacks to precipitation in southern Africa. J. Climate, 19, 4198–4206.

Costa, M.H., J.A. Foley, 2000: Combined effects of deforestation and doubled atmospheric CO2 concentrations on the climate of Amazonia. J. Clim., 13:35–58

Cuxart, J., Bougeault, Ph. and Redelsperger, J-L., 2000. A turbulences scheme allowing for mesoscale and large eddy simulations. Quart. J. Roy. Meteor. Soc., 126, 1-30.

Davies, H.C., 1976: A lateral boundary formulation for multi-level prediction models. Quart. J. Roy. Meteor. Soc., 102, 405–418.

Denis, B., R. Laprise, D. Caya, and J. Côté, 2002: Downscaling ability of one-way nested regional climate models: The big-brother experiments. Climate Dyn., 18, 627–646.

Dickinson, R.E., and A. Henderson-Sellers, 1988: Modelling tropical deforestration: A study of GCM land-surface parameterizations. Quart. J Roy. Meteor. Soc., 114, 439-462.

Dickinson, R. E., R. M. Errico, F. Giorgi, and G. T. Bates, 1989: A regional climate model for the western US. Climatic Change, 15, 383-422.

Dirmeyer P.A, 2003: The Role of the Land Surface Background State in Climate Predictability ***J. of Hydromet.,*** 4, 599–610

Dirmeyer P. A., R. D. Koster, and Z. Guo, 2006: Do Global Models Properly Represent the Feedback between Land and Atmosphere? ***J. of Hydromet***., 7, 1177–1198

Dirmeyer P. A. and L. K. Brubaker, 2007: Characterization of the Global Hydrologic Cycle from a Back-Trajectory Analysis of Atmospheric Water Vapor. ***J. of Hydromet***., 8, 20–37.

Druyan L. M., M. Fulakeza, P. Lonergan, 2006: The impact of vertical resolution on regional model simulation of the west African summer monsoon, Intern. J. Clim., vol. 28, issue 10, pp. 1293-1314

Ducoudre N, Laval K, Perrier A (1993) SECHIBA, a new set of parameterizations of the hydrologic exchanges at the land-atmosphere interface within the LMD atmospheric general circulation model. J Clim 6:248-273.

Dümenil L, Todini E (1992) A rainfall–runoff scheme for use in the Hamburg climate model. In: O'Kane JP (ed) Advances in theoretical hydrology, EGS series of hydrological sciences 1, Elsevier pp 129–157

Ek, M., and L. Mahrt, 1994: Daytime evolution of relative humidity at the boundary layer top, Mon. Weather Rev., 122, 2709-2721.

Eltahir, E. A. B., and R. L. Bras, 1994: Precipitation recycling in the Amazon basin Quart. J. Roy. Meteor. Soc., 120, 861–880.

Eltahir, E. A. B., and R. L. Bras, 1996: Precipitation recycling. *Rev. Geophys.,* **34,** 367–378.
Emanuel KA (1993) A scheme for representing cumulus convection in large-scale models. J Atmos Sci 48:2313-2335.

Eltahir, E.A.B., 1998: A soil moisture-rainfall feedback mechanism. 1. Theory and observations. Water Resour. Res., 34**,** 765–776.

Emori, S. 1998. The interaction of cumulus convection with soil moisture distribution: An idealized simulation*, J. Geophys. Res.*, **103**(D8), 8873-8884.

Feddema J.J., K. Oleson, G. Bonan, L. Mearns, W. Washington, G. Meehl, D. Nychka, 2005: A comparison of a GCM response to historical anthropogenic land cover change and model sensitivity to uncertainty in present-day land cover representations. Climate Dyn., 25, 581–609.

Fennessy M.J., J. Shukla, 1999: Impact of initial soil wetness on seasonal atmospheric prediction. J. Clim., 12, 3167–3180

Fernandez J. P. R., S. H. Franchito, and V. B. Rao, 2006: Simulation of the summer circulation over South America by two regional climate models. Part II: A comparison between 1997-1998 El Niño and 1998-1999 La Niña events. Theor. Appl. Climatol. 86, 261–270

Figueroa, S., P. Satyamurti, and P. L. Silva Dias, 1995: Simulation of the summer circulation over the South American region with an Eta coordinate model. J. Atmos. Sci., 52, 1573–1584

Findell, K.L, E.A.B., Eltahir 2003: Atmospheric Controls on Soil Moisture–Boundary Layer Interactions. Part II: Feedbacks within the Continental United States. ***J. of Hydromet.***, 4, 570–583

Fischer E. M., S. I. Seneviratne, P. L. Vidale, D. Lüthi, and C. Schär, 2007: Soil Moisture Atmosphere Interactions during the 2003 European Summer Heat Wave. J. Clim., 20, 5081-5099.

Figueroa, S., P. Satyamurti, and P. L. Silva Dias, 1995: Simulation of the summer circulation over the South America region with Eta coordinate model. J. Atmos. Sci., 52, 573–584.

Frich, P., Alexander, L.V., Della-Marta P., Gleason B., Haylock M., Klein Tank A.M.G. and Peterson T. 2002. Observed coherent changes in climatic extremes during the second half of the twentieth century. *Clim. Res.* **19**, 193-212.

Fu, R., B. Zhu, and R. E. Dickinson, 1999: How do atmosphere and land surface influence seasonal changes of convection in the tropical Amazon? J. Clim., 12, 1306–1321.

Fu, R., R. E. Dickinson, M. Chen, and H. Wang, 2001: How do tropical sea surface temperatures influence the seasonal distribution of precipitation in the equatorial Amazon? J. Clim., 14, 4003– 4026.

Fu.R and W. Li, 2004: The influence of the land surface on the transition from the dry to wet season in Amazonia, Theoretical and Applied Climatology, 78, 97-110

Fu C., S. Wang, Z. Xiong, W. J. Gutowski, D.-K. Lee, J. L. McGregor, Y. Sato, H. Kato, J.-W. Kim, and M.-S. Suh, 2005: Regional Climate Model Intercomparison Project for Asia Bulletin of the American Meteorological Society 86: 257–266

Gan, M. A., V. E. Kousky, and C. F. Ropelewski, 2004: The South America monsoon circulation and its relationship to rainfall over west-central Brazil. J. Clim., 17, 47–66.

Garand L, 1983: Some improvements and complements to the infrared emissivity algorithm including a parameterization of the absorption in the continuum region. J Atmos Sci 40:230-244

Garratt, J.R., 1993: Sensitivity of Climate Simulations to Land-Surface and Atmospheric Boundary-Layer Treatments - A Review. J. Clim., 6, 419–448

Giorgetta M, Wild M (1995) The water vapour continuum and its representation in ECHAM4, Max Planck Institut fuer Meteorologie Report vol 162, p38.

Giorgi, F., 1995: Perspectives for regional earth system modeling. Glob. Planet. Change, 10, 23-42.

Giorgi, F., and G.T. Bates, 1989: The climatological skill of a regional model over complex terrain. Mon. Wea. Rev., 117, 2325–2347.

Giorgi, F., and L.O. Mearns, 1999: Introduction to special section: Regional climate modeling revisited. J. Geophys. Res., 104, 6335–6352.

Giorgi, F., M. R. Marinucci, G. T. Bates, and De Canio, 1993: Development of a second generation regional climate model (RegCM2). Part II: Convective processes and assimilation of lateral boundary conditions. Mon. Wea. Rev., 121, 2814–2832.

Giorgi, F., and X. Bi, 2000: A study of internal variability of a regional climate model. J. Geophys. Res., 105, 29503–29521.

Grimm, A. M., J. S Pal, F. Giorgi, 2007: Connection between Spring Conditions and Peak Summer Monsoon Rainfall in South America: Role of Soil Moisture, Surface Temperature, and Topography in Eastern Brazil. J. Clim., 20, 5929-5945

Guo, Z., P.A. Dirmeyer, R.D.Koster, G. Bonan, E. Chan, P. Cox, C. T. Gordon, S. Kanae, E. Kowalczyk, D. Lawrence, P. Liu, C.-H. Lu, S. Malyshev, B. McAveney, J. L. McGregory, K. Mitchel, D. Mocko, T. Oki, K.W. Oleson, A. Pitman, Y.C. Sud, C.M. Taylor, M. Christopher, D. Verseghy, R. Vasic, Y. Xue, T. Yamada, 2006 GLACE: The Global Land-Atmosphere Coupling Experiment. Part II: Analysis**.** J. of Hydromet**.**, 7, 611-625.

Hagemann, S., Botzet, M., Dumenil, L., and Machenhauer, B., 1999: Derivation of global GCM boundary conditions from 1 km land use satellite data. Report No. 289. Max-Planck-Institut fur Meteorologie, Hamburg.

Hansen, M. C., DeFries, R. S., Townshend, J. R. G., Sohlberg, R., 2000: Global land cover classification at 1km spatial resolution using a classification tree approach, Int. J. Remote Sensing 21: 1331–1364.

Henderson-Sellers A., and K. McGuffie, 1987: Climate Modelling Primer. John Wiley and sons 217pp.

Hewitt, C.D., 2005: ENSEMBLES – providing ensemble-based predictions of climate changes and their impacts. *Parliament Magazine*, 11 July 2005, p. 57.

Hourdin F, Musat I, Bony S, Braconnot P, Codron F, Dufresne J-L, Fairhead L, Filiberti M-A, P Friedlingstein, J-Y Grandpeix, G Krinner, P LeVan, Z-X Li, F Lott (2006) The LMDZ4 general circulation model: climate performance and sensitivity to parametrized physics with emphasis on tropical convection. Clim Dyn 27: 787-813.

Jacob D (2001) A note on the simulation of the annual and inter-annual variability of the water budget over the Baltic Sea drainage basin. Met Atmos Phys 77:61-73.

Ji, Y., and A. D. Vernekar, 1997: Simulation of the Asian summer monsoons of 1987 and 1988 with a regional model nested in a global GCM. J. Clim., 10, 1965–1979.

Jones C.G. and E. Sanchez, 2002. The representation of shallow cumulus convection and associated cloud fields in the Rossby Centre Atmospheric Model. *HIRLAM Newsletter 41*, Available on request from SMHI, S-60176 Norrköping, Sweden.

Jones, C., G. Nikulin, A. Ullerstig, P. Samuelsson and U. Willén, 2009: Simulating Precipitation over Africa with a new version of RCA. Rossby Centre Newsletter, May 2009, available online at: http://www.smhi.se/content/1/c6/04/14/79/attatchments/RCnews_may_2009.pdf

Juang, J. Y., G.G., Katul, A., Porporato, P.C., Stoy, M.S., Siqueira, M., Detto, H.-S., Kim, and R. Oren, 2007. Eco-hydrological controls on summertime convective rainfall triggers. Global Change Biol., 13, 887–896.

Kain, J.S. 2004: The Kain–Fritsch Convective Parameterization: An Update John S. Kain Journal of Applied Meteorology, 43: 170–181.

Kain, J.S. and J.M. Fritsch, 1993. Convective parameterizations for MEsoscale Models: The Kain-Fritsch scheme. In: The representation of cumulus convection in numerical models, Eds: K.A. Emanuel and D.J. Raymond. *AMS Monograph*, 46, 246 pp.

Khairoutdinov, M. F., and Y. L. Kogan, 2000: A new cloud physics parameterization in a large-eddy simulation model of marine stratocumulus. Mon. Wea. Rev 128: 229–243

Kjellström E, Bärring L, Gollvik S, Hansson U, Jones C, Samuelsson P, Rummukainen M, Ullerstig A, Willén U, Wyser K (2005) A 140-year simulation of European climate with the new version of the Rossby Centre regional atmospheric climate model (RCA3). Reports Meteorology and Climatology No. 108, SMHI, SE-60176 Norrköping, Sweden, 54pp

Kleidon A and Heimann M (2000) Assessing the role of deep rooted vegetation in the climate system with model simulations: mechanism, comparison to observations and implications for Amazonian deforestation. Climate Dyn., 16, 183-199.

Koeppe, C. E. and Delong, G. C. (1958) *Weather and Climate*. McGraw-Hill.

Kodama, Y., 1992: Large-scale common features of subtropical precipitation zones (the Baiu frontal zone, the SPCZ, and the SACZ), Part I, Characteristics of subtropical zones. *J. Meteorol. Soc. Jpn*, 70: 813 – 835.

Kodama, Y., 1993: Large-scale common features of subtropical precipitation zones (the Baiu frontal zone, the SPCZ, and the SACZ), Part II, Conditions of the circulations for generating STCZs, *J. Meteorol. Soc*. Jpn. 71: 581–610.

Koster R., Z. Guo and P.A. Dirmeyer, 2003: GLACE: Quantifying Land-Atmosphere Coupling Strength Across a Broad Range of Climate Models. CLIVAR Exchanges 28:1-3

Koster R.D., P.A. Dirmeyer, Z. Guo, G. Bonan, E. Chan, P. Cox, C.T. Gordon, S. Kanae, E. Kowalczyk, D. Lawrence, P. Liu, C.-H. Lu, S. Malyshev, B. McAvaney, K. Mitchell, D. Mocko, T. Oki, K. Oleson, A. Pitman, Y.C. Sud, C.M. Taylor, D. Verseghy, R. Vasic, Y. Xue and T. Yamada, 2004: Regions of Strong Coupling Between Soil Moisture and Precipitation. Science, 305,1138-1140

Koster R.D., Z. Guo, P.A. Dirmeyer, G. Bonan, E. Chan, P. Cox, H. Davies, C.T. Gordon, S. Kanae, E. Kowalczyk, D. Lawrence, P. Liu, C. Lu, S. Malyshev, B. McAvaney, K. Mitchell, D. Mocko, T. Oki, K.W. Oleson, A. Pitman, Y.C. Sud, C.M. Taylor, D. Verseghy, R. Vasic, Y. Xue and T. Yamada, 2006: GLACE: The Global Land–Atmosphere Coupling Experiment. Part I: Overview. *J. of Hydromet*., 7, 590-610

Kousky V.E., 1988: Pentad outgoing longwave radiation climatology for the South American sector. Rev Bras Meteorol 3: 217–231.

Krinner G, Viovy N, de-Noblet-Ducoudré N, Ogée J, Polcher J, Friedlingstein P, Ciais P, Sitch S, Prentice C (2005) A dynamic global vegetation model for studies of the coupled atmosphere-biosphere system. Global Change Biology 19:1015:1048.

Lawford, R. G., Roads, J., Lettenmaier, D. P., and Arkin, P. 2007. GEWEX Contributions to Large-Scale Hydrometeorology, *J. Hydrometeror*, 8, 629–641.

Lawrence D. M. and J. M. Slingo, 2005: Weak Land–Atmosphere Coupling Strength in HadAM3: The Role of Soil Moisture Variability. *J. of Hydromet.*, 6, 670–680

Lean, J., and D.A. Warrolow, 1989: Simulation of the regional climatic impact of Amazon deforestation. Nature, 342: 411-413.

Lenderink, G., and de Rooy, W., 2000. A robust mixing length formulation for a TKE-1 turbulence scheme, *Hirlam Newsletter*, 36, 25-29.

Lenderink, G., and Holtslag, A. A. M., 2004. An updated length-scale formulation for turbulent mixing in clear and cloudy boundary layers. Quart. J. Roy. Meteor. Soc., 130, 3405-3427.

Lenters, J. D., and K. H. Cook, 1995: Simulation and diagnosis of the regional summertime precipitation climatology of South America J. Clim., 8, 2988–3005.

Li, W., R. Fu, 2004: Transition of the Large-Scale Atmospheric and Land Surface Conditions from the Dry to the Wet Season over Amazonia as Diagnosed by the ECMWF Re-Analysis. J. Clim., 17, 2637–2651.

Lin Y.-L., R.D. Farley, H.D. Orville 1983: Bulk Parameterization of the Snow Field in a Cloud Model. Journal of Applied Meteorology 22:1065–1092.

Liebmann, B., G. Kiladis, J. Marengo, and T. Ambrizzi, 1999: Submonthly convective variability over South America and the South Atlantic Convergente Zone. J. Clim., 12, 1877–1891.

Liebmann, B. and J. Marengo, 2001: Interannual Variability of the Rainy Season and Rainfall in the Brazilian Amazon Basin, J. Clim, 14: 4308.

Liebmann B., G. N. Kiladis, C. S. Vera and A. C. Saulo, L. M. V. Carvalho, 2004: Subseasonal Variations of Rainfall in South America in the Vicinity of the Low-Level Jet East of the Andes and Comparison to Those in the South Atlantic Convergence Zone. J. Clim., 17, 3829–3842

Ljungemyr P., Gustafsson N. and Omstedt A., 1996. Parameterization of lake thermodynamics in a high resolution weather forecasting model. *Tellus*, 48A, 608–621.

Loveland, T. R & Belward, A. S. (1997) The IGBP-DIS global 1 km land cover data set, DISCover: first results. *Int. J. Remote Sensing* 18: 3289–3295.

Lucas-Picher, P., D. Caya, and S. Biner, 2004: RCM's internal variability as function of domain size. *Research Activities in Atmospheric and Oceanic Modelling,* J. Côté, Ed., World Meteorological Organization, 7.27–7.28.

Marengo J.A., B. Liebmann, V.E. Kousky, N.P. Filizola, I.C. Wainer, 2001: Onset and end of the rainy season in the Brazilian Amazon Basin. J. Clim,.14, 833–852

Marengo J.A., W.R. Soares, C. Saulo, M. Nicolini, 2004: Climatology of the Low-Level Jet East of the Andes as Derived from the NCEP–NCAR Reanalyses: Characteristics and Temporal Variability. J. Clim., 17, 2261-2280

Marengo, J.A., 2007: Integrating across spatial and temporal scales in climate projections: Challenges for using RCM projections to develop plausible scenarios for future extreme events in South America for vulnerability and impact studies. Extended Abstracts and Draft Papers. IPCC TGICA Expert Meeting on Integrating Analysis of Regional Climate Change and Response Options. Nadi, Fiji, 20-22 June 2007, p. 141-147.

Masson, V., Champeaux, J.-L., Chauvin, F., Meriguet, C., Lacaze, R., 2003: A global database of land surface parameters at 1-km resolution in meteorological and climate models. J. Clim., 16, 1261–1282.

Mearns L.O., F. Giorgi, L. McDaniel, C. Shields, 2003, Analysis of daily variability of precipitation in a nested regional climate model: comparison with observations and doubled CO, results. Global and Planetary Change 10 (199.5) 55-78

Menéndez, C.G., de Castro, M., Boulanger, J.-P., D'Onofrio, A., Sanchez, E., Sörensson, A.A., Blazquez, J., Elizalde, A., Jacob, D., Le Treut, H., Li, Z.X., Núñez, M.N., Pfeiffer, S., Pessacg, N., Rolla, A., Rojas, M., Samuelsson, P., Solman, S.A. and Teichmann, C. 2010. Downscaling extreme month-long anomalies in southern South America. *Climatic Change*, 98, 379 - 403

Menéndez C.G, Sörensson A.A, Samuelsson P., Willén U., Hansson U., de Castro M., Boulanger J.-P., 2009: CLARIS Project: towards climate downscaling in South America using RCA3. 2nd Lund Regional-scale Climate Modelling Workshop: 21st Century Challenges in Regional-scale Climate Modelling. Lund, Sweden, 4 - 8 May 2009.

Mironov D.V. 2008. Parameterization of lakes in numerical weather prediction. Description of a lake model. COSMO Technical Report, No. 11, Deutscher Wetterdienst, Offenbach am Main, Germany, 41 pp.

Misra, V., P. A. Dirmeyer, B. P. Kirtman, H.-M. Juang, and M. Kanamitsu, 2002: Regional simulation of interannual variability over South America, J. Geophys. Res., 107(D20), 8036, doi:10.1029/2001JD900216

Misra V., 2005: Simulation of the Intraseasonal Variance of the South American Summer Monzón Mon. Wea. Rev., 133, 663-676.

Morcrette J-J, Smith L, Fourquart Y (1986) Pressure and temperature dependance of the absorption in longwave radiation parameterizations. Beitr Phys Atmos 59:455-469

Morcrette J-J (1991) Radiation and cloud radiative properties in the ECMWF operational weather forecast model. J Geophys Res 96D:9121-9132

Moura, A. D., and J. Shukla, 1981: On the dynamics of droughts in northeast Brazil: Observations, theory, and numerical experiments with a general circulation model. J. Atmos. Sci., 38, 2653– 2675.

Nepstad D.C., C.R. de Carvalho, E.A. Davidson, P.H. Jipp, P.A. Lefebvre, H.G. Negreiros, E.D. da Silva, T.A. Stone, S.E. Trumbore, S. Vieira, 1994: The role of deep roots in the hydrological and carbon cycles of Amazonian forests and pastures. Nature 372:666-669

Nesbitt, S.W., Zipser, E.J. 2003. The Diurnal Cycle of Rainfall and Convective Intensity to Three Years of TRMM Measurements. *J. Climate*. **16**, 1456-1475.

New M., M. Hulme, P. Jones, 1999: Representing twentieth-century space time climate variability. Part I. Development of a 1961-1990 mean monthly terrestrial climatology. J. Clim., 12, 829-856

New M., M. Hulme, P. Jones, 2000: Representing twentieth-century space time climate variability. Part II: Development of 1901-1996 monthly grids of terrestrial surface climate. J. Clim., 13, 2217-2238.

Nicolini, M., P. Salio, G. Ulke, J. Marengo, M. Douglas, J. Paegle, and E. Zipser, 2004: South American low-level jet diurnal cycle and three-dimensional structure. *CLIVAR Exchanges,* Vol. 9, No. 1, International CLIVAR Project Office, 6–9.

Nobre, C. A., P. J. Sellers and J. Shukla, 1991: Amazonian deforestation and regional climate change. J. Clim., 4, 957-988.

Nogués-Paegle, J., and K. C. Mo, 1997: Alternating wet and dry conditions over South America during summer, Mon. Wea. Rev., 125: 279–291.

Nogués-Paegle J., C.R. Mechoso, R. Fu, E.H. Berbery, W.C. Chao, T.-C. Chen, K. Cook, A.F. Diaz, D. Enfield, R. Ferreira, A.M. Grimm, V.Kousky, B. Liebmann, J. Marengo, K. Mo, D. Neelin, J. Paegle, A.W. Robertson, A. Seth, C.S. Vera, J. Zhou, 2002: Progress in Pan American CLIVAR research: understanding the South American monsoon. Meteorologica 27:1-30.
Nordeng TE (1994) Extended versions of the convective parametrization scheme at ECMWF and their impact on the mean and transient activity of the model in the tropics. ECMWF Research Department, Technical Momorandum No. 206, October 1994, 41 pp, European Centre for Medium Range Weather Forecasts, Reading, UK.

Nuñez M. N., S. A. Solman, M. F. Cabre, 2008: Regional climate change experiments over southern South America. II: Climate change scenarios in the late twenty-first century. Climate Dyn. DOI 10.1007/s00382-008-0449-8

Oyama M. D., and C. A. Nobre, 2004: Climatic Consequences of a Large-Scale Desertification in Northeast Brazil: A GCM Simulation Study. J. Clim., 17, 3203–3213.

Pielke R.A. Sr, 2001: Influence of the spatial distribution of vegetation and soils on the prediction of cumulus convective rainfall. Reviews of Geophysics, 39: 151–177

Pitman, A.J. and M. Zhao, 2000: The relative impact of observed change in land cover and carbon dioxide as simulated by a climate model, Geophysical Research Letters, 27: 1267-1270

Qian J.-H, A. Seth, and S. Zebiak, 2003: Reinitialized versus Continuous Simulations for Regional Climate Downscaling. Mon. Wea. Rev., 131, 2857-2874

Rao, G. V., and S. Erdogan, 1989: The atmospheric heat source over the Bolivian plateau for a mean January. Bound-Layer Meteor., 46, 13–33.

Rasch, P.J. and Kristjansson, J.E., 1998. A comparison of the CCM3 model climate using diagnosed and predicted condensate parameterisations, J. Clim., 11, 1587-1614.

Räisänen P, Rummukainen M, Räisänen J (2000) Modification of the HIRLAM radiation scheme for use in the Rossby Centre regional atmospheric climate model. Report No. 49, Department of Meteorology, University of Helsinki, 71 pp.

Rauscher S. A. , A. Seth, J.-H. Qian and S. J. Camargo, 2006: Domain choice in an experimental nested modeling prediction system for South America. Theor. and appl. clim. 86: 229-246

Rauscher S. A., A. Seth, B. Liebmann, J.-H. Qian, and S. J. Camargo, 2007: Regional Climate Model–Simulated Timing and Character of Seasonal Rains in South America. Mon. Wea. Rev., 135, 2642–2657

Rial J.A., R.A. Pielke Sr., M. Beniston, M. Claussen, J. Canadell, P. Cox, H. Held, N. de Noblet-Ducoudré, R. Prinn, J. F. Reynolds, J. D. Salas 2004: Nonlinearities, Feedbacks and Critical Thresholds within the Earth's Climate System. Climatic Change 65, 11-38.

Roads, J., S. Chen, S. Cocke, L. Druyan, M. Fulakeza, T. LaRow, P. Longergan, J.-H. Qian, and S. Zebiak, 2003: International Research Institute/Applied Research Centers (IRI/ARCs) regional model intercomparison over South America. J. Geophys. Res., 108 (D14), 4425, doi:10.1029/2002JD003201.

Robertson, A. W., and C. Mechoso, 2000: Interannual and interdecadal variability of the South Atlantic Convergence Zone, Mon. Wea. Rev., 128: 2947– 2957.

Rodell, M., P.R. Houser, A.A. Berg, J.S. Famiglietti, 2004: Evaluation of 10 Methods for Initializing a Land Surface Model. ***J. of Hydromet.,*** 6, 146-155.

Rogers R.F. and J.M. Fritsch 1996: A General Framework for Convective Trigger Functions Mon. Wea. Rev., 124, 2438–2452.

Rojas, M., and A. Seth, 2003: Simulation and sensitivity in a nested modeling system for South America. Part II: GCM boundary forcing. J. Clim., 16, 2454-2471.

Ropelewski, C.F., and M.S. Halpert, 1989: Precipitation patterns associated with the high index phase of the Southern Oscillation. J. Clim., 2, 268–284.

Roy B. S., R. Avissar, 2002: Impact of land use/land cover change on regional hydrometeorology in Amazonia. J. Geophys. Res., 107(D20), 8037, DOI 10.1029/2000JD000266

Ruane, A.C. and Roads, J.O. 2007. 6-Hour to 1-Year Variance of Five Global Precipitation Sets. *Earth Interactions*, **11**, doi:10.1175/EI225.1

Sadershmukh, P.D., and B. J., Hoskins (1985) Vorticity balances in the tropics during the 1982-1983 El Niño-Southern Oscillation event, J. Roy. Meteor. Soc., 111, 261-278

Salio, P., M. Nicolini, and A. C. Saulo, 2002: Chaco low-level jet events characterization during the austral summer season. J. Geophys. Res.*,* 107, 4816

Salio P., M. Nicolini and E. J. Zipser, 2007: Mesoscale Convective Systems over Southeastern South America and Their Relationship with the South American Low-Level Jet. Mon. Wea. Rev., 135, 1290–1309

Samuelsson P., E. Kourzeneva and D. Mironov, 2009: The impact of lakes on the European climate as simulated by a regional climate model. Accepted for publication in Boreal Environmental Research

Samuelsson P, Gollvik S, Ullerstig A, 2006: The land-surface scheme of the Rossby Centre regional atmospheric climate model (RCA3). Report in Meteorology 122, SMHI. SE-601 76 Norrköping, Sweden

Sass B.H., Rontu L., Savijärvi H., Räisänen P., 1994. HIRLAM-2 Radiation scheme: Documentation and tests. *Hirlam technical report No 16.,* SMHI. SE-601 76 Norrköping, Sweden, 43 pp.

Satyamurty, P., C. C. Ferreira, and M. A. Gan, 1990: Cyclonic vortices over South America. Tellus, 42A, 194–201.

Sato N., P.J. Sellers, D.A. Randall, E.K. Schneider, J. Shukla, J.L. Kinter III, Y.-T. Hou and E. Albertazzi, 1989: Effects of implementing the simple biosphere model in a general circulation model. J. Atmos. Sci., 46:2757–2782

Saulo, A. C., L. J. Ferreira, J. Mejia, and M. Seluchi, 2004: Description of the thermal low characteristics using SALLJEX special observations. *CLIVAR Exchanges,* Vol. 9, No. 1, International CLIVAR Project Office, 9–11.

Savijärvi H., 1990. A fast radiation scheme for mesoscale model and short-range forecast models. *J. Appl. Met*., 29, 437-447.

Schär C., D. Lüthi, U. Beyerle, and E. Heise, 1999: The Soil–Precipitation Feedback: A Process Study with a Regional Climate Model. J. Clim., 12, 722–741

Seluchi, M. E., and J. A. Marengo, 2000: Tropical-midlatitude exchange of air masses during summer and winter in South America: Climatic aspects and examples of intense events, Int. J. Climatol., 20: 1167– 1190.

Seneviratne, S.I., P. Viterbo, D. Luthi and C. Schar, 2004: Inferring Changes in Terrestrial Water Storage Using ERA-40 Reanalysis Data: The Mississippi River Basin. J. Clim., 17, 2039–2057.

Seneviratne S. I., D. Lüthi, M. Litschi and C. Schär, 2006: Land–atmosphere coupling and climate change in Europe. Nature 443, 205 – 209

Seth, A., and F. Giorgi, 1998: The effects of domain choice on summer precipitation simulation and sensitivity in a regional climate model. J. Clim., 11, 2698–2712.

Seth, A., and M. Rojas, 2003: Simulation and sensitivity in a nested modeling system for South America. Part I: Reanalyses boundary forcing. J. Clim., 16, 2437–2453.

Seth A., M. Rojas, B. Liebmann, and J.-H. Qian, 2004: Daily rainfall analysis for South America from a regional climate model and station observations, J. Geophys. Res., 31, L07213, doi:10.1029/2003GL019220

Shukla, J., C. Nobre, and P. Sellers 1990: Amazon deforestation and climate change. Scienece, 247: 1322-1325.

Silva, V. B. S., and E. H., Berbery, 2006: Intense rainfall events affecting the La Plata basin. J. Hydrometeor., 7, 769–787.

Silvestri G., C. Vera, D. Jacob, S. Pfeifer, C. Teichmann, 2008: A high-resolution 43-year atmospheric hindcast for South America generated with the MPI regional model. Climate Dyn., DOI 10.1007/s00382-008-0423-5

Simmons A., S. Uppala, D. Dee, S. Kobayashi, 2006: ERA-Interim: New ECMWF reanalysis products from 1989 onwards, ECMWF Newsletter No. 110, http://www.ecmwf.int/publications/newsletters/pdf/110_rev.pdf

Slingo J.M., 1987: The development and verification of a cloud prediction model for the ECMWF model Quart. J. Roy. Meteor. Soc., 113, 899-927

Solman S. A., M. N. Nuñez and M. F. Cabre, 2007: Regional climate change experiments over southern South America. I: present climate. Climate Dyn., DOI 10.1007/s00382-007-0304-3.

Stephens G. L., 1978: Radiation profiles in extended water clouds: II. Parameterization schemes. J Atmos Sci 35: 2123-2132.

Sundquist H. 1978: A parameterization scheme for non-convective condensation including precipitation including prediction of cloud water content. Quart J R Met Soc 104:677-690.

Sörensson A.A., Ruscica R, Menéndez C.G., Alexander P., Samuelsson P., Willén U., Hansson U, 2009, South America's Present and Future Climate as Simulated by the Rossby Centre

Regional Atmospheric Model, 9th International Conference on Southern Hemisphere Meteorology and Oceanography.

Swenson, S. C., and P. C. D. Milly (2006), Climate model biases in seasonality of continental water storage revealed by satellite gravimetry, Water Resour. Res., 42, W03201, doi:10.1029/2005WR004628.

Takle E. S., W. J. Gutowski Jr., R. W. Arritt, Z. Pan, C. J. Anderson, R. R. da Silva, D. Caya, S.-C. Chen, F. Giorgi, J. Hesselbjerg Christensen, S.-Y. Hong, H.-M. H. Juang, J. Katzfey, W. M. Lapenta, R. Laprise, G. E. Liston, T.M. Philippe Lopez, J. McGregor, R. A. Pielke Sr. and J. O. Road, 1999: Project to Intercompare Regional Climate Simulations (PIRCS): Description and initial results. J. Geophys. Res., 104 (D16), 19,443–19,461

Takle E. S., J. Roads, B. Rockel, W. J. Gutowski Jr., R. W. Arritt, I. Meinke, C. G. Jones, and A. Zadra, 2007: Transferability Intercomparison: An Opportunity for New Insight on the Global Water Cycle and Energy Budget. Bulletin of the American Meteorological Soviet. 88: 375–384

Taylor, C. M., and R. J., Ellis, 2006. Satellite Detection of Soil Moisture Impacts on Convection at the Mesoscale. Geophysical Research Letters, 33**,** doi:10.1029/2005GL02525.

Taylor C.M, D. J. Parker, and P. P. Harris, 2007: An observational case study of mesoscale atmospheric circulations induced by soil moisture. Geophys. Res. Lett., Vol 34, L15801, doi:10.1029/2007GL030572,

Tiedtke M., 1989: A comprehensive mass flux scheme for cumulus parameterization in large scale models. Mon Wea Rev 117:1779-1800

Trenberth, K. E., 1999: Atmospheric moisture recycling: Role of advection and local evaporation, J. Clim., 12, 1368–1381.

Uppala S.M., P.W. Kållberg, A.J. Simmons, U. Andrae, V. da Costa Bechtold, M. Fiorino, J.K. Gibson, J. Haseler, A. Hernandez, G.A. Kelly, X. Li, K. Onogi, S. Saarinen, N. Sokka, R.P. Allan, E. Andersson, K. Arpe, M.A. Balmaseda, A.C.M. Beljaars, L. van de Berg, J. Bidlot, N. Bormann, S. Caires, F. Chevallier, A. Dethof, M. Dragosavac, M. Fisher, M. Fuentes, S. Hagemann, E. Hólm, B.J. Hoskins, L. Isaksen, P.A.E.M. Janssen, R. Jenne, A.P. McNally, J.-F. Mahfouf, J.-J. Morcrette, N.A. Rayner, R.W. Saunders, P. Simon, A. Sterl, K.E. Trenberth, A. Untch, D. Vasiljevic, P. Viterbo and J. Woollen, 2005: The ERA-40 re-analysis. Quart. J. Roy. Meteor. Soc., 131, 2961-3012

van den Hurk B., P. Viterbo, A. Beljaars, and A. Betts, 2000: Off-line validation of the ERA40 surface scheme. European Centre for Medium-Range Weather Forecasts Tech. Memo. 295, 42 pp.

van den Hurk B., M. Hirschi, C. Schär, G. Lenderink, E. van Meijgaard E, A. van Ulden, B. Rockel, S. Hagemann, P. Graham, E. Kjellström and R. Jones, 2005: Soil control on runoff response to climate change in regional climate model simulations. J. Clim. 18, 3536–3551.

Vannitsem, S., and F. Chomé, 2005: One-way nested regional climate simulations and domain size. J. Clim., 18**,** 229–233.

Vautard, R., P. Yiou, F. D'Andrea, N. de Noblet, N. Viovy, C. Cassou, J. Polcher, P. Ciais, M. Kageyama, and Y. Fan, 2007: Summertime European heat and drought waves induced by wintertime Mediterranean rainfall déficit. *Geophys. Res. Lett.*, 34, L07711, doi:10.1029/2006GL028001.

Velasco, I. and Fritsch, J.M. 1987. Mesoscale convective complexes in the Americas. *J. Geophys. Res*. **92**(D8), 9591–9613.

Vera C., J. Baez, M. Douglas, C. B. Emmanuel, J. Marengo, J. Meitin, M. Nicolini, J. Nogues-Paegle, J. Paegle, O. Penalba, P. Salio, C. Saulo, M. A. Silva Dias, P. Silva Dias, and E. Zipser, 2004: The South American Low-Level Jet Experiment. Bulletin of the American Meteorological Society, 87: 63–77

Vera C., W. Higgins, J. Amador, T. Ambrizzi, R. Garreaud, D. Gochis, D. Gutzler, D. Lettenmaier, J. Marengo, C. R. Mechoso, J. Nogues-Paegle, P. L. Silva Dias, and C. Zhang, 2006a: Toward a Unified View of the American Monsoon Systems. Journal of Climate,19: 4977–5000

Vera, C., G. Silvestri, B. Liebmann, P. Gonzalez, 2006b: Climate change scenarios for seasonal precipitation in South America from IPCC-AR4 models, Geophys. Res. Lett., 33, L13707, doi:10.1029/2006GL025759.

Voldoire, A., and J.F. Royer, 2004: Tropical deforestation and climate variability. Climate Dyn., 22, 857–874.

Voldoire A., J.F. Royer, 2005: Climate sensitivity to tropical land surface changes with coupled versus prescribed SSTs. Climate Dyn., 24, 843–862.

von Storch, H., 2005: Models of global and regional climate. *Meteorology and Climatology,* M. G. Anderson, Ed., *Enciclopedia of Hydrological Sciences,* Vol. 1, Wiley, 478–490.

Wang, G., Y. Kim, and D. Wang, 2007: Quantifying the strength of soil moisture-precipitation coupling and its sensitivity to changes in surface water budget, ***J. of Hydromet.***, 8, 551– 570.

Wang Y., L. R. Leung, J. L. McGregor, D.-K. Lee, W.-C Wang, Y. Ding, F. Kimura, 2004: Regional Climate Modeling: Progress, Challenges, and Prospects. Journal of the Meteorological Society of Japan. Vol. 82, 1599-1628.

Wyser, K., L. Rontu and H. Savijärvi, 1999. Introducing the effective radius into a fast radiation scheme of a mesoscale model. *Contr. Atm. Phys.*, 72, 205-218.

Webster, P. J., V. Magana, T. N. Palmer, J. Shukla, R. A. Tomas, M. Yanai, and T. Yasunari, 1998: Monsoons: Processes, predictability, and the prospects for prediction. J. Geophys. Res., 103 (C7), 14 451–14 510.

Weisse, R., H. Heyen, and H. von Storch, 2000: Sensitivity of a regional atmospheric model to a sea state–dependent roughness and the need of ensemble calculations. Mon. Wea. Rev., 128, 3631–3642.

Wu, W., A. H. Lynch, and A. Rivers, 2005: Estimating the uncertainty in a regional climate model related to initial and boundary conditions. J. Clim., 18, 917–933.

Xu, K.-M., and D. A. Randall, 1996: A semiempirical cloudiness parameterization for use in climate models. J. Atmos. Sci., 53, 3084-3102.

Xue Y, De Sales F, Li W-P, Mechoso CR, Nobre CA, Juang H-M, 2006: Role of land surface processes in South American monsoon development. J. Clim. 19, 741-762.

Yamada T. J., R. D. Koster, S. Kanae, and T. Oki, 2007: Estimation of Predictability with a Newly Derived Index to Quantify Similarity among Ensemble Members. Mon. Wea. Rev.,135, 2674–2687

Zhou, J., and K.-M. Lau, 1998: Does a monsoon climate exist over South America? J. Clim., 11, 1020–1040.

Zipser, E. J., D. J. Cecil, C. Liu, S. W. Nesbitt, and D. P. Yorty, 2006: Where are the most intense thunderstorms on Earth?, Bull. Am. Meteorol. Soc., 87, 1057–1071.

Volume II: Figures

Index Volume II: Figures

MODEL DOMAIN AND TOPOGRAPHY

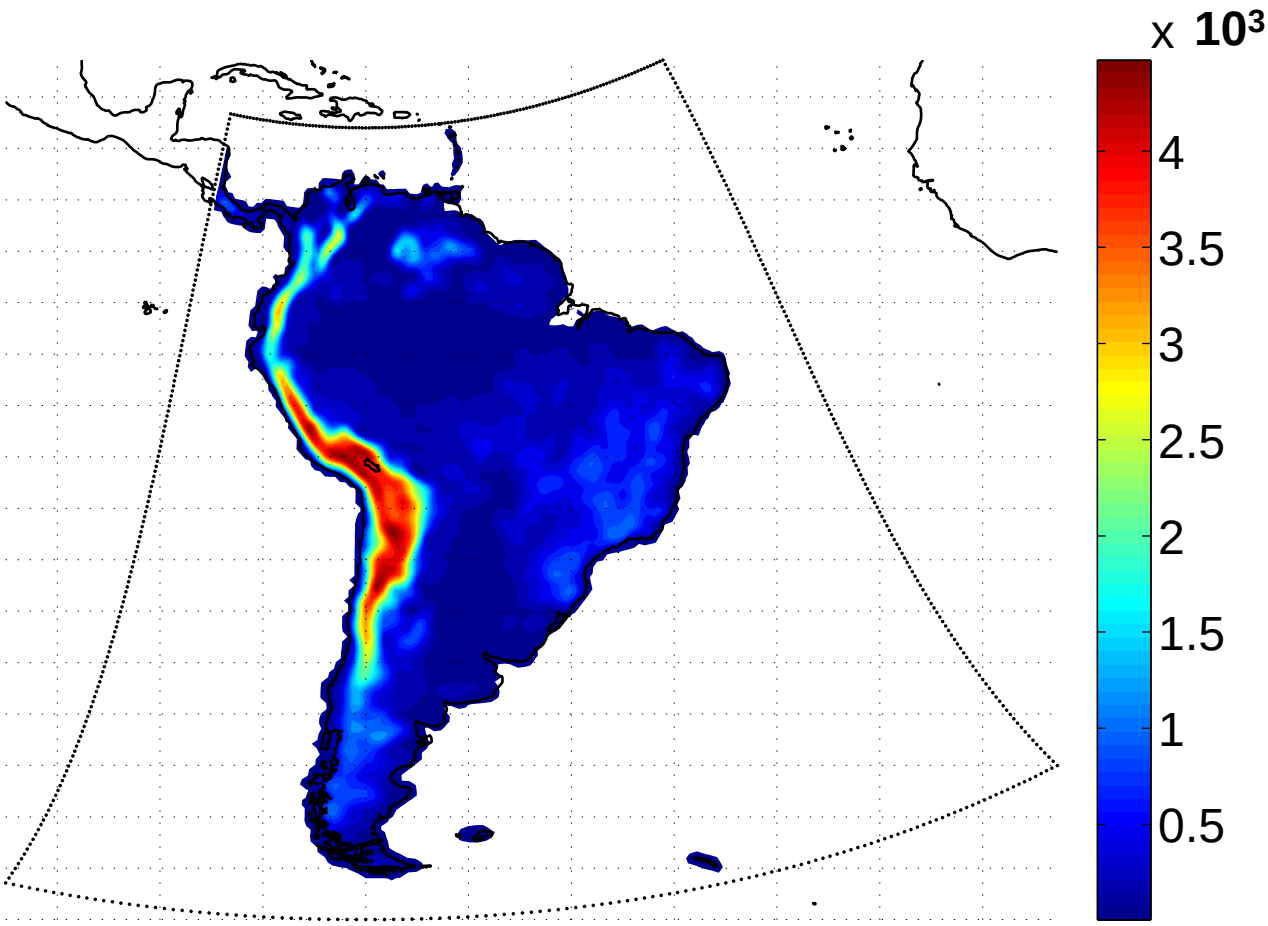

Figure 2.1: The RCA3-E domain over South America and the model topography in meters.

REGIONS

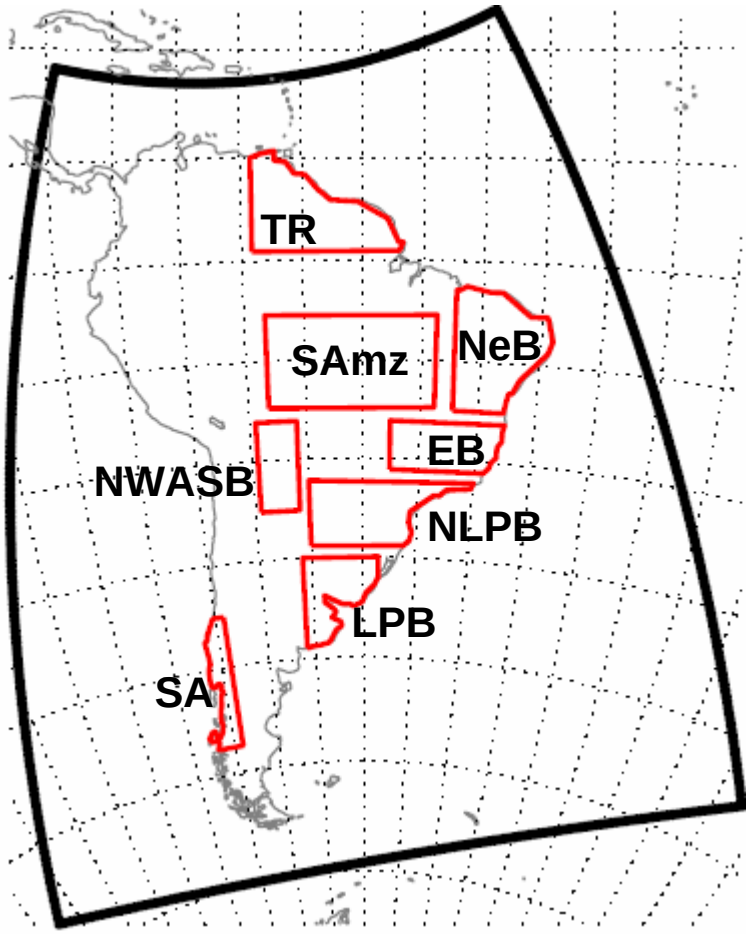

Figure 3.1: The 8 regions considered in this study: **TR** (Tropical), **SAms** (Southern Amazonia), **NeB** (Northeastern Brazil), **EB** (Eastern Brazil), **NWASB** (Northwestern Argentina, Southern Bolivia), **NLPB** (Northern la Plata Basin), **LPB** (La Plata Basin), **SA** (Southern Andes).

PRECIPITATION BIASES

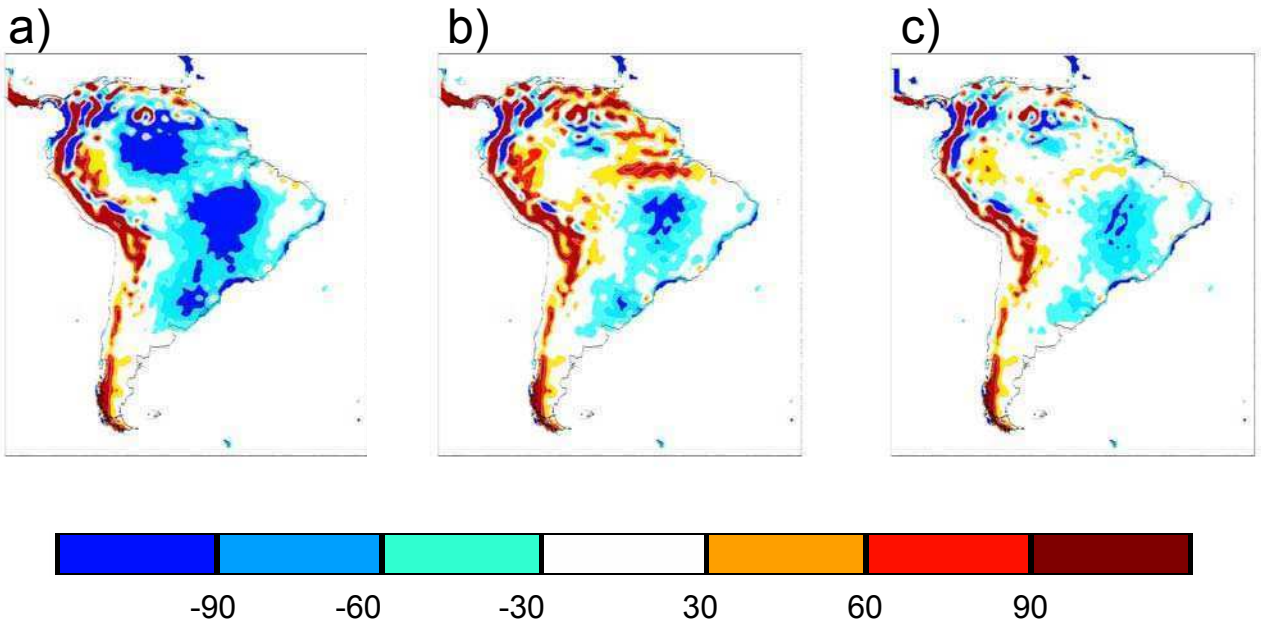

Figure 3.2:Annual precipitation bias (mm/month) relative to CRU for a) RCA3, b) RCA3_ECO, c) RCA3-E.

PRECIPITATION ANNUAL CYCLES

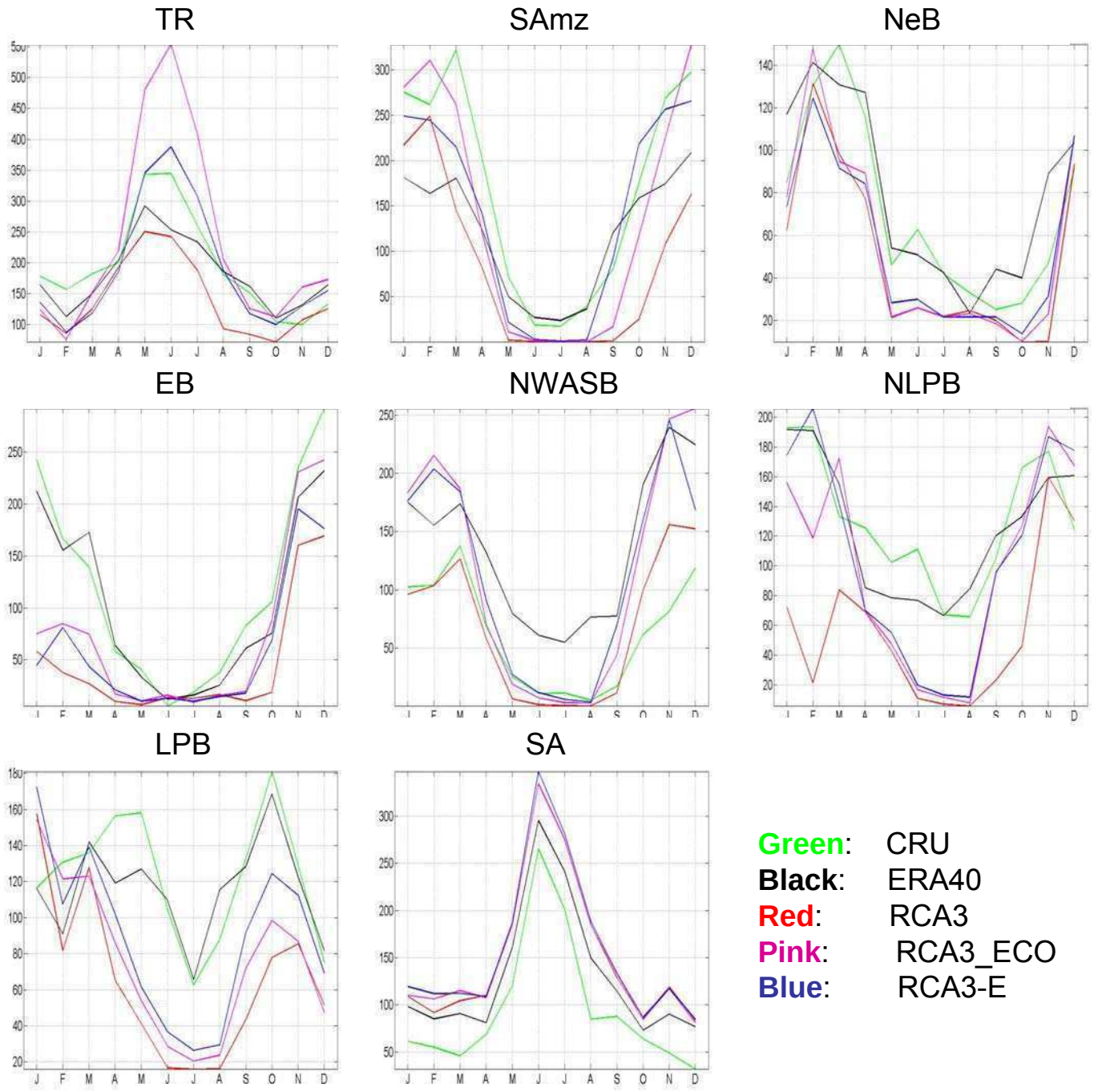

Figure 3.3: Annual cycles of precipitation (mm/month). Note different scales on the y-axis.

NEAR SURFACE TEMPERATURE BIASES

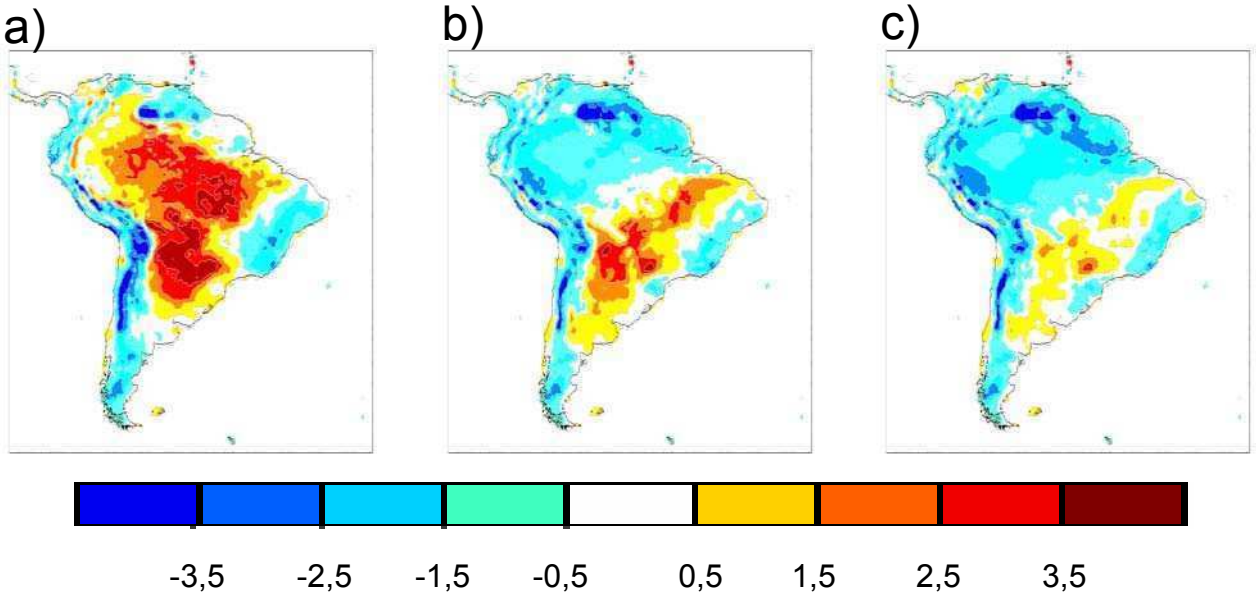

Figure 3.4:Annual t2m bias (C°) relative to CRU for a) RCA3, b) RCA3_ECO, c) RCA3-E.

T2M ANNUAL CYCLES

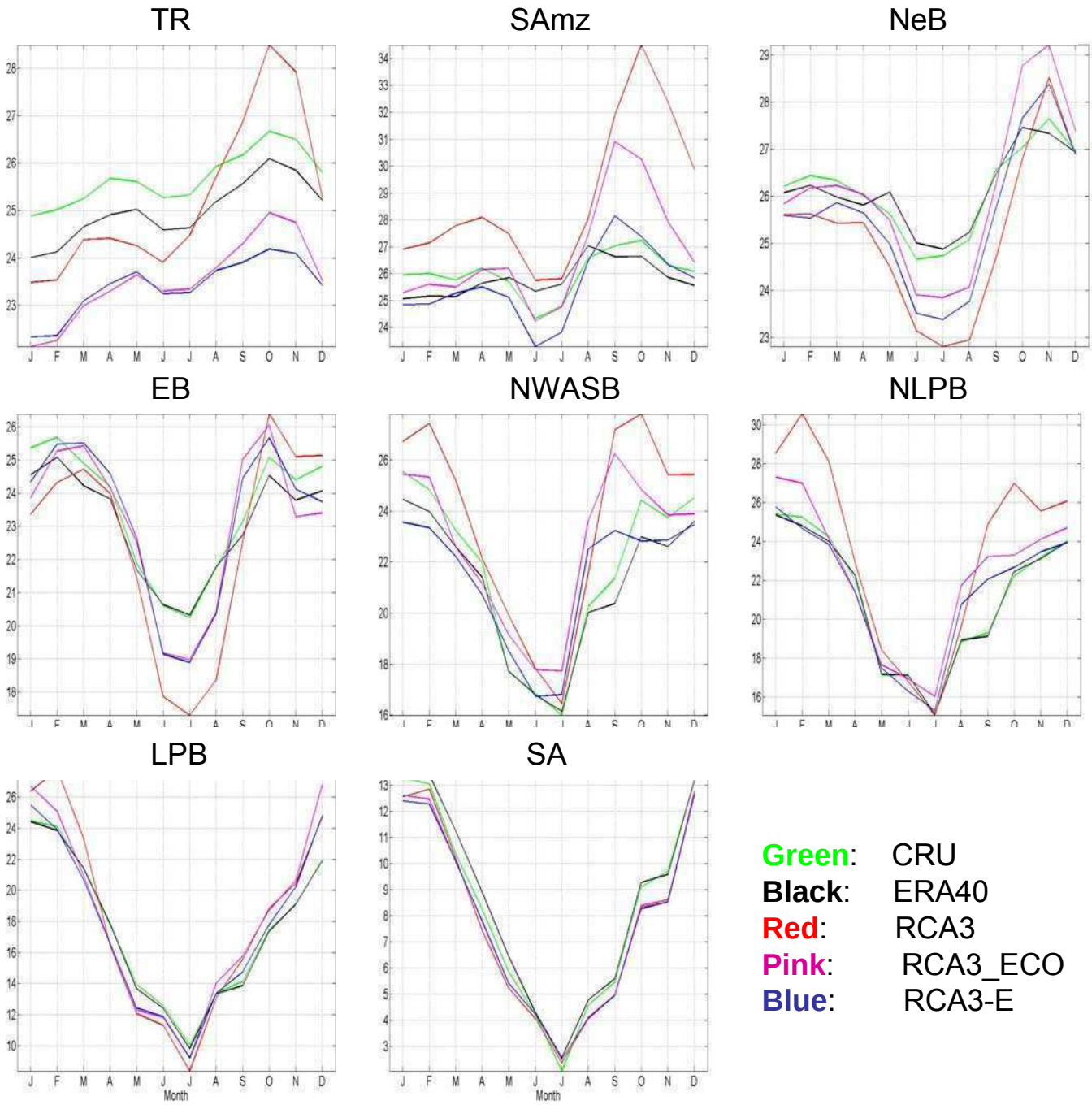

Figure 3.5: Annual cycles of t2m (°C). Note different scales on the y-axis.

CLOUD COVER

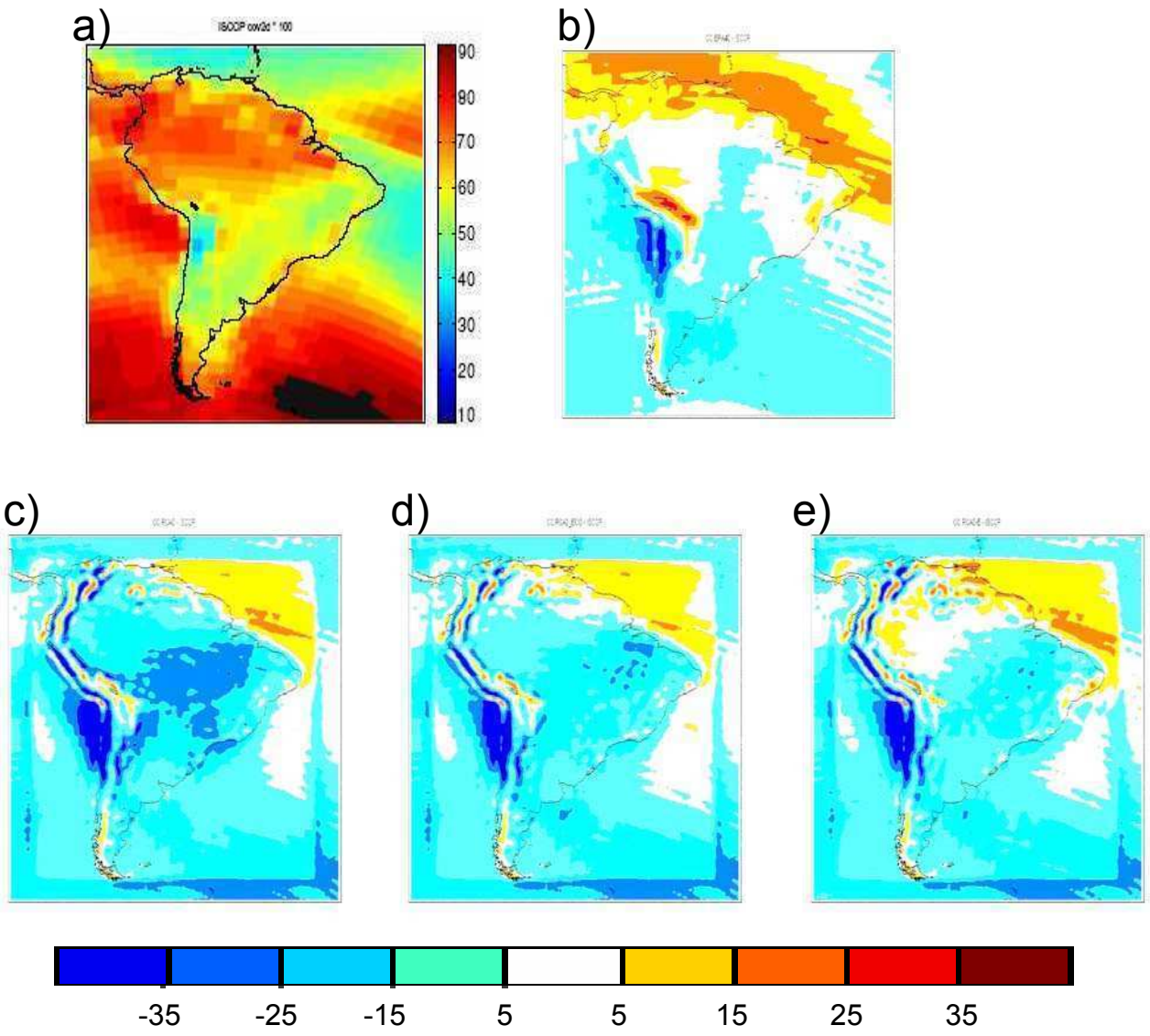

Figure 3.6: Annual cloud cover (percentage), a) ISCCP, biases relative to ISCCP for b) ERA40, c) RCA3, d) RCA3_ECO and e) RCA3-E.

T2M MEAN AND INTERNAL VARIABILITY

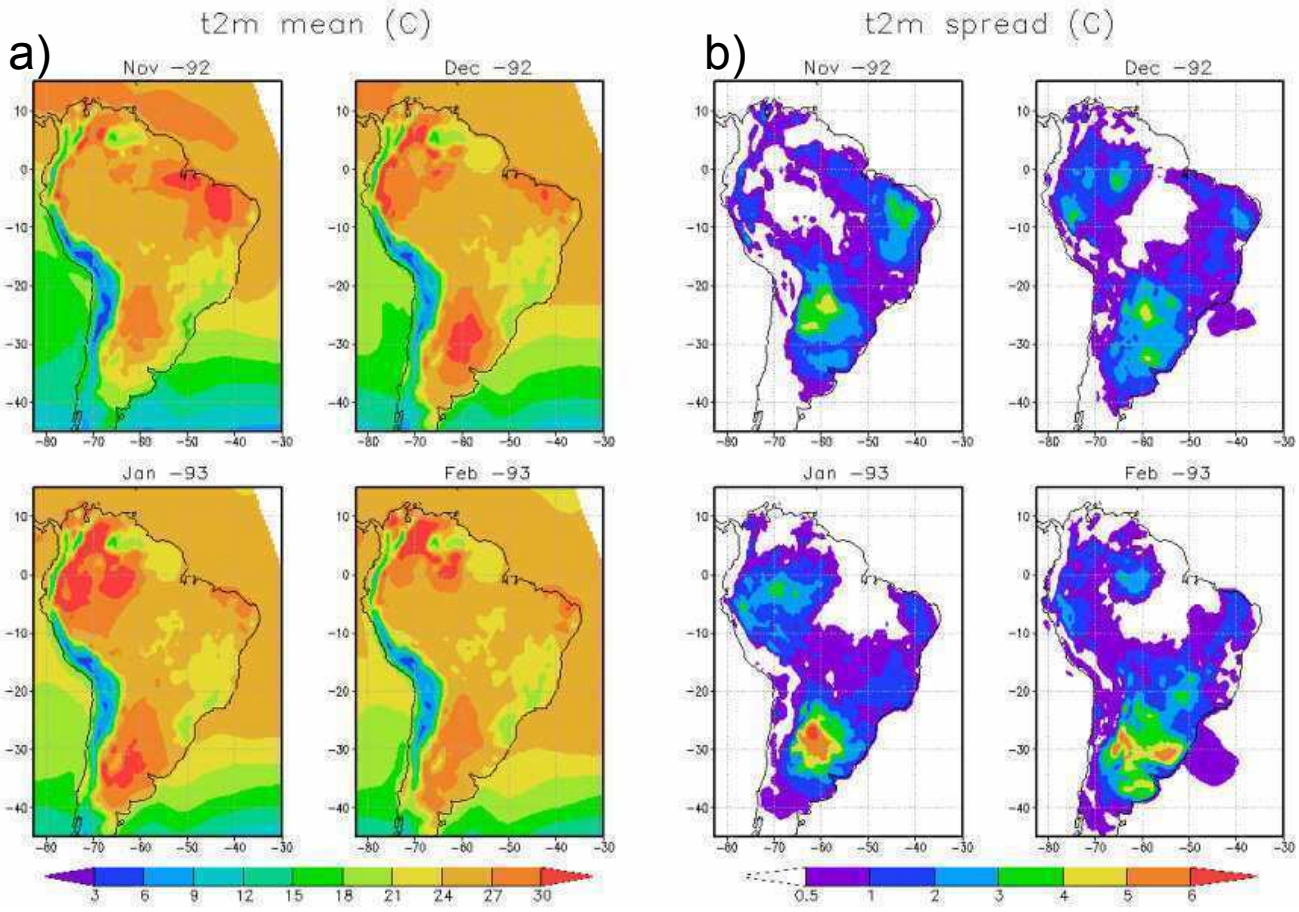

Figure 4.1: a) Monthly means of t2m (C°) for Nov -92 to Feb -93. b) Ensemble spread as a measure of model internal variability.

PRECIPITATION MEAN AND INTERNAL VARIABILITY

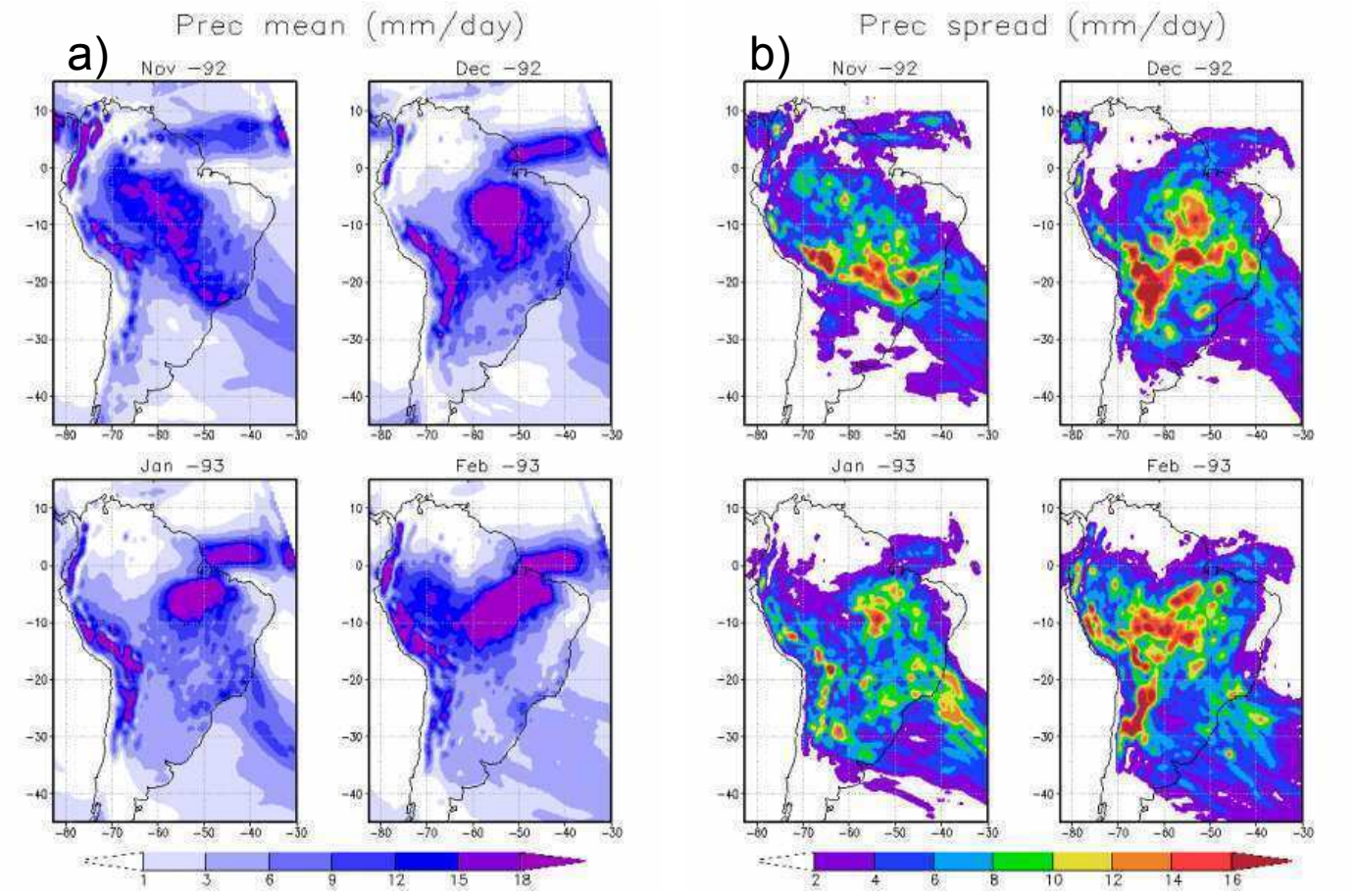

Figure 4.2: a) Monthly means of precipitation for Nov -92 to Feb -93 (mm/day). b) Ensemble spread as a measure of model internal variability.

GRID POINT DISTRIBUTIONS OF INTERNAL VARIABILITY

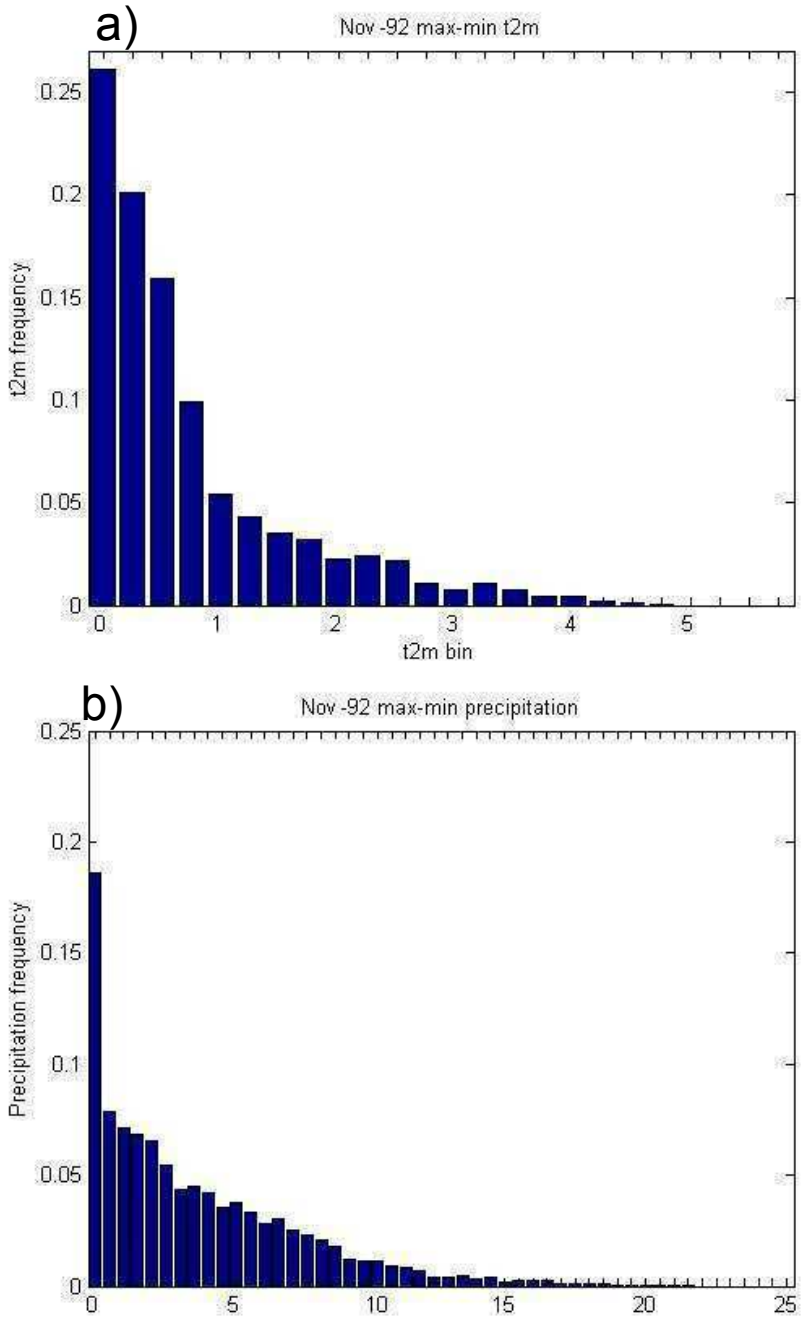

Figure 4.3: Distributions of internal variability grid point-by-gridpoint for a) t2m (C°) and b) precipitation (mm/day)for the whole continent excluding the Andes for November.

ACCUMULATED DISTRIBUTIONS OF INTERNAL VARIABILITY

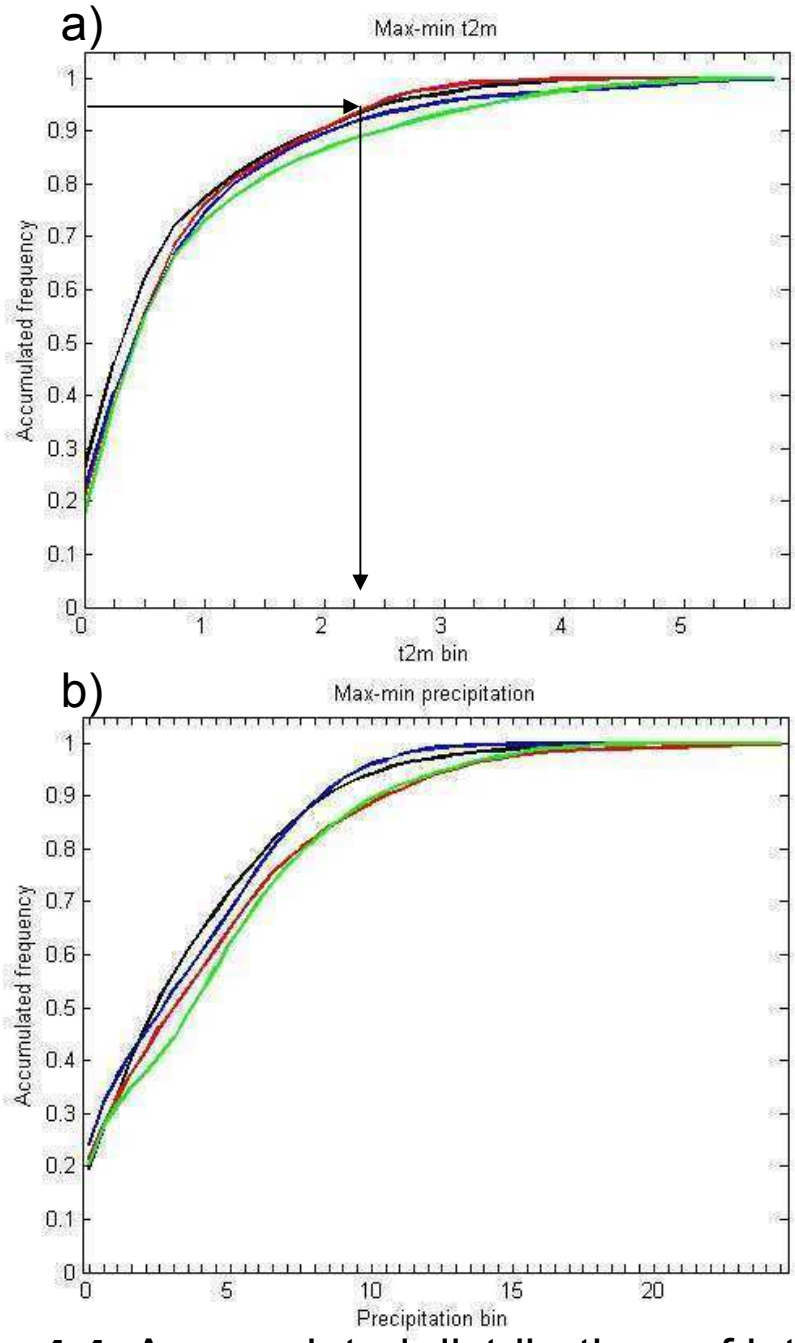

Figure 4.4: Accumulated distributions of internal variability of a) t2m and b) precipitation. November – black, December – red, January – blue and February – green. The arrows in a) indicate how the 95th percentile (ΔT) is calculated.

Chapter 5

SOIL MOSTURE EVOLUTION

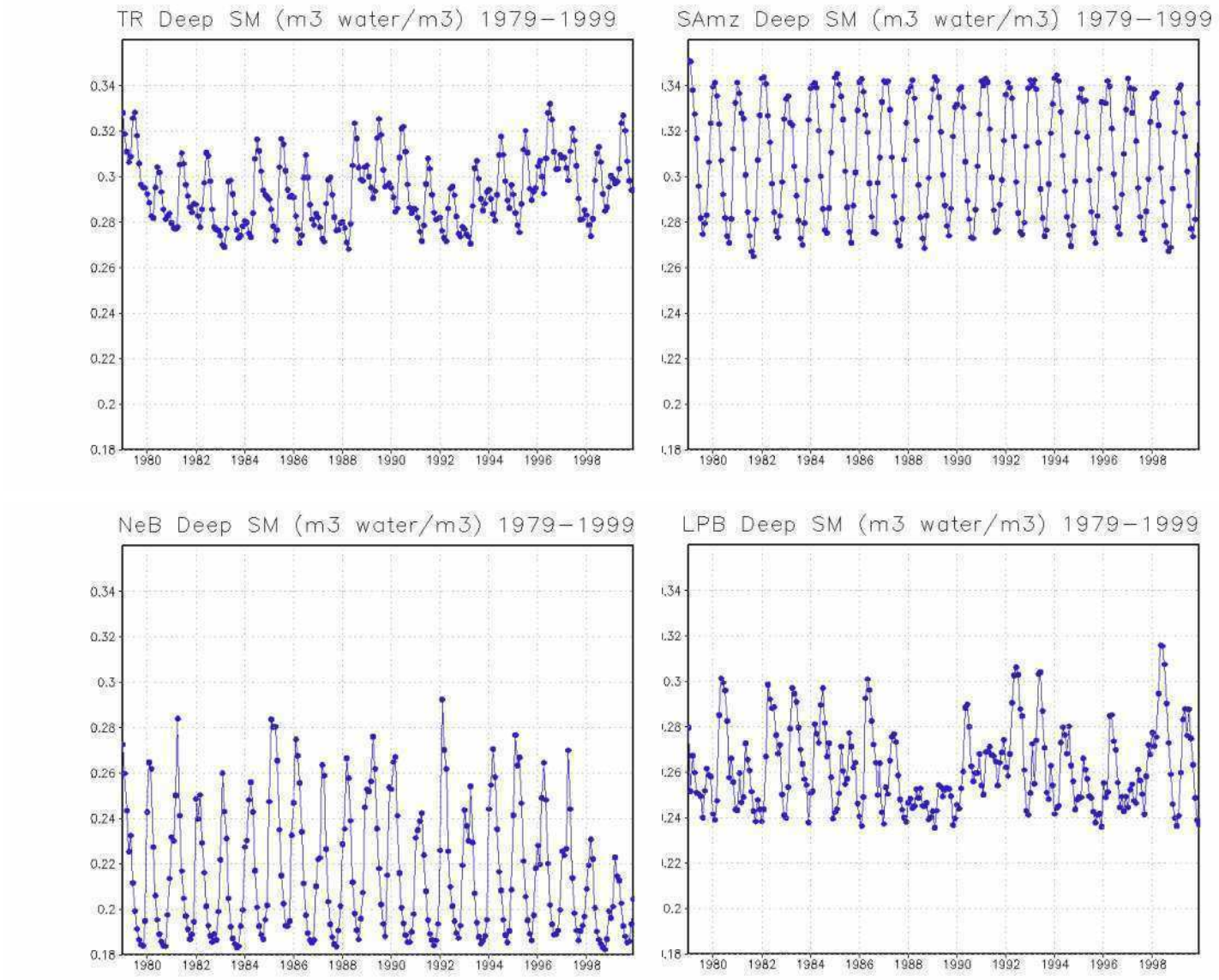

Figure 5.1:Deep soil moisture monthly evolution from January 1979 (initialization of the simulation) to December 1999 for regions a) TR, b) SAmz, c) NeB and d) LPB.

PRECIPITATION – SEASONAL MEANS

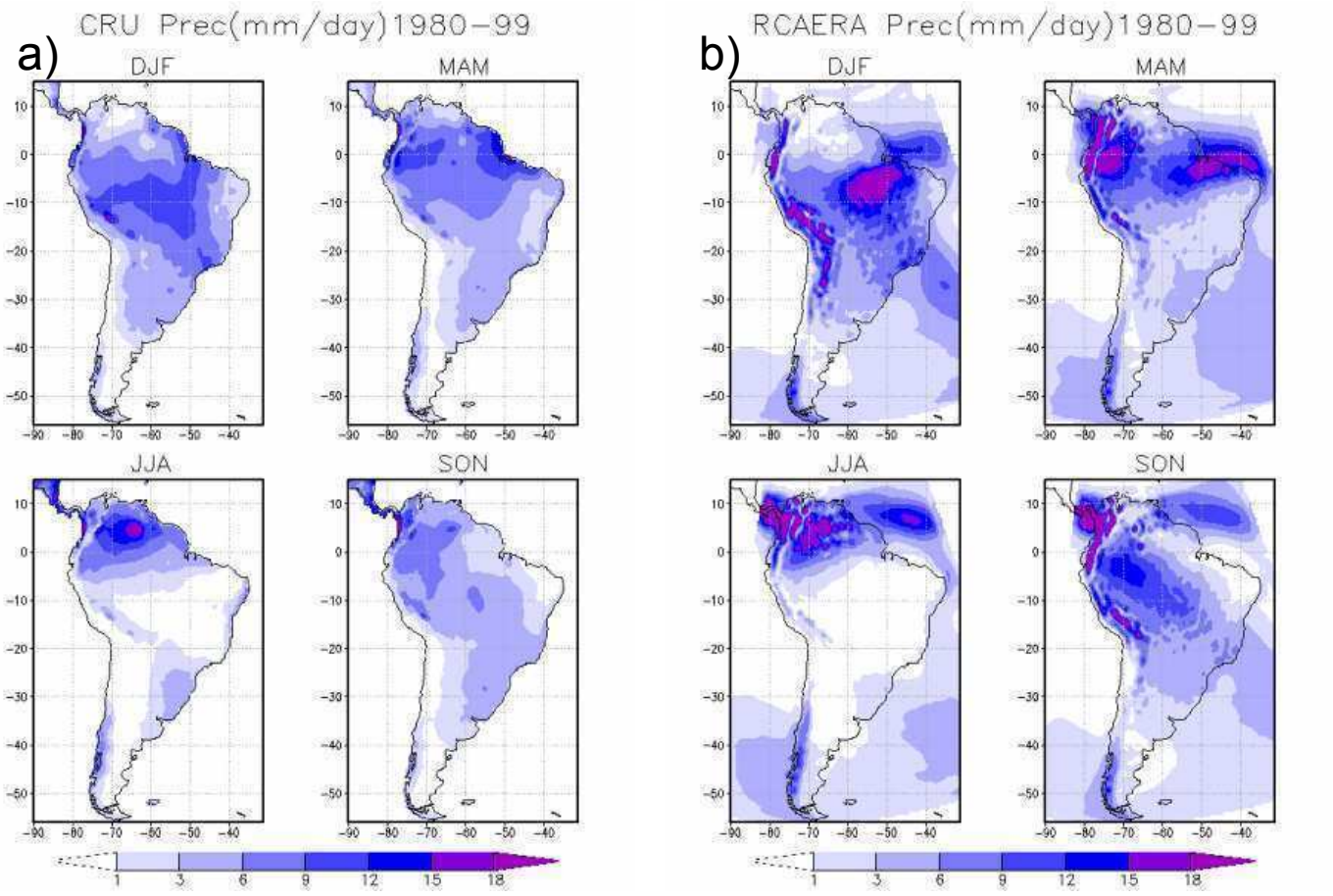

Figure 5.2: Seasonal means of precipitation 1980-1999 for a) CRU b) RCAERA.

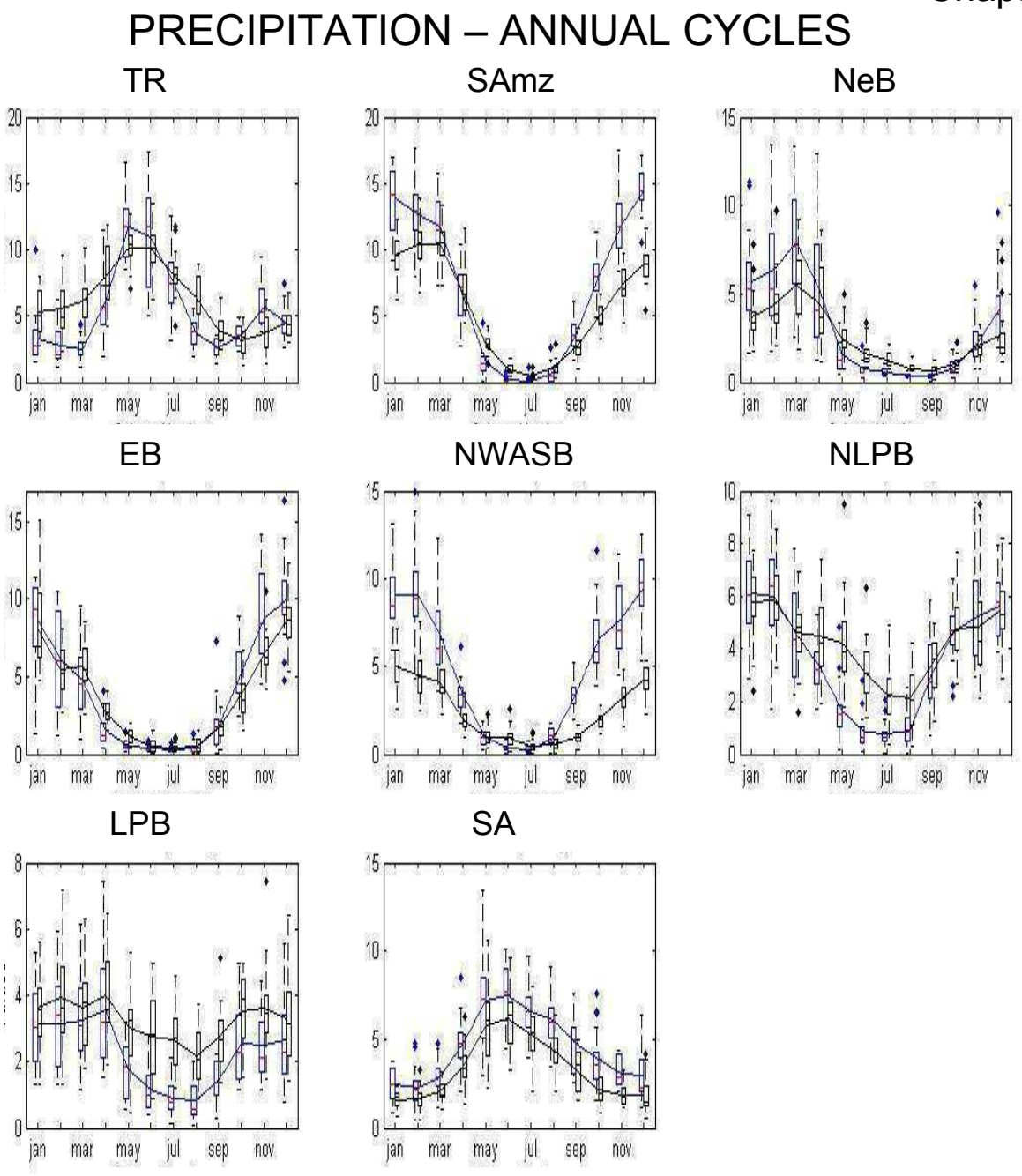

Figure 5.3: Annual cycles of precipitation (mm/day), note different scales for different regions) together with boxplots representing the interannual variability of each month. Black – CRU, Blue – RCAERA. The boxes have lines at the lower quartile, median, and upper quartile values. The whiskers are lines extending from each end of the box to show the extent of the rest of the data. The dots mark outliers beyond the ends of the whiskers.

PRECIPITATION – ANNUAL MEANS

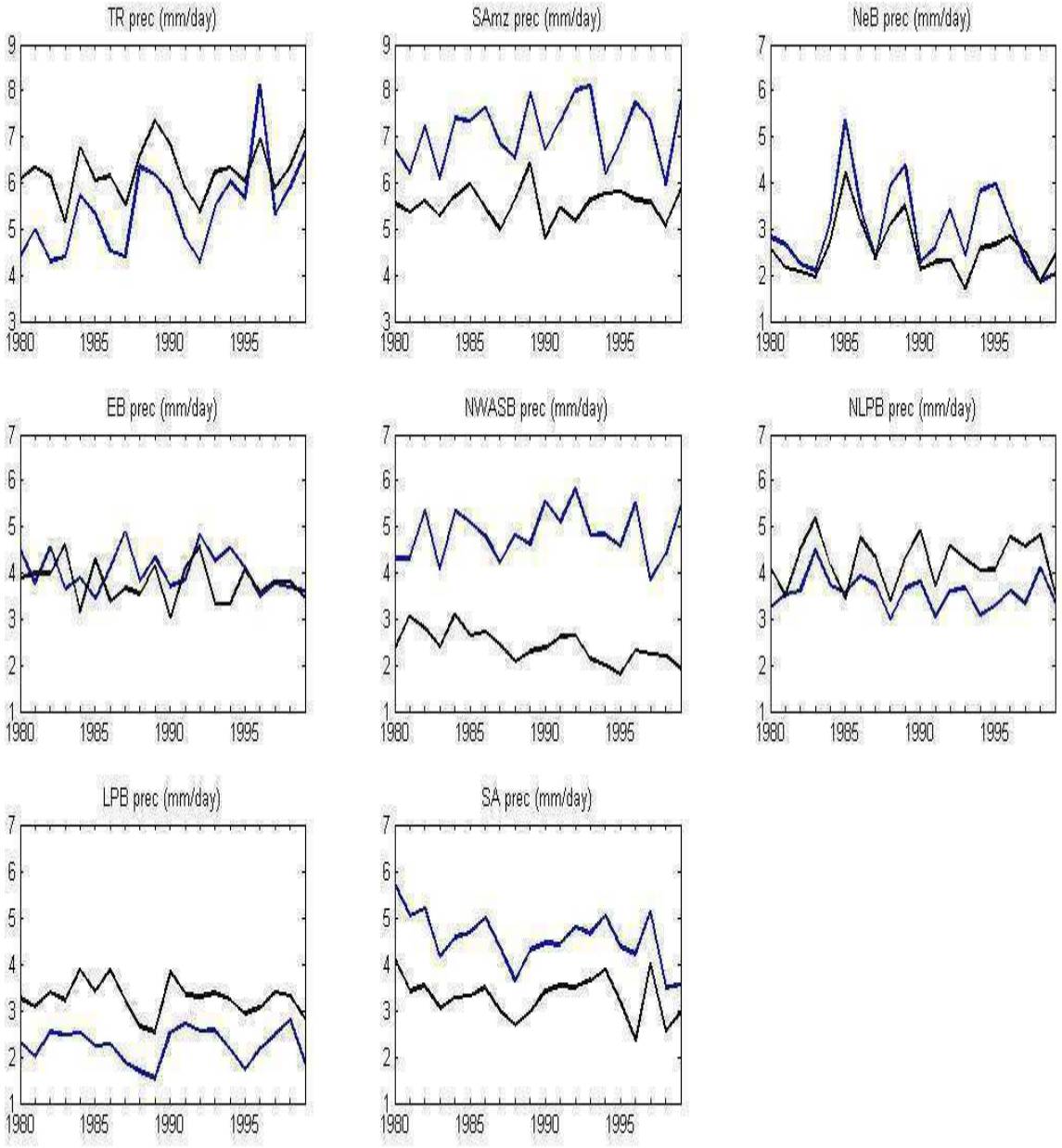

Figure 5.4: Annual means of precipitation (mm/day) for the whole simulation period (1980-1999). Black – CRU, Blue – RCAERA.

PRECIPITATION – EVOLUTION DURING THE SAMS

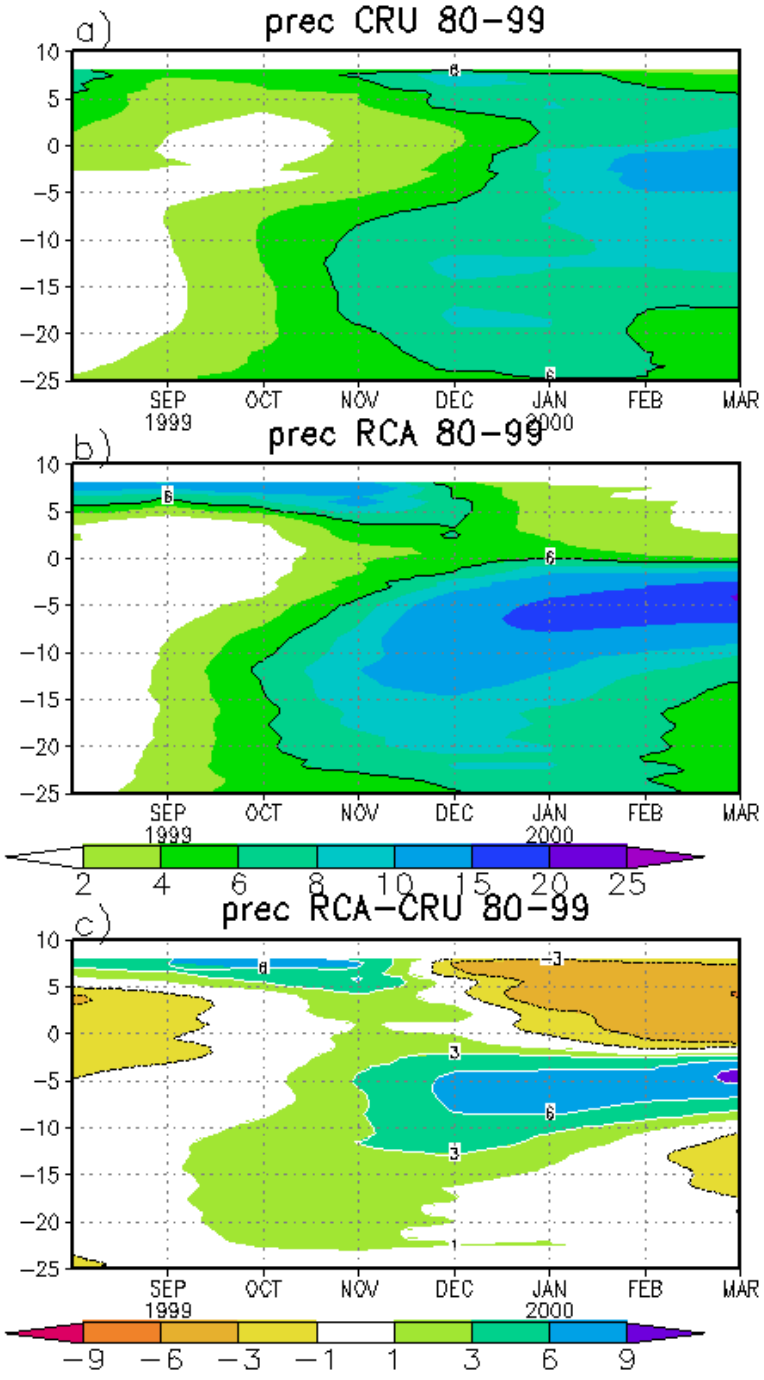

Figure 5.5: Evolution of the August-March precipitation (mm/day) 1980-1999 between 60°W and 40°W, a) CRU, b) RCAERA, c) RCAERA bias. In a) and b) the isoline 6 mm/day is highlighted for clarity. Y-axes show latitude.

T2M – SEASONAL MEANS

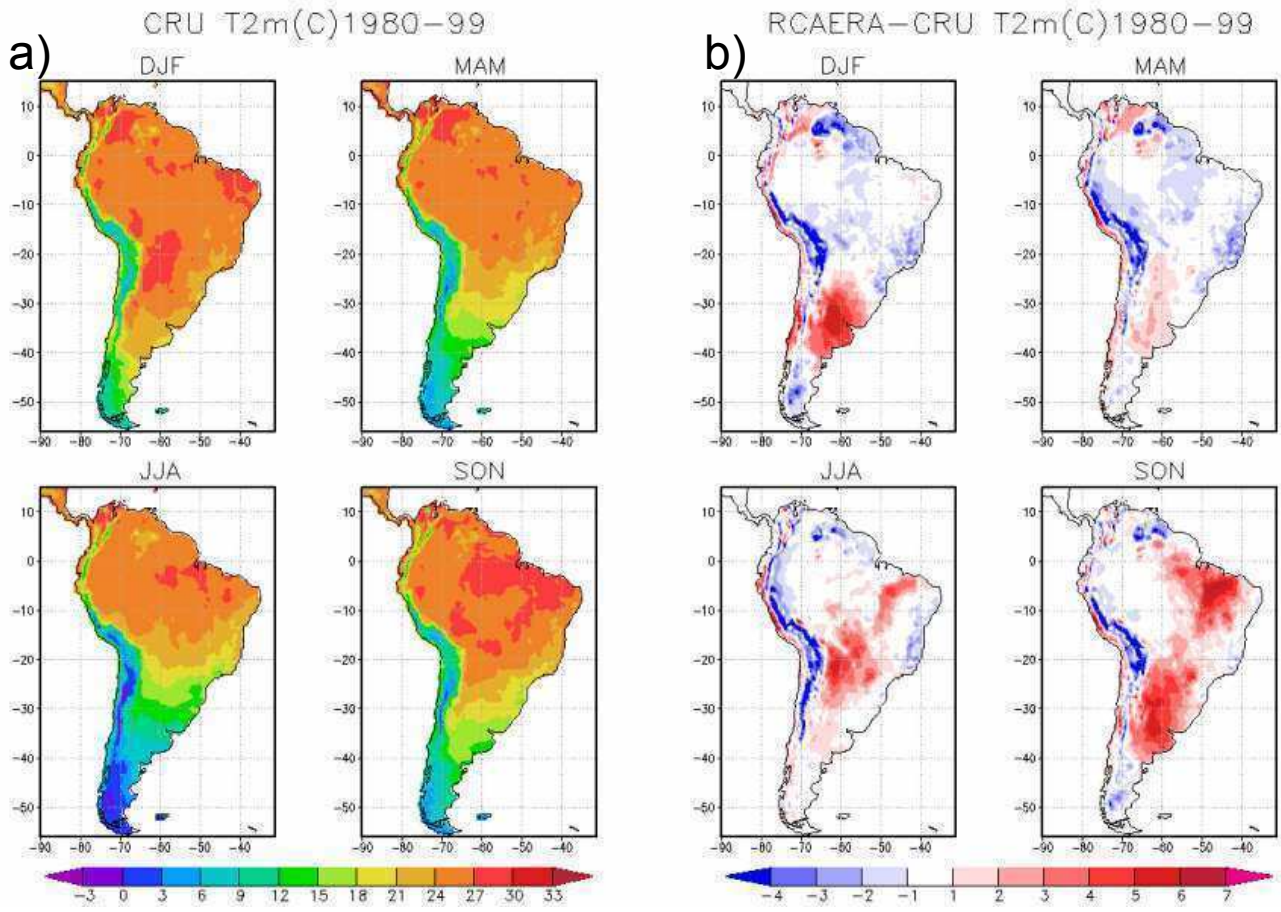

Figure 5.6: Seasonal means of t2m (C°) 1980-1999 for a) CRU b) RCAERA bias.

T2M – ANNUAL CYCLES

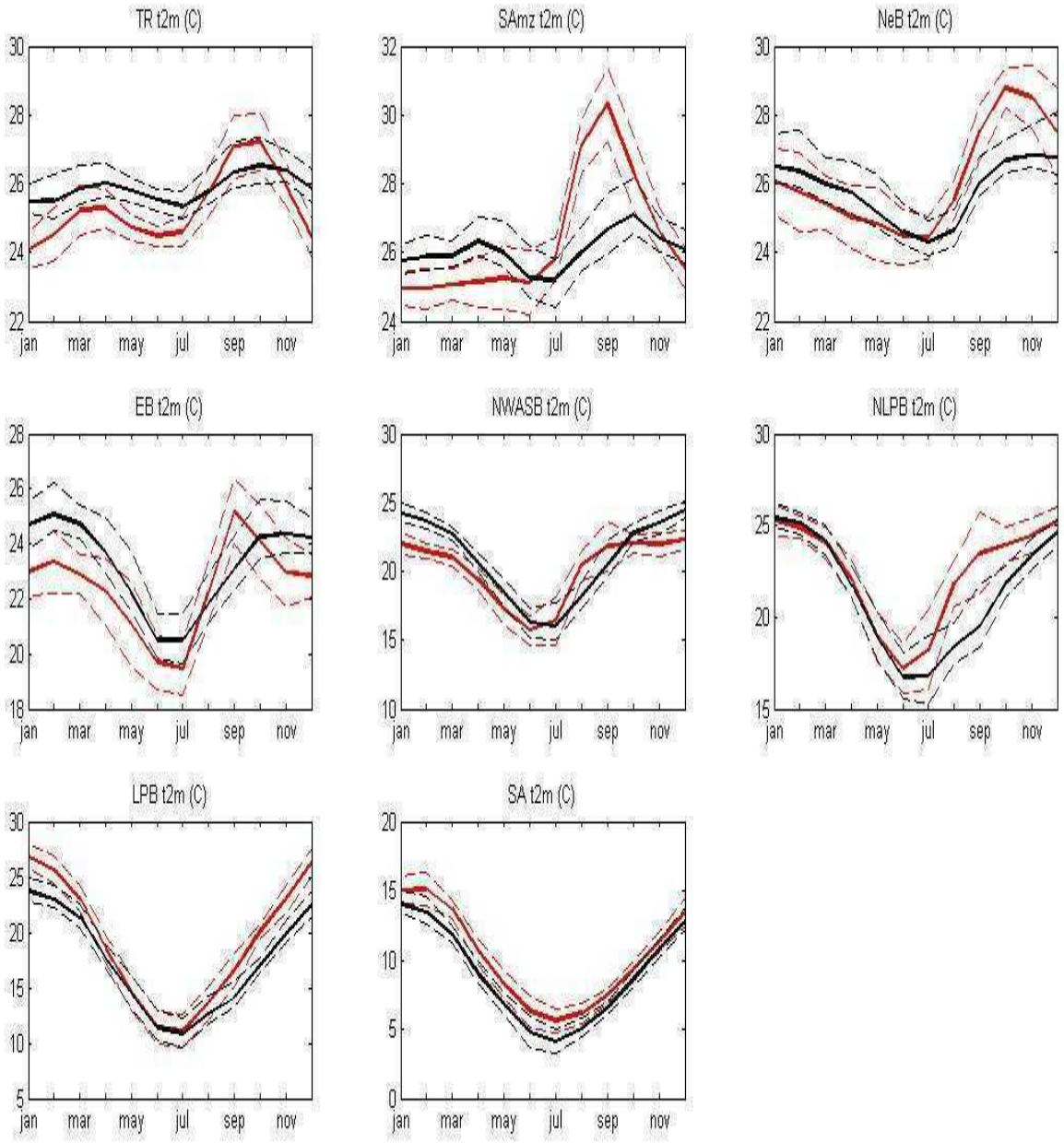

Figure 5.7: Annual cycles of t2m together with the standard deviation of each month. Black – CRU, Red – RCAERA. Solid lines are monthly means and dashed lines indicate the standard deviation.

T2M – ANNUAL MEANS

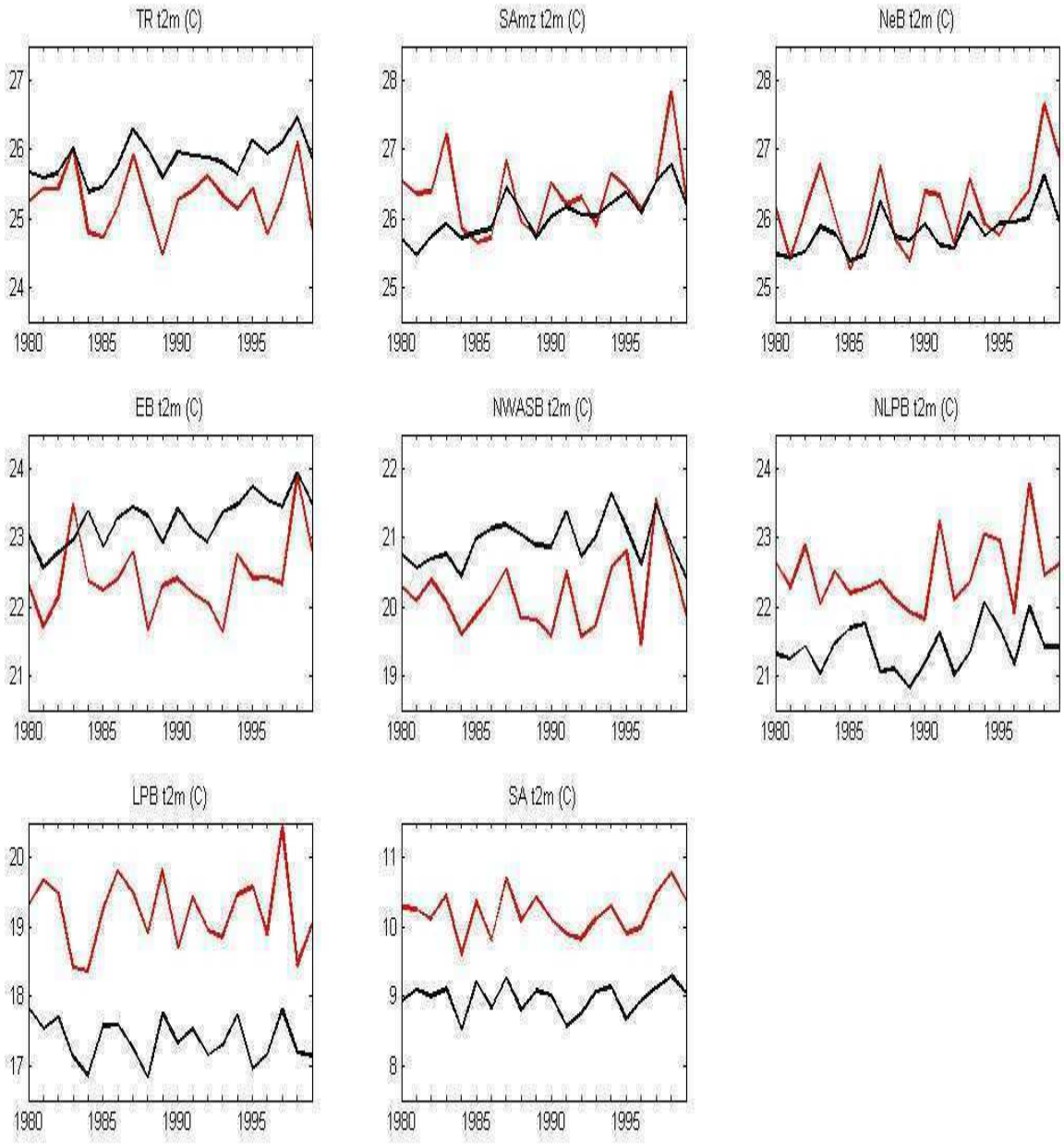

Figure 5.8: Annual means of t2m for the whole simulation period (1980-1999). Black – CRU, Red – RCAERA.

TOTAL COLUMN WATER - SEASONAL MEANS

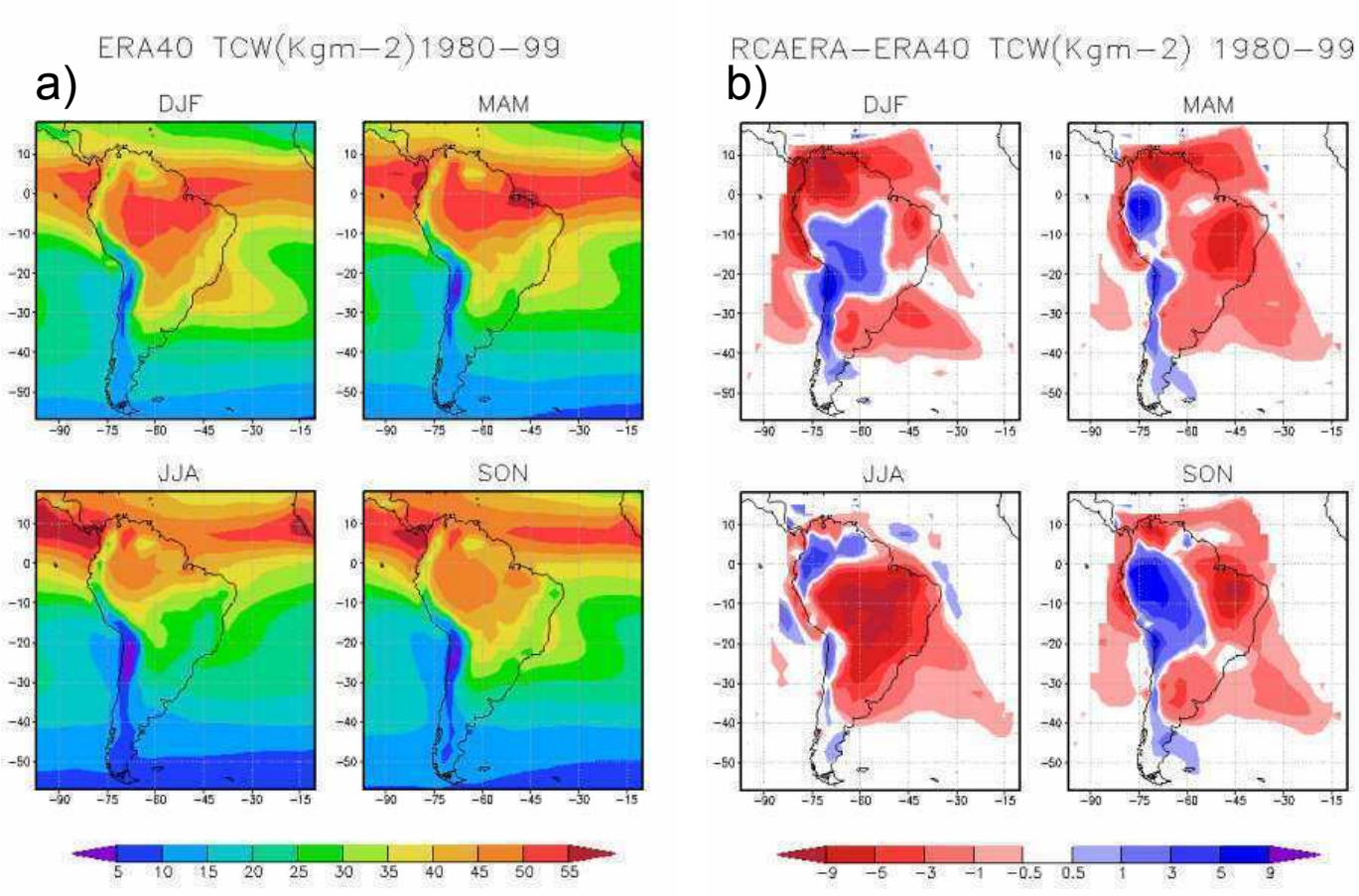

Figure 5.9: Seasonal means total column water 1980-1999 for a) ERA40 b) RCAERA – ERA40.

850hPa VINDS - SEASONAL MEANS

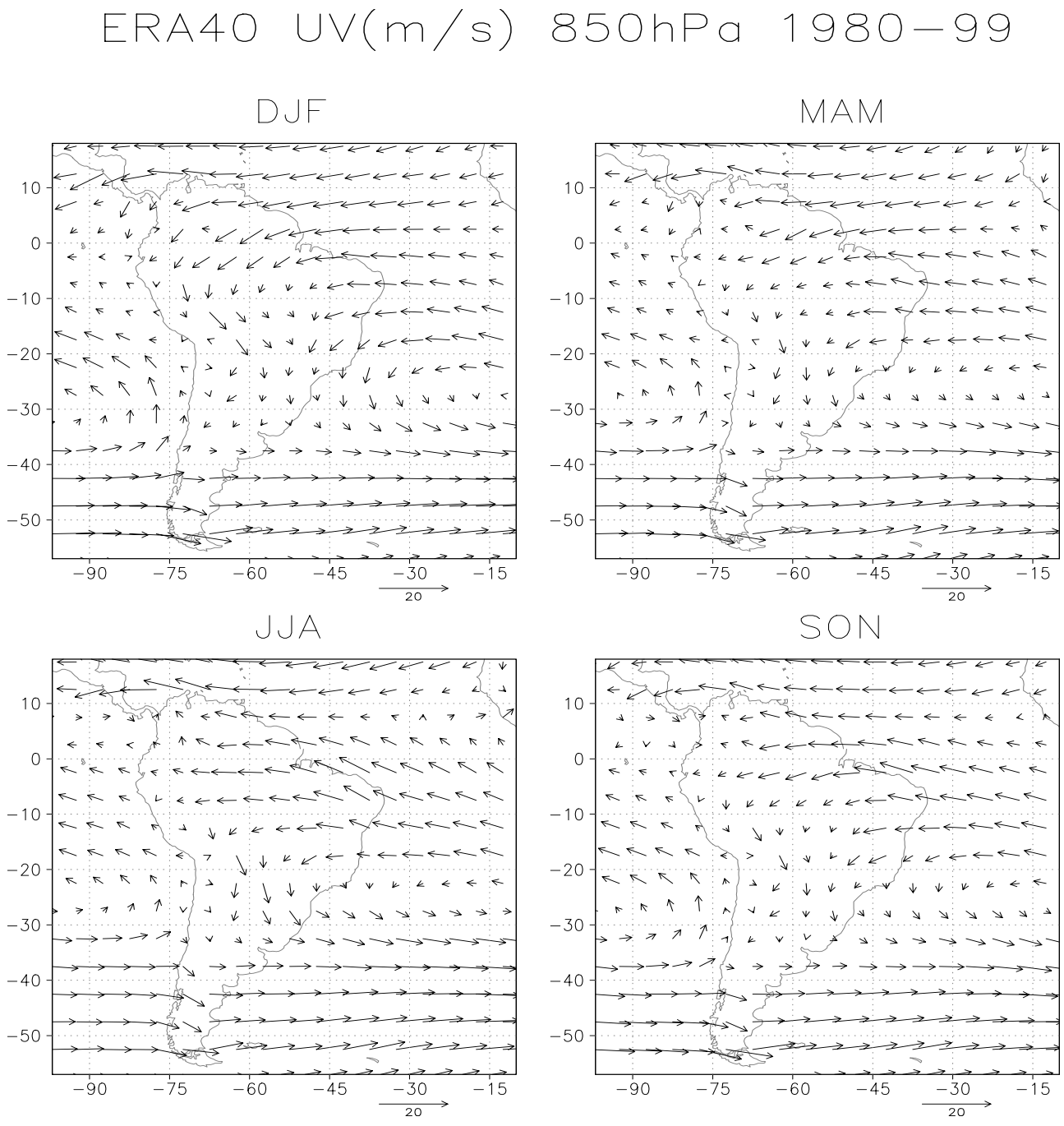

Figure 5.10a: Seasonal means of 850hPa vinds 1980-1999 for ERA40 (scale 20 m/s).

850hPa VINDS - SEASONAL MEANS

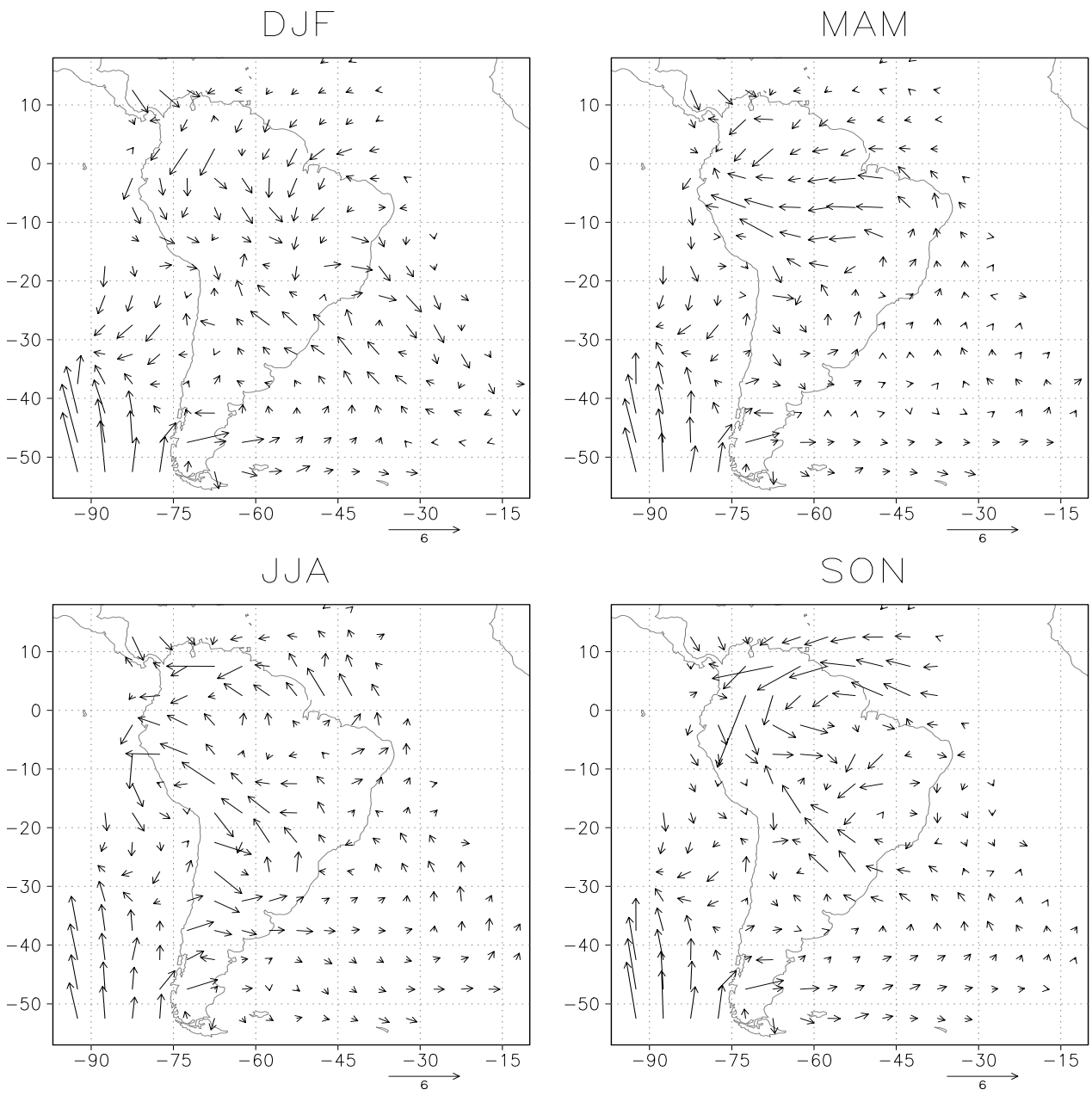

Figure 5.10b: Seasonal mean RCAERA biases of of 850hPa vinds 1980-1999 (scale 6 m/s).

PRECIPITATION - SEASONAL MEANS

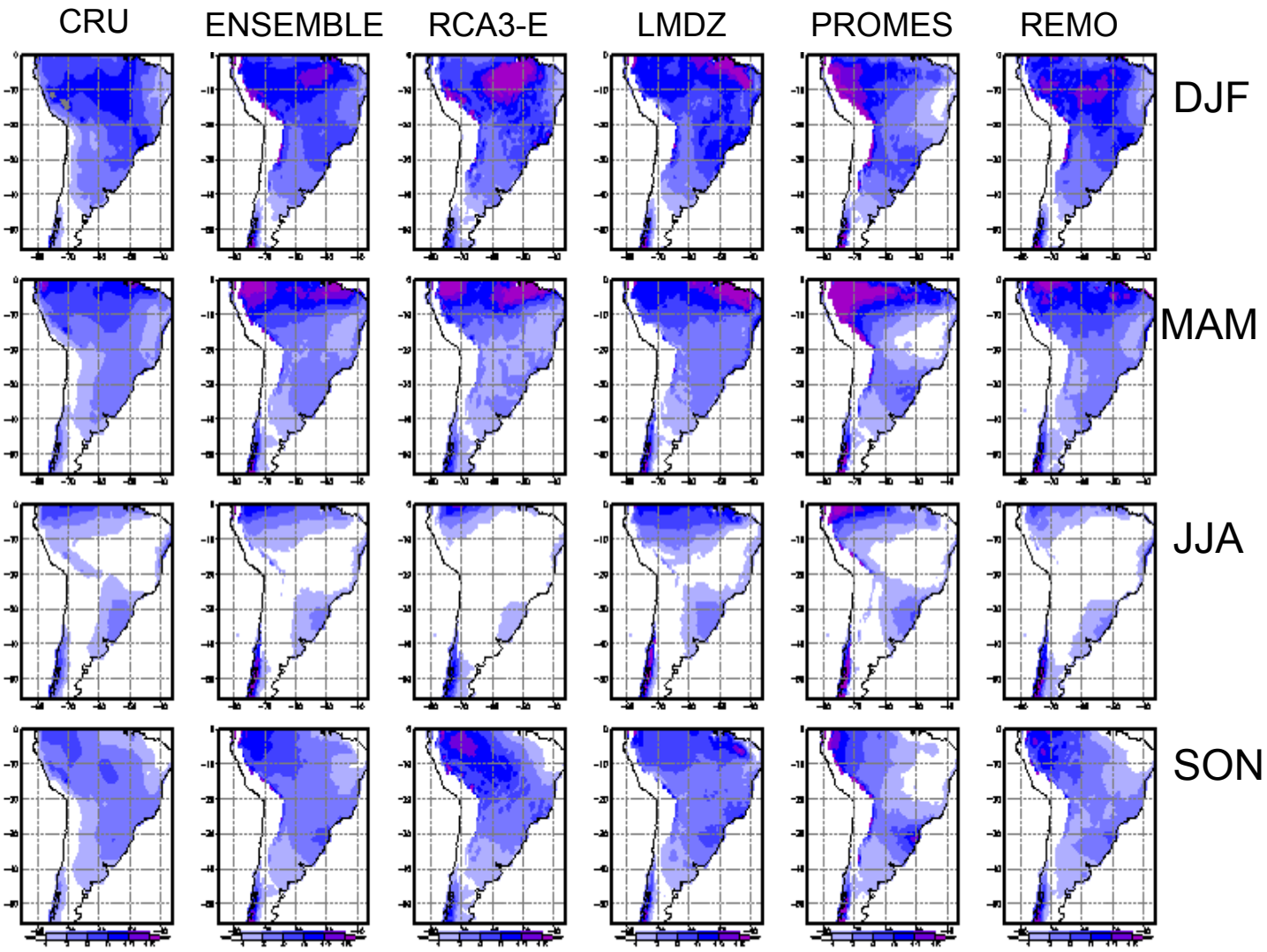

Figure 5.11: Seasonal precipitaton means (mm/day) of CRU, ensemble and of each model.

T2M - SEASONAL MEANS

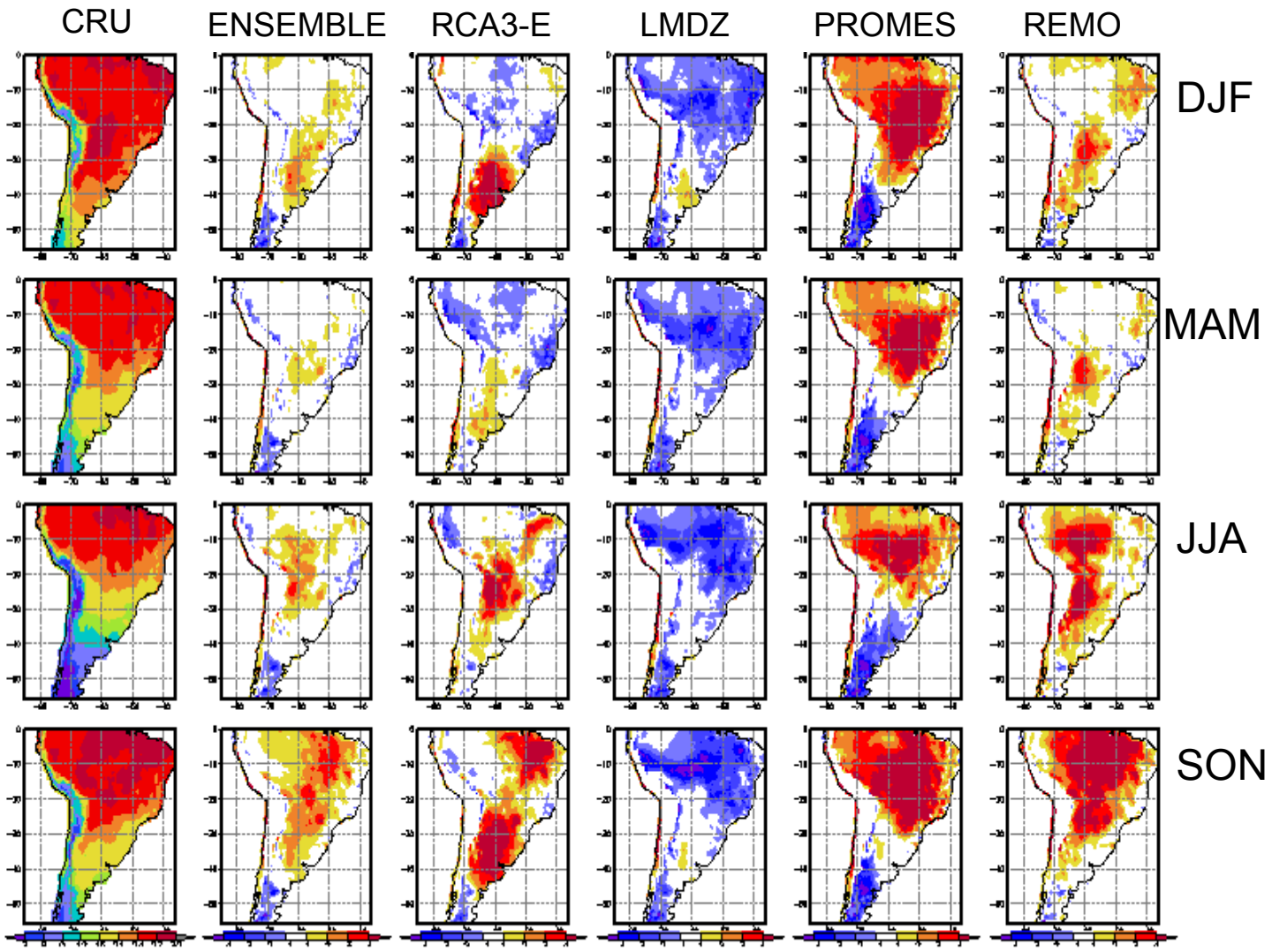

Figure 5.12: Seasonal means of CRU t2m (C°)1991-2000 and the corresponding biases of the ensemble and of each model.

INITIAL DEEP SOIL MOISTURE

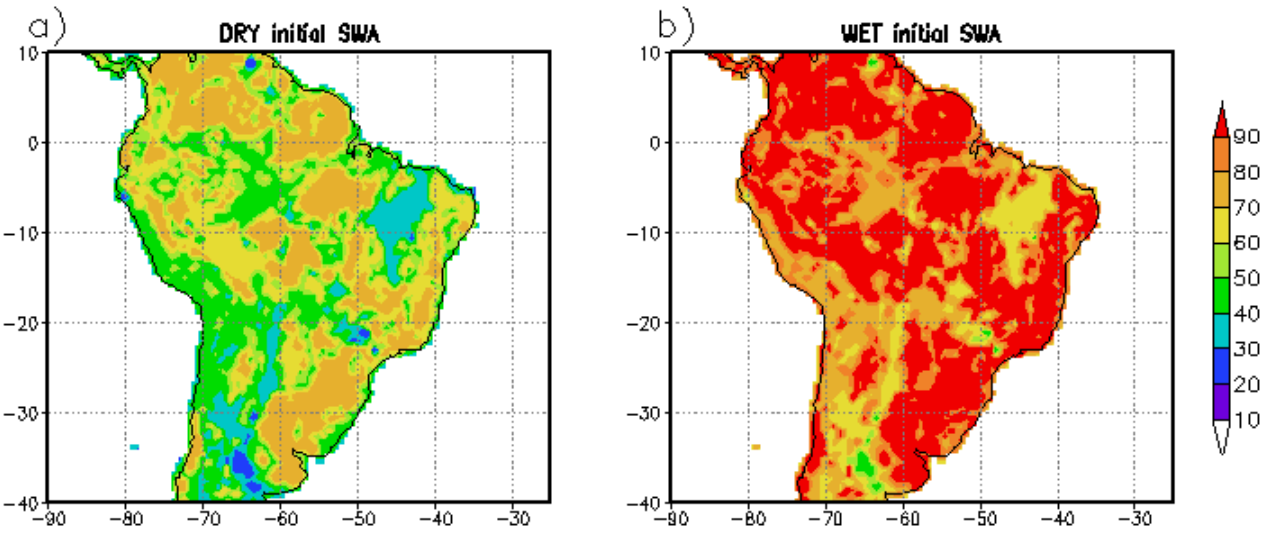

Figure 6.1: The initial deep soil moisture (% of saturation level) of the two ensembles a) DRY and b) WET.

PRECIPITATION

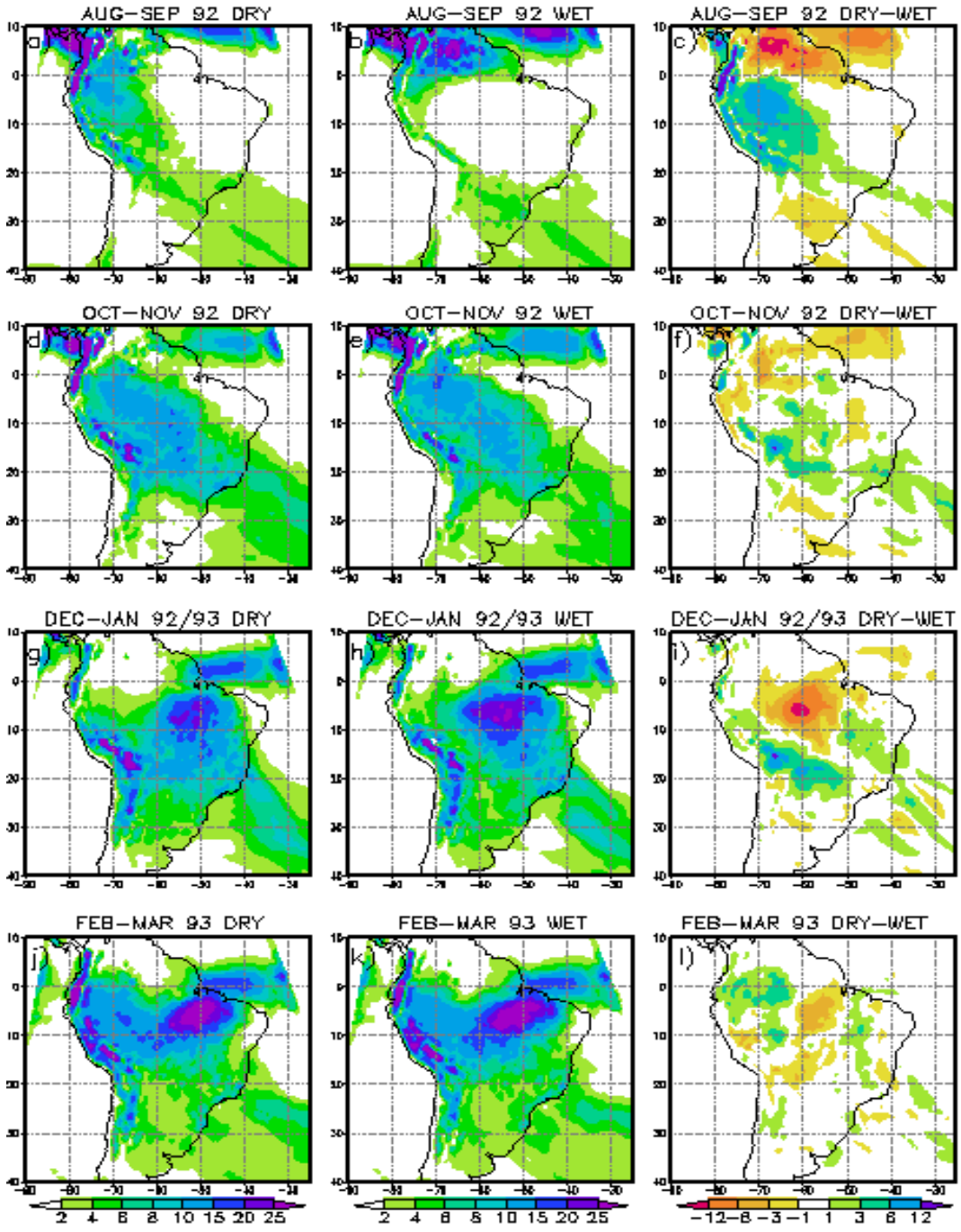

Figure 6.2: The bi-monthly development of precipitation (mm/day): Left column – DRY, middle column – WET, right column – DRY-WET.

PRECIPITATION

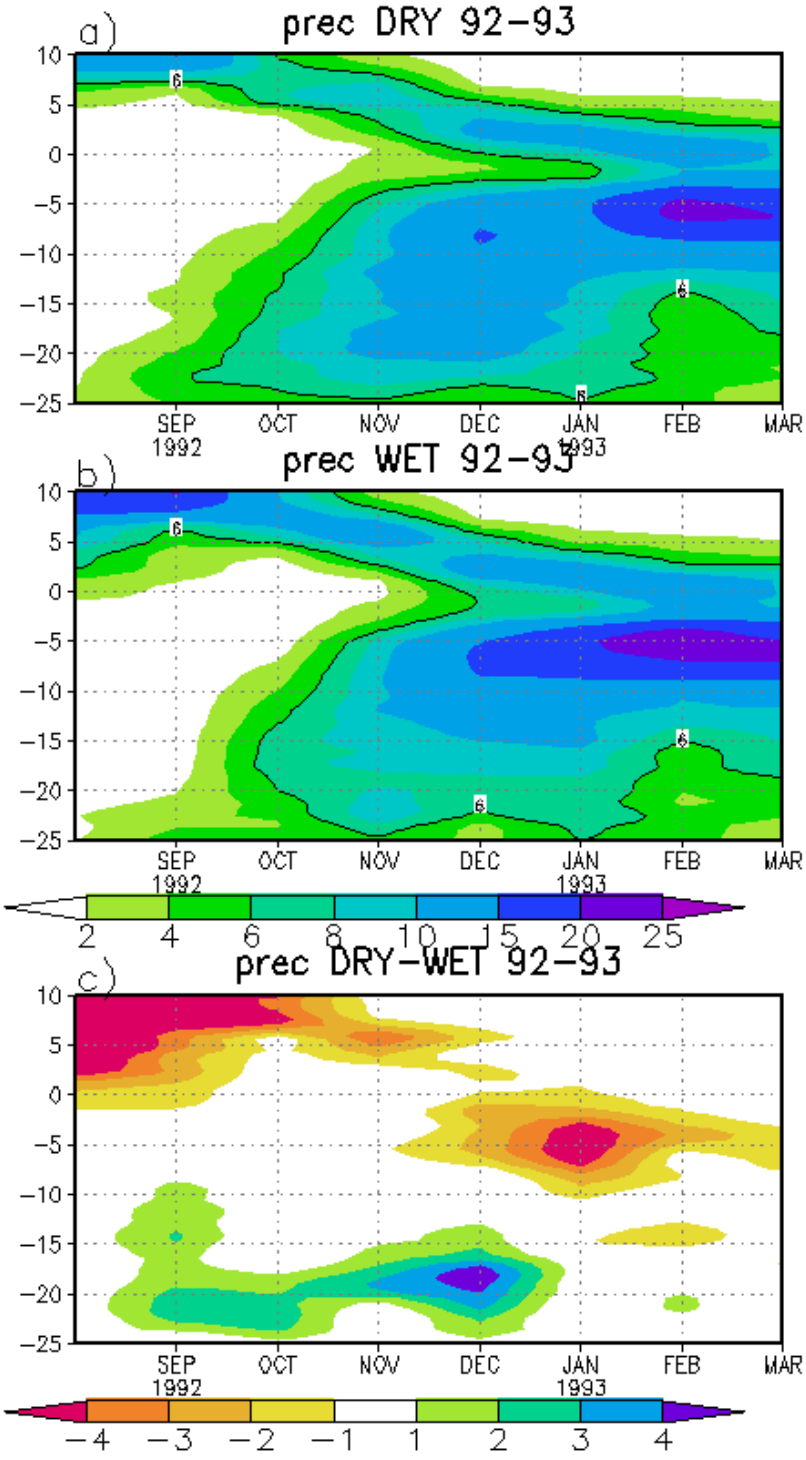

Figure 6.3: Evolution of the August-March precipitation (mm/day) 1992-93 between 60°W and 40°W, a) DRY, b) WET, c) DRY-WET. Y-axes show latitude.

850hPa TEMPERATURE AND HUMIDITY TRANSPORT

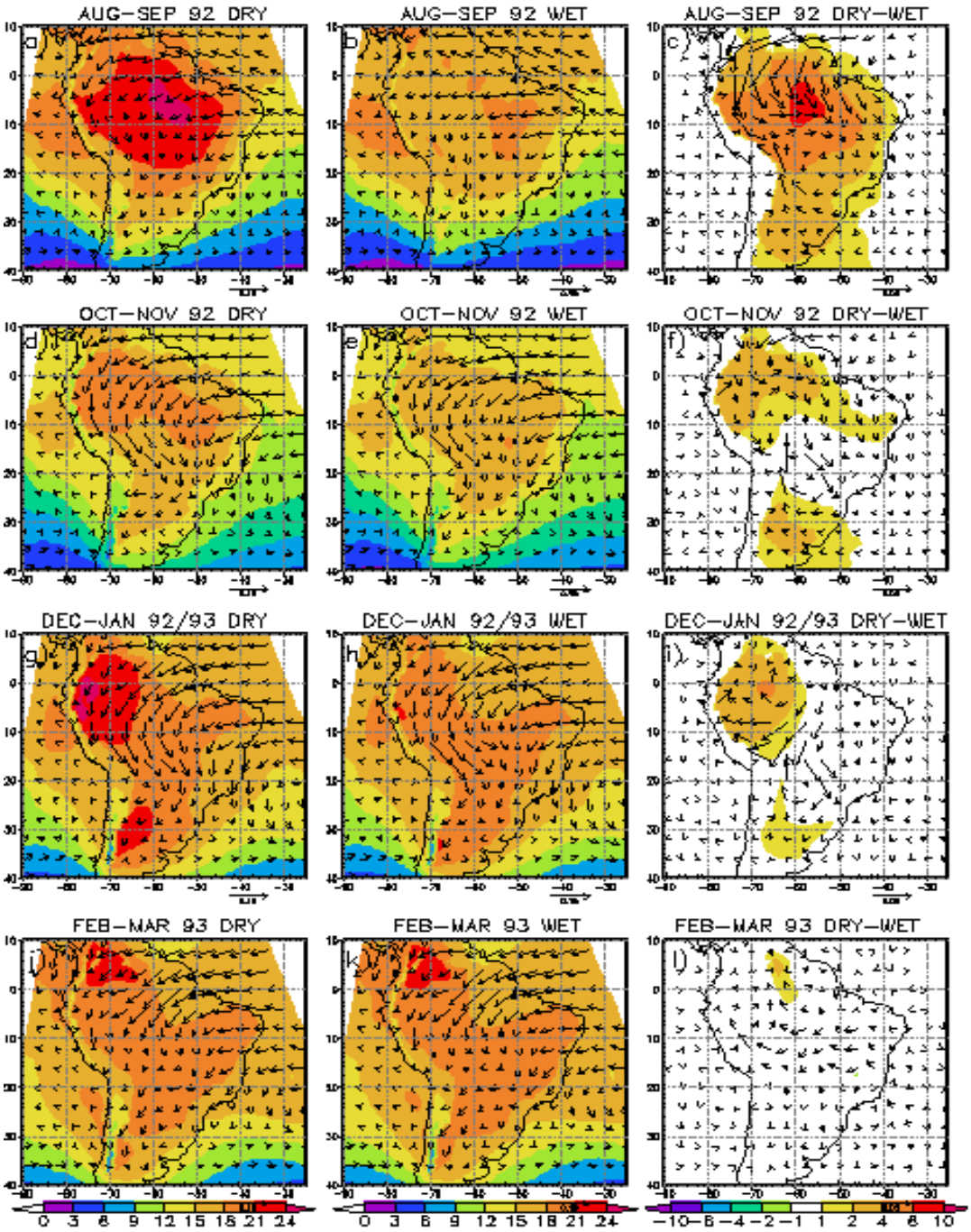

Figure 6.4: The bi-monthly development of 850hPa temperature (°C) and humidity transport (g/m²s): Left column – DRY, middle column – WET, right column – DRY-WET. Scale: length of arrow = 0.15 g/m²s.

EVAPORATIVE FRACTION

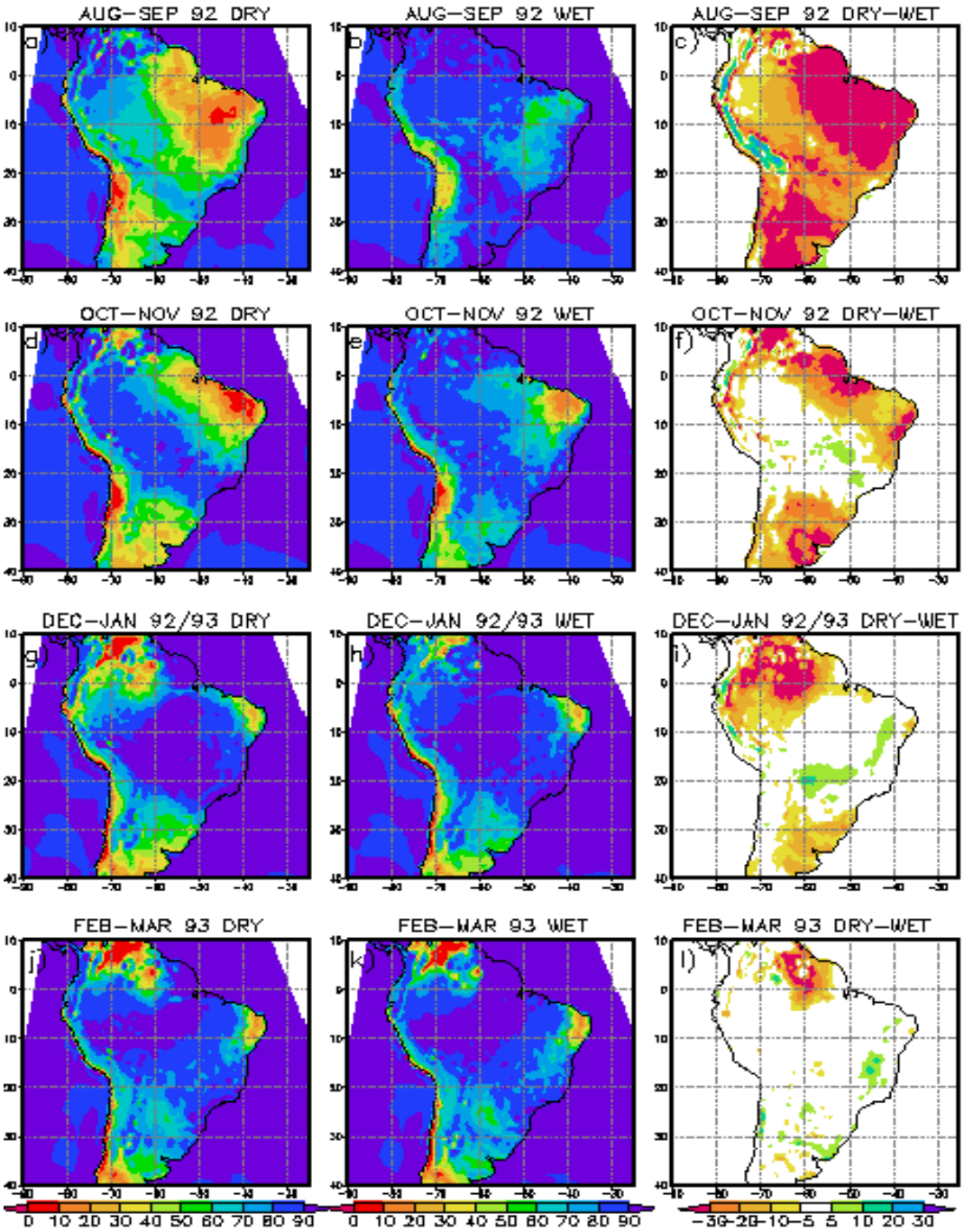

Figure 6.5: The bi-monthly development of evaporative fraction (%): Left column – DRY, middle column – WET, right column – DRY-WET.

DEEP SOIL MOISTURE

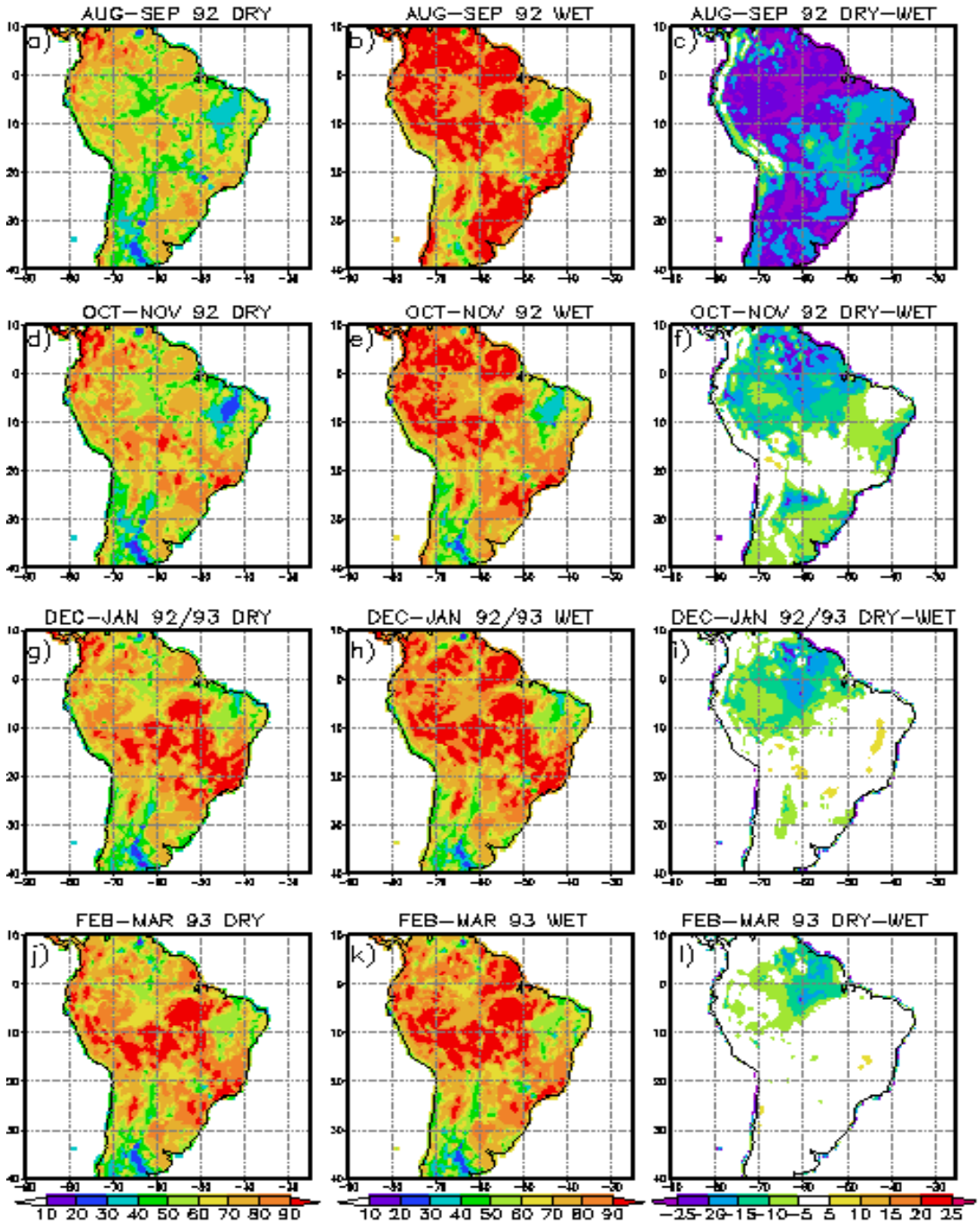

Figure 6.6: The bi-monthly development of deep soil water content (% of saturation level): Left column – DRY, middle column – WET, right column – DRY-WET.

DAILY PRECIPITATION FREQUENCY

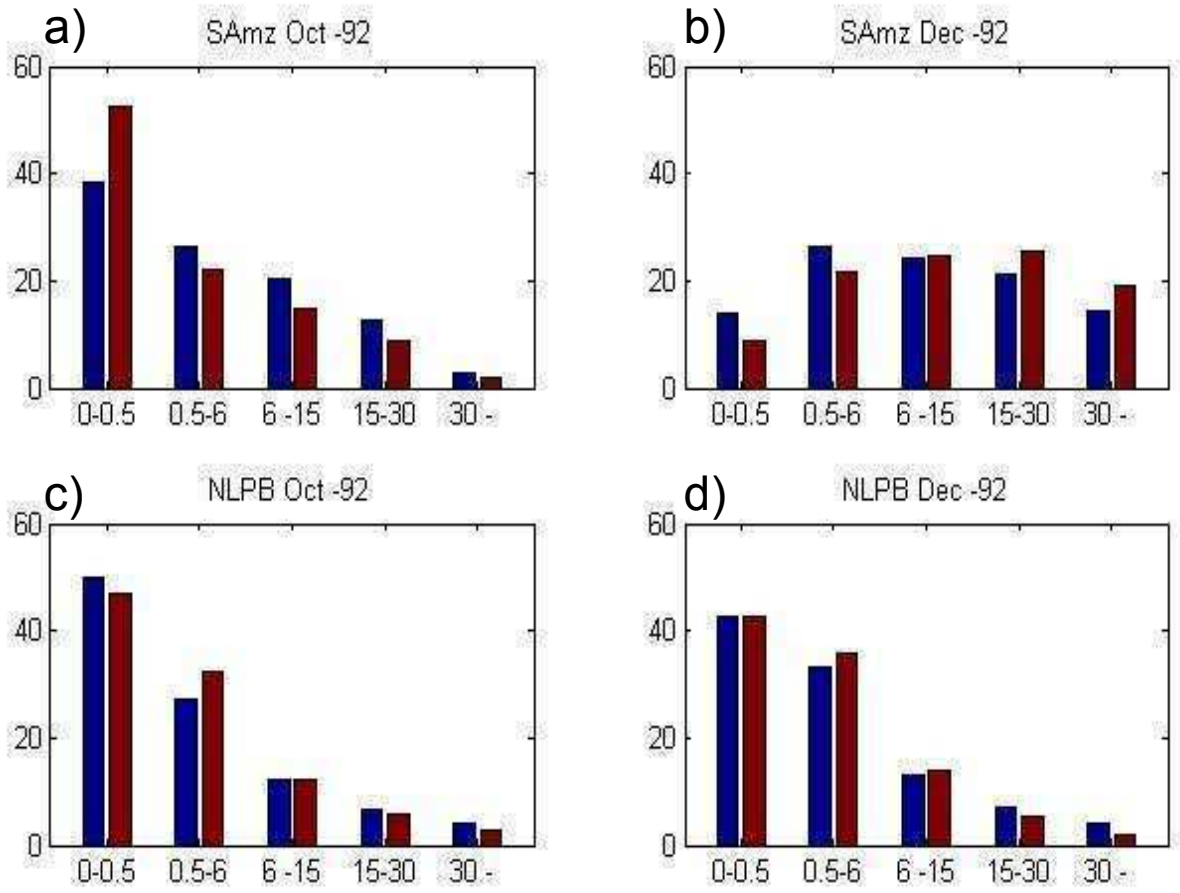

Figure 6.7: Frequency diagrams of daily precipitation (mm/day), a) SAmz region October, b) SAmz region December, c) NLPB region October, d) NLPB region December. Blue bars – DRY, Red bars – WET.

Chapter 7

SOIL DEPTH OF ECOCLIMAP

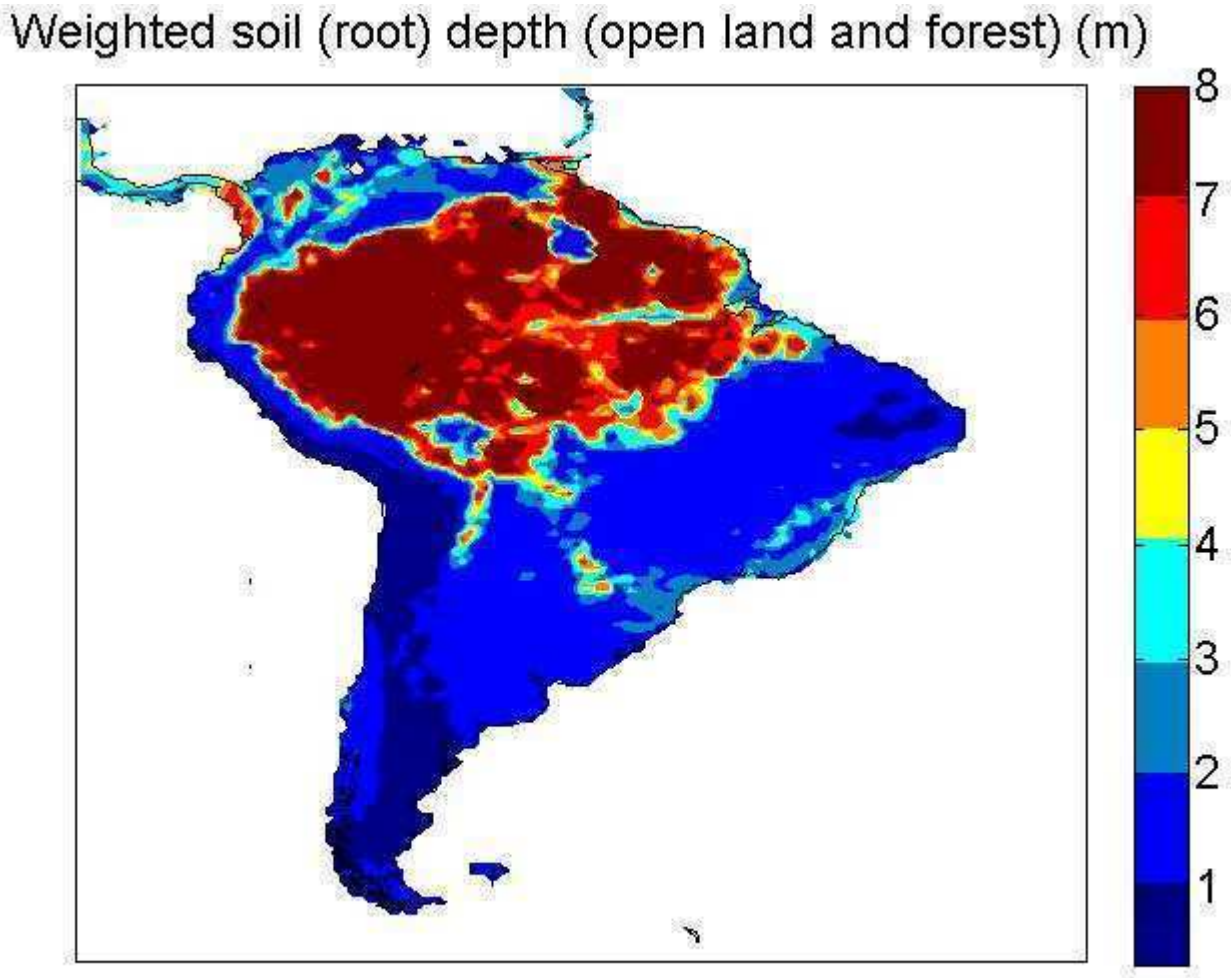

Figure 7.1: The soil depth in Ecoclimap, which is employed for the soil and the rooting depth in RCA3-E.

PRECIPITATION - SEASONAL

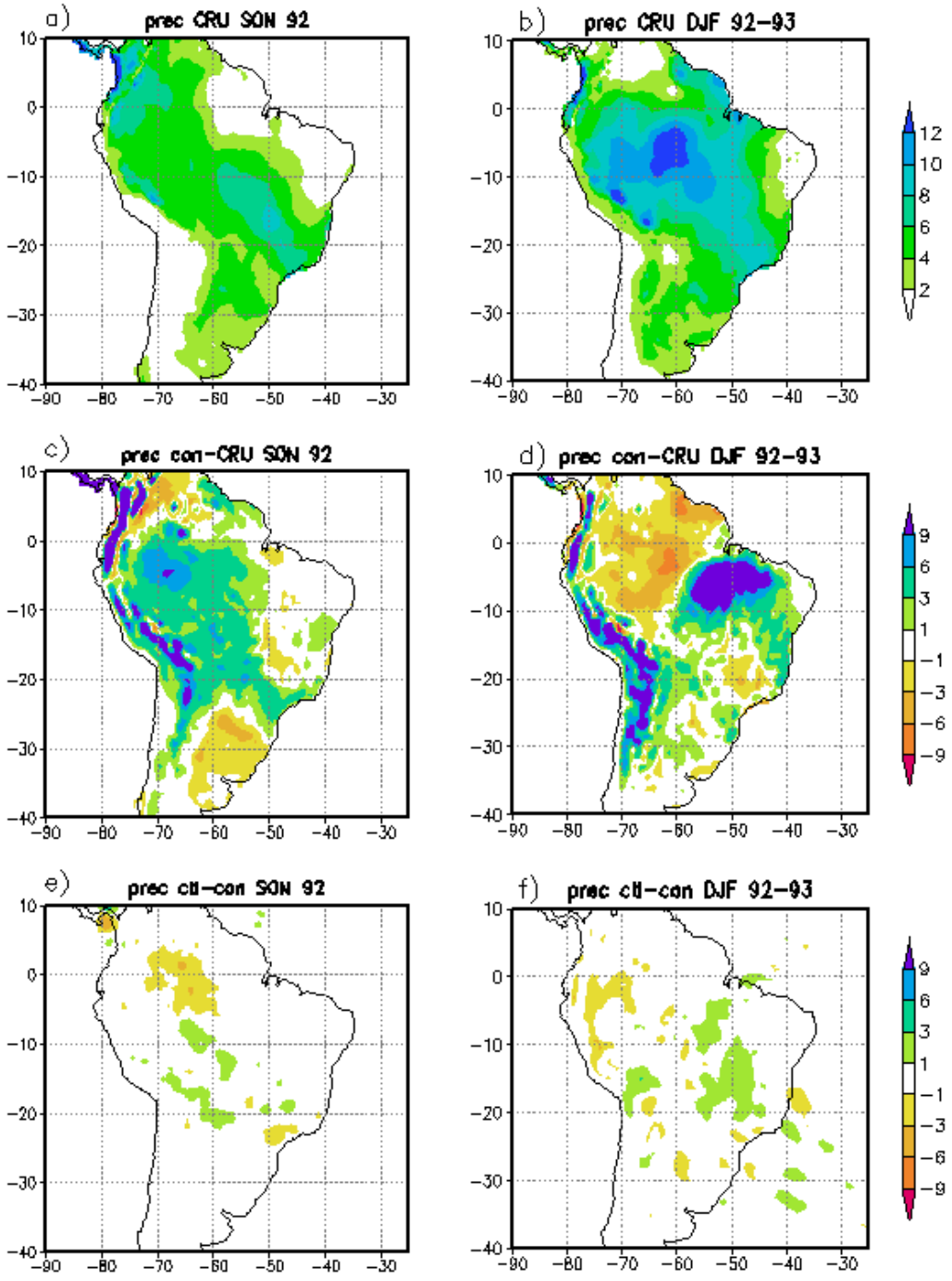

Figure 7.2: Seasonal precipitation (mm/day): left column – SON, right column – DJF. Upper panel – CRU, middel panel – CON-CRU, lower panel – CTL - CON.

PRECIPITATION – MONTLY DIFFERENCE BETWEEN ENSEMBLES

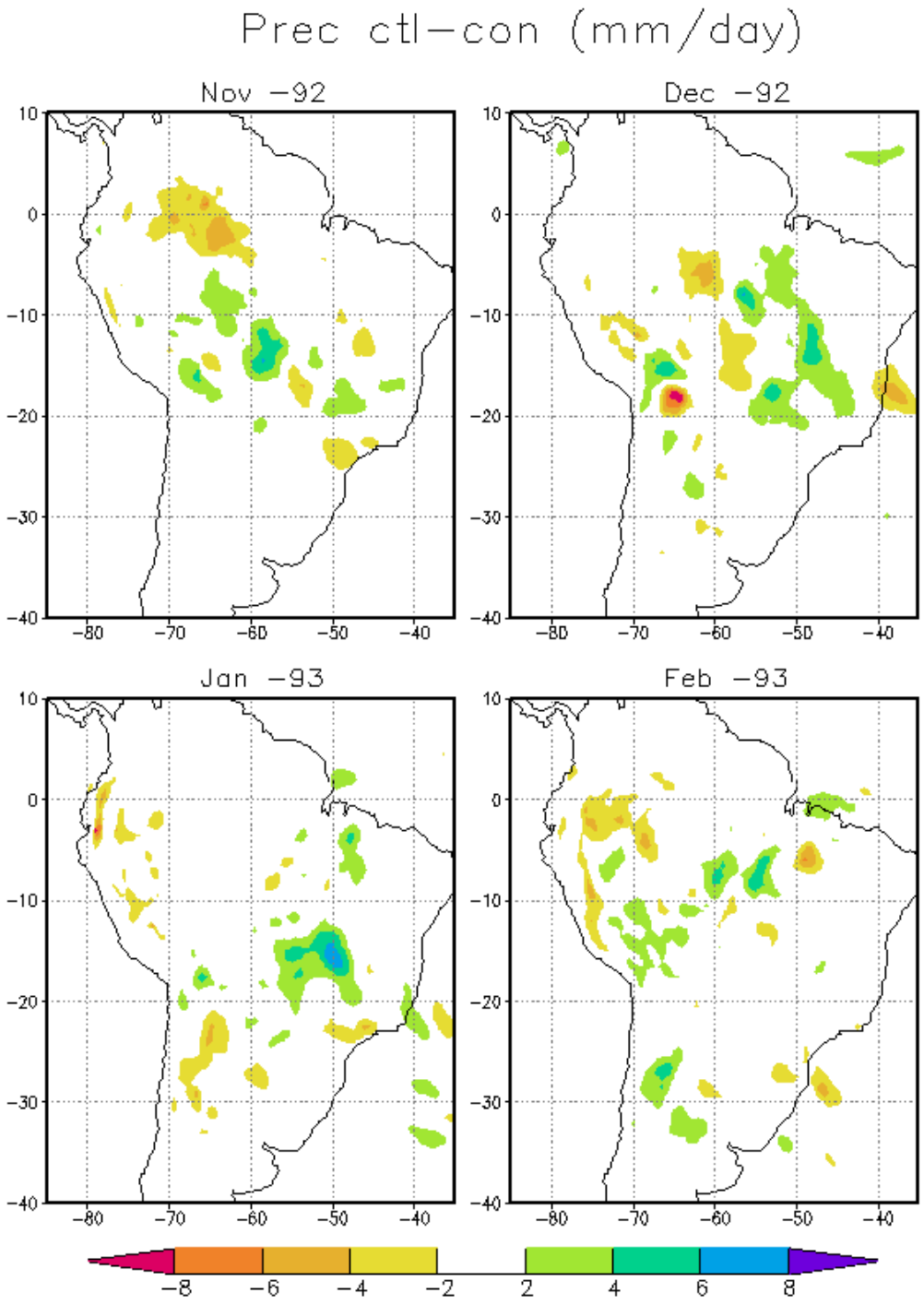

Figure 7.3: Monthly precipitation difference (mm/day) CTL-CON for November to Feburary.

Ω PRECIPITATION

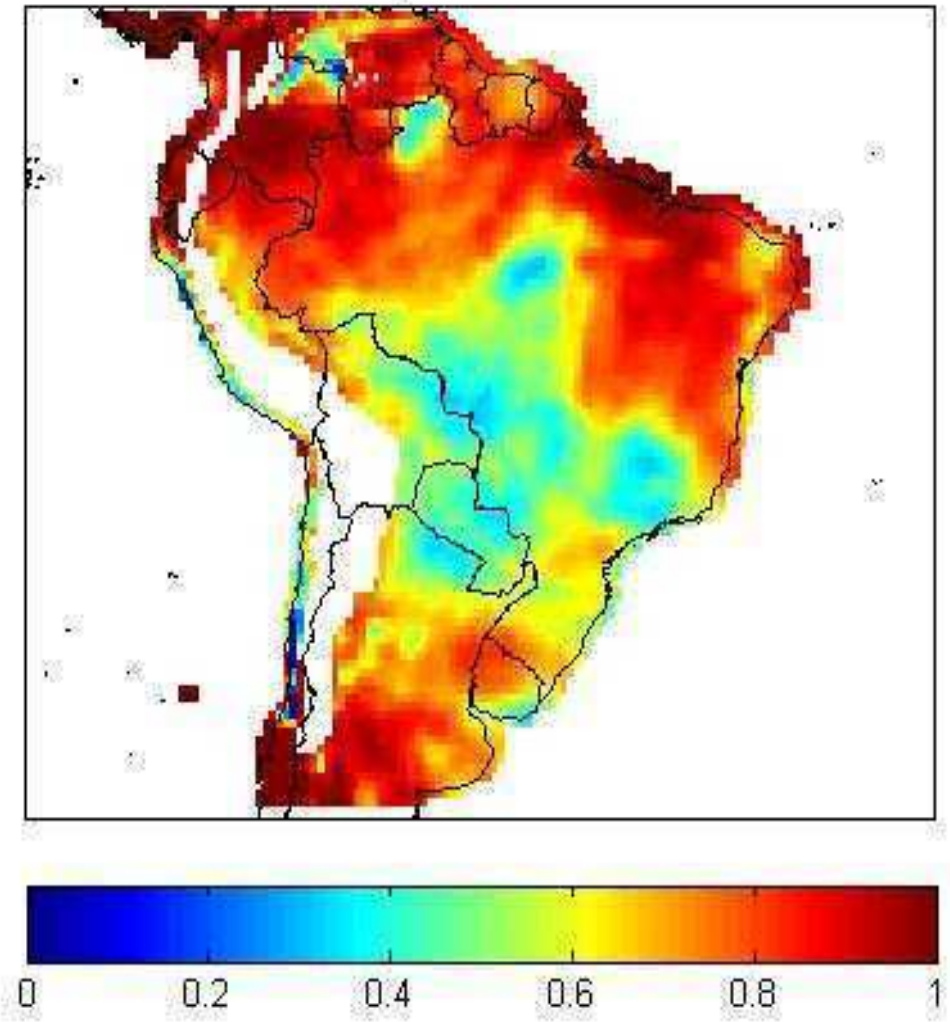

Figure 8.1: Ω(S) for precipitation DJF (92-93).

ΔΩ PRECIPITATION

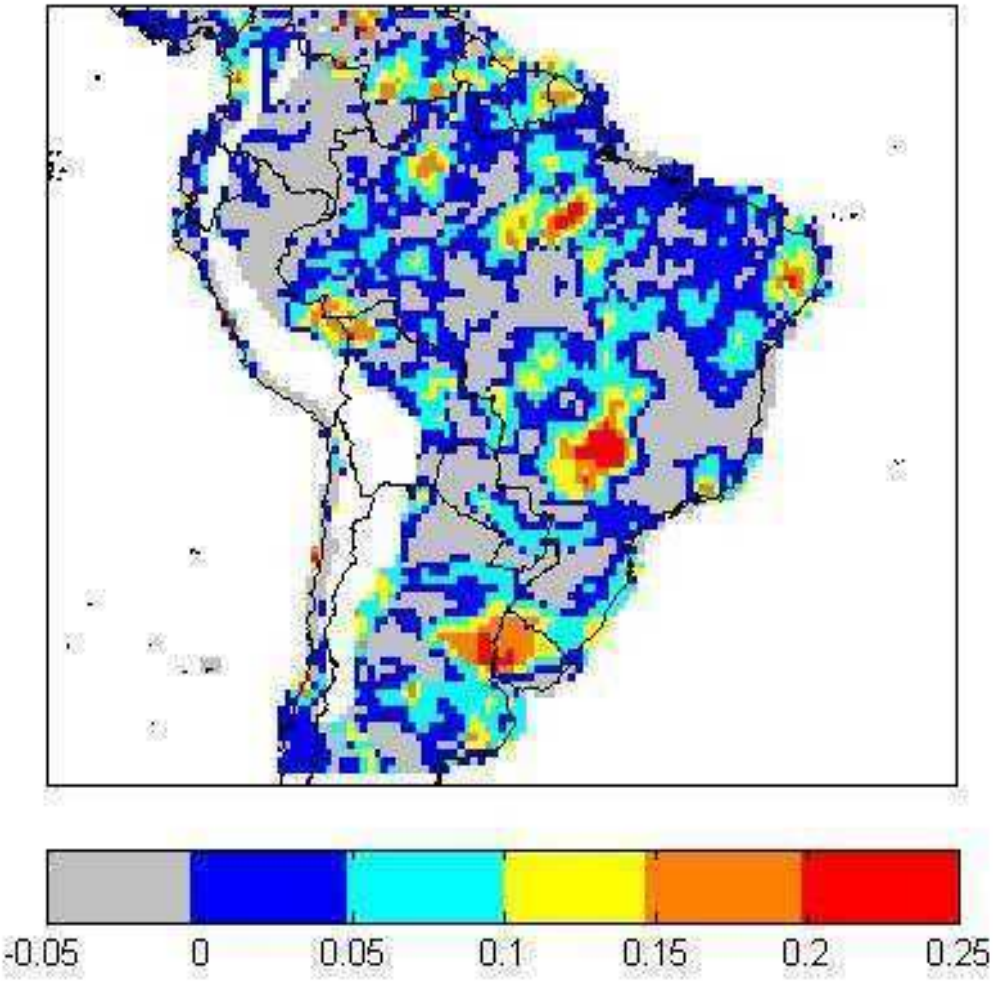

Figure 8.2: Ω coupling strength index for precipitation ($\Delta\Omega_P$).

ΔΩ EVAPOTRANSPIRATION

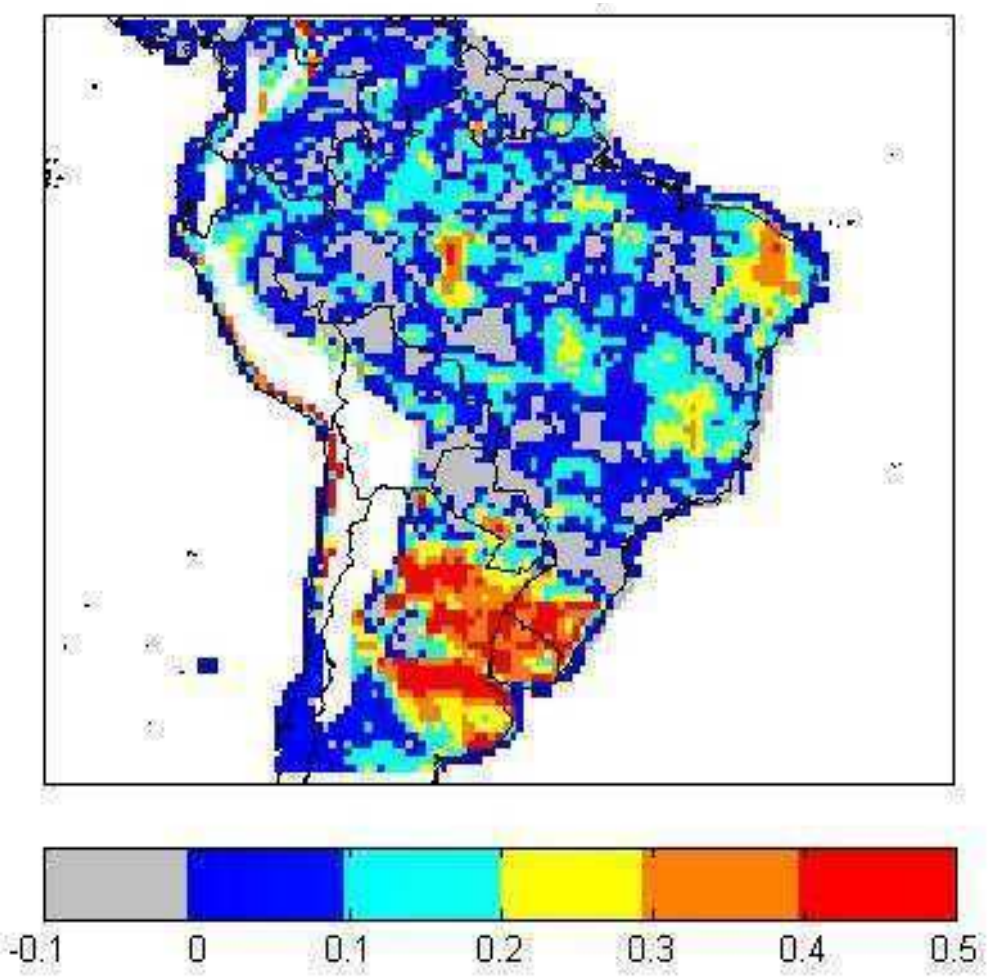

Figure 8.3: Ω coupling strength index for evapotranspiration ($\Delta\Omega_E$).

$\Delta\Omega_E * \sigma_E$

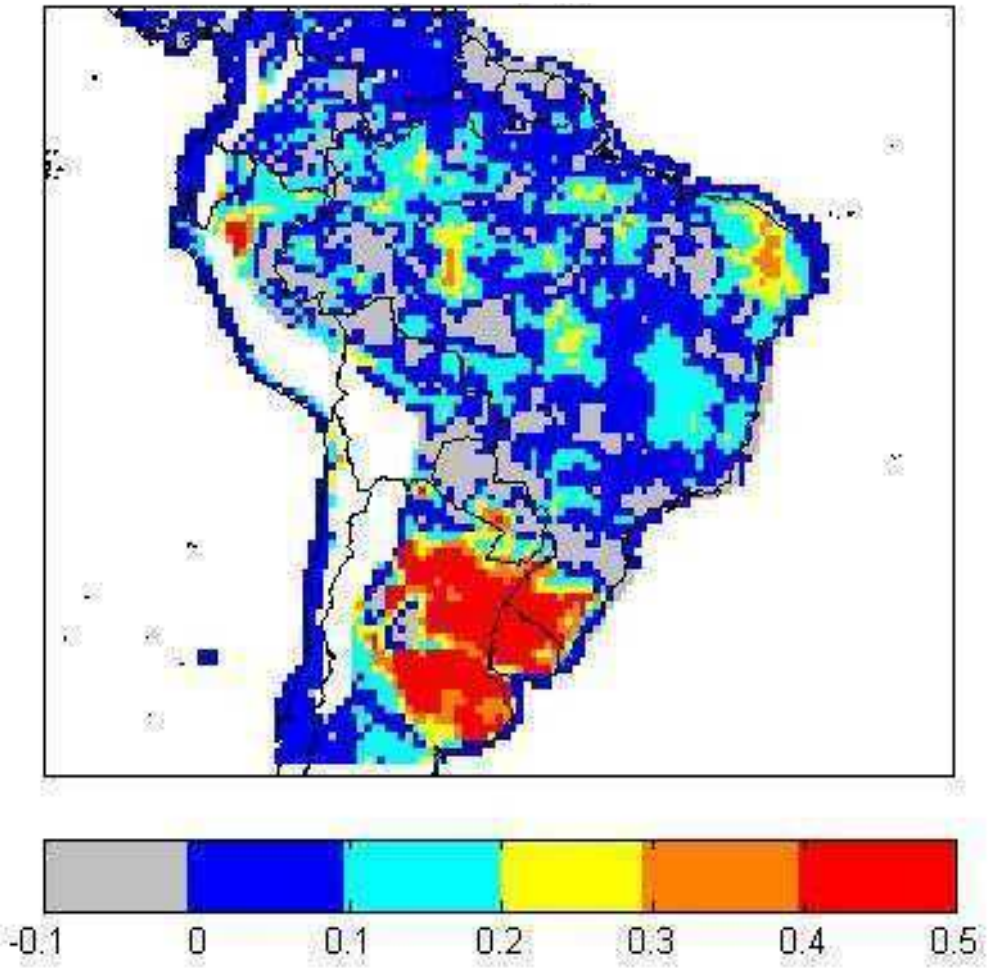

Figure 8.4: The product of evapotranspiration Ω coupling strength and standard deviation of evapotranspiration ($\Delta\Omega_E * \sigma_E$).

$\Delta\Omega_E * \sigma_E$ binned by SWA

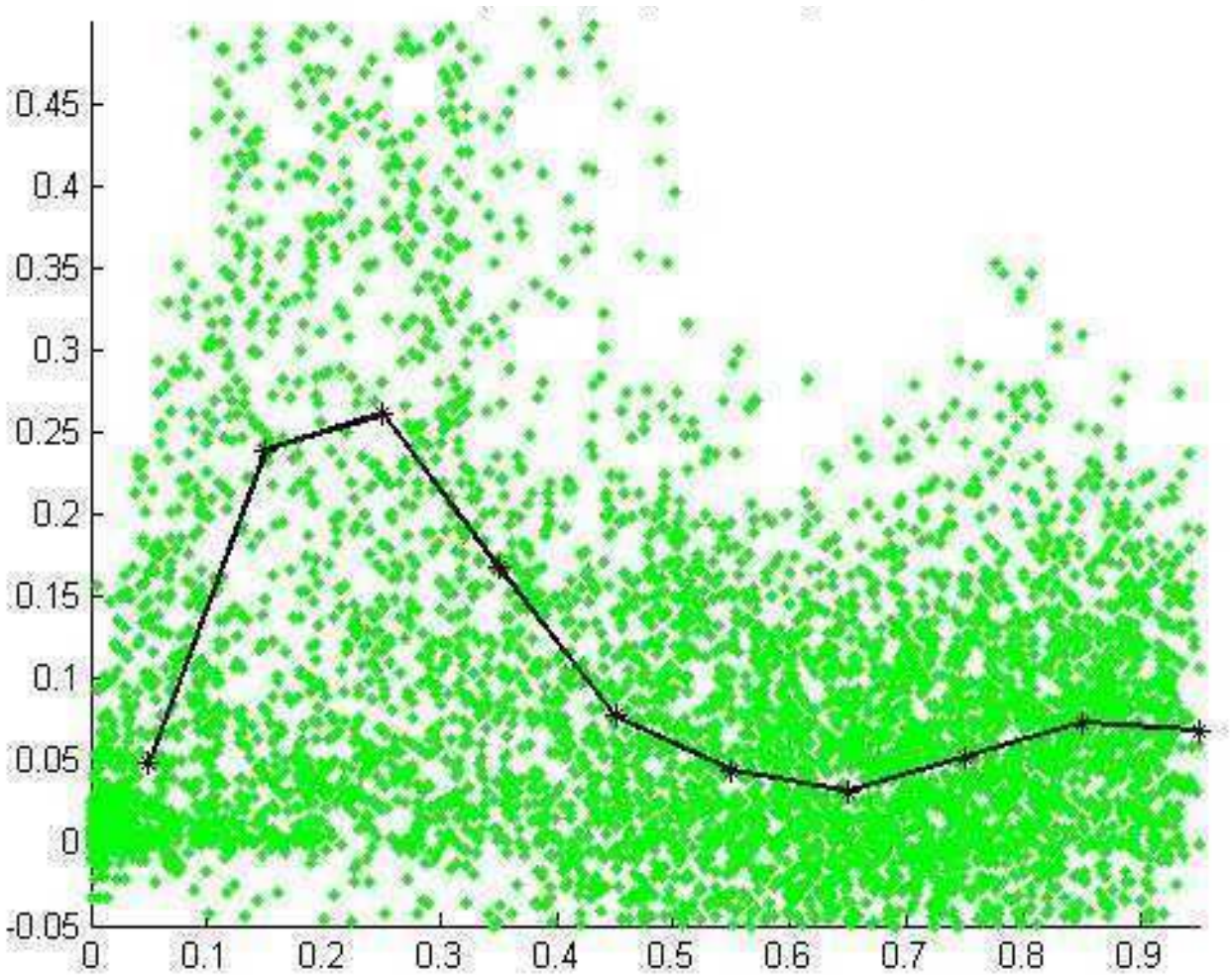

Figure 8.5: The product of evapotranspiration coupling strength and standard deviation of evapotranspiration ($\Delta\Omega_E * \sigma_E$) binned by the soil water content (SWA).

ΔΘ EVAPOTRANSPIRATION

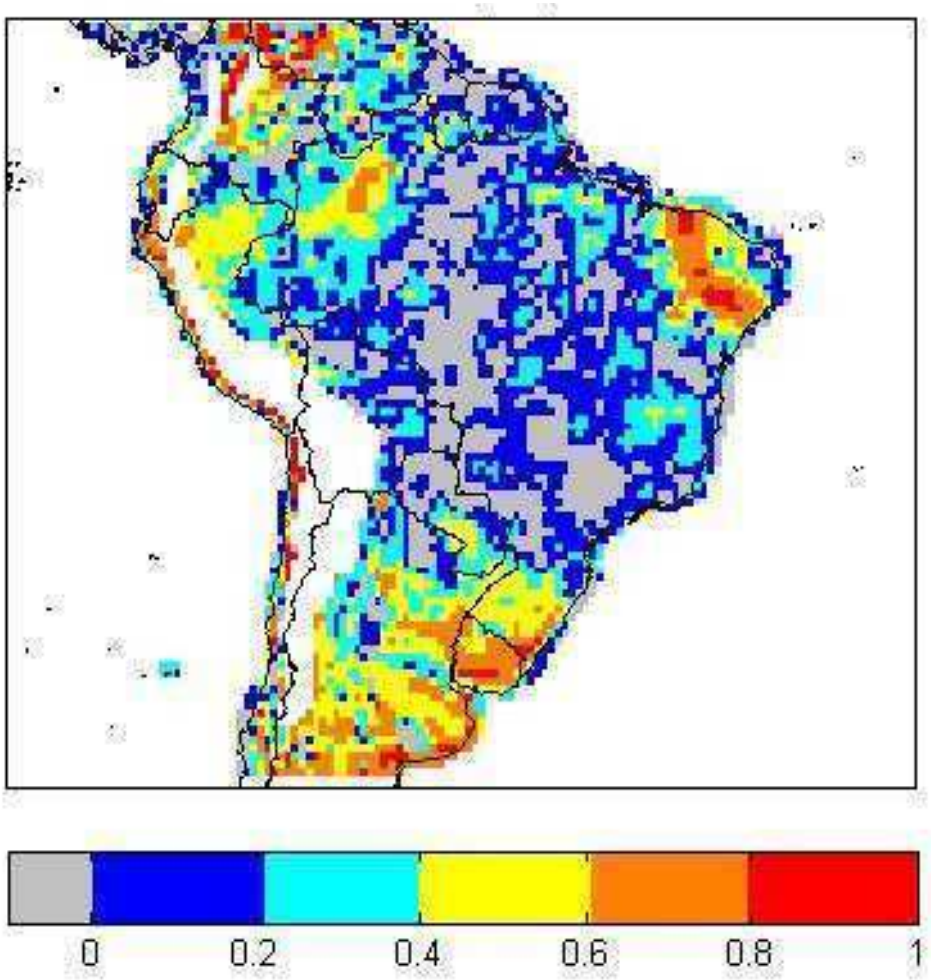

Figure 8.6: Θ coupling strength index for evapotranspiration ($\Delta\Theta_E$).

$$\sigma_{DJF}(E_W) - \sigma_{DJF}(E_S)$$

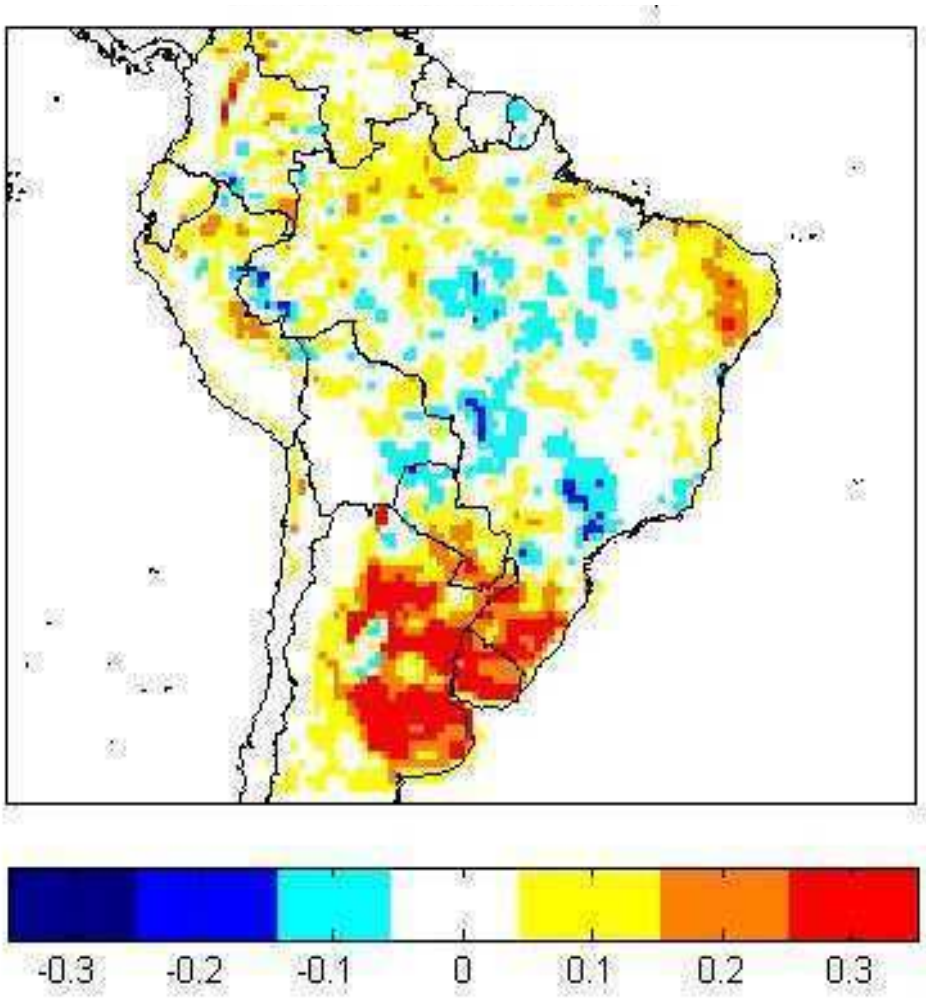

Figure 8.7: The difference between the ensemble mean standard deviations of ensemble W and ensemble S.

ΔΘ PRECIPITATION

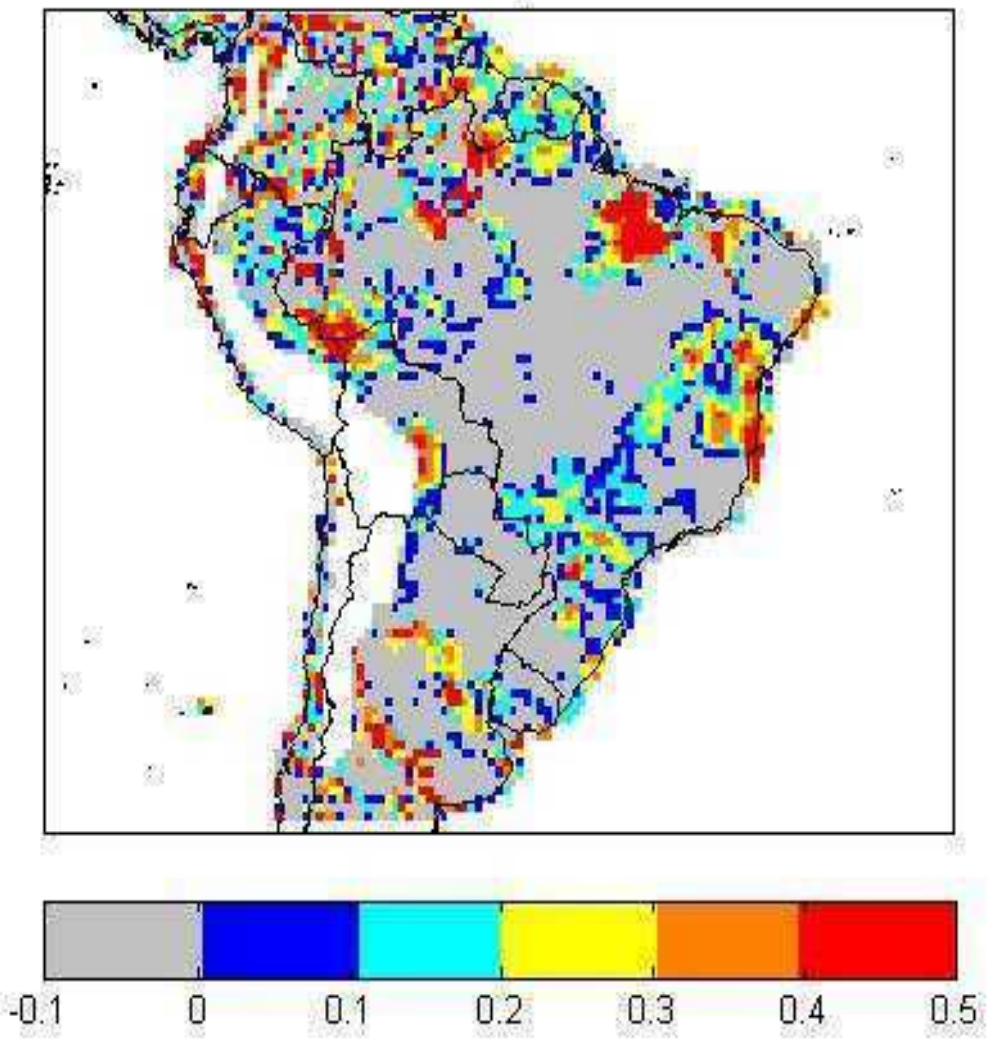

Figure 8.8: Θ coupling strength index for precipitation ($\Delta\Theta_P$).

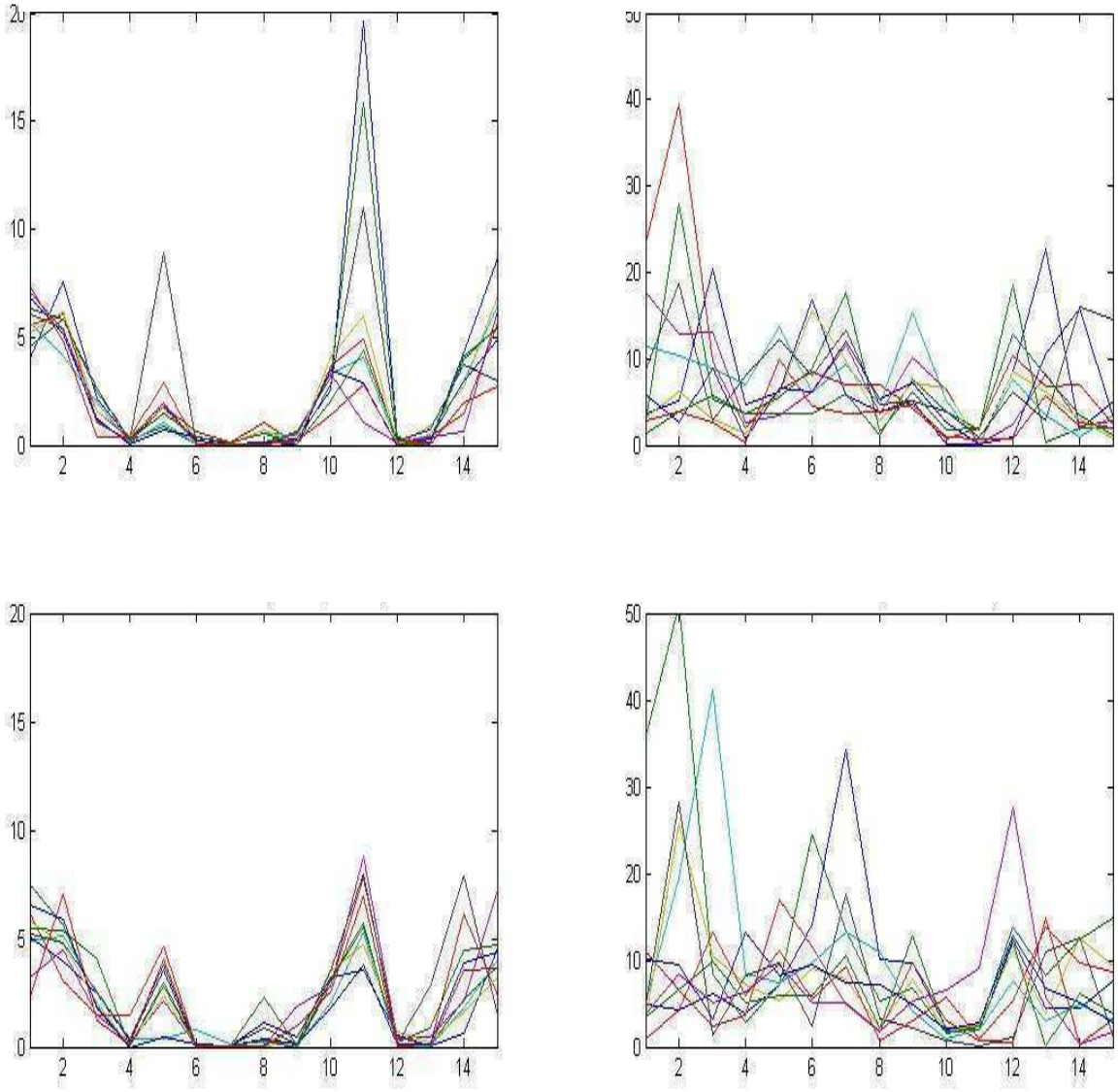

Figure 8.9: Timeseries of the different ensemble members precipitation (mm/day). Left panel: gridpoint with positive $\Delta\Theta_P$ and right panel: gridpoint with negative $\Delta\Theta_P$. Upper panels: ensemble S and lower panels: ensemble W.

THE DEPENDENCE OF $\Delta\Theta_P$ AND $\Delta\Omega_P$ ON ENSEMBLE SEASONAL MEAN (SEM_P)

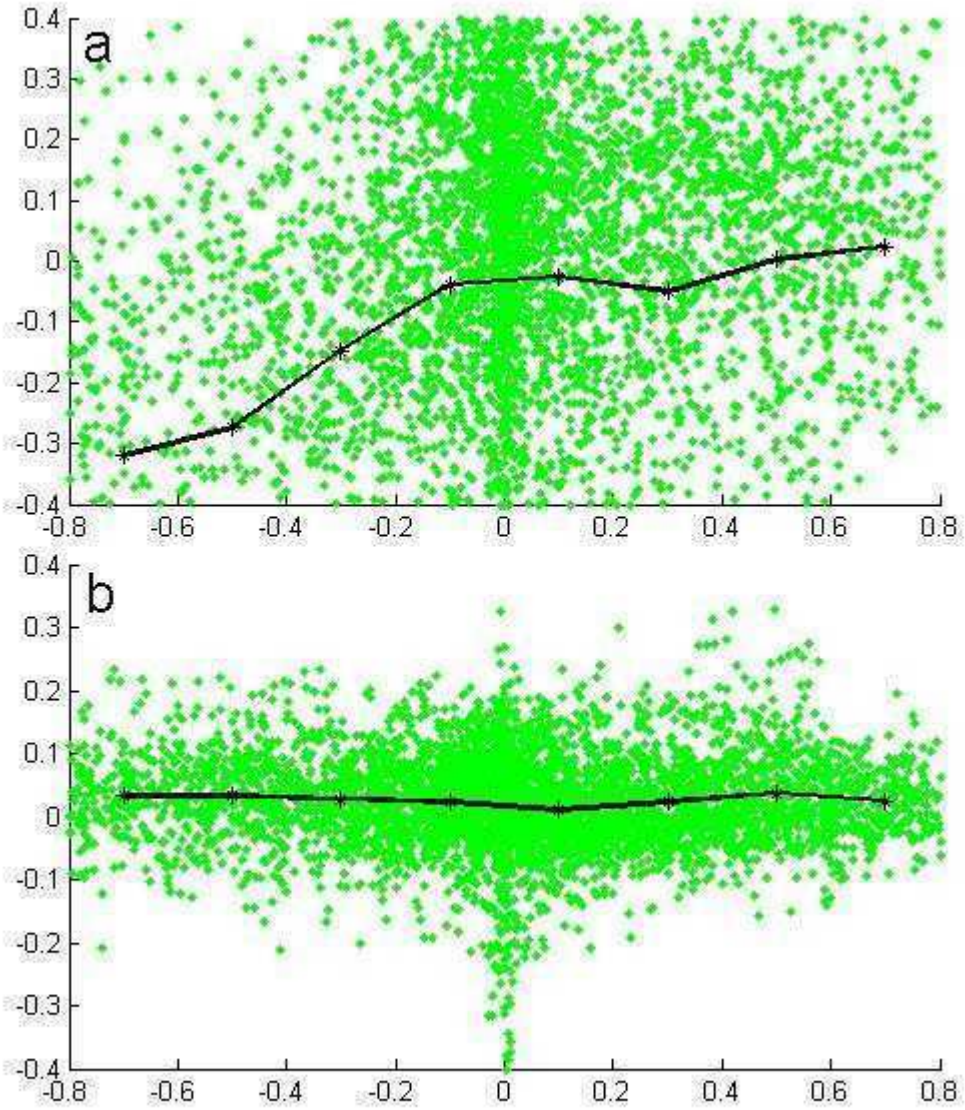

Figure 8.10: a) $\Delta\Theta_P$ binned by ensemble seasonal mean differences between the ensembles (mm/day), and b) Same but for $\Delta\Omega_P$ The differences are defined as the ensemble S minus the ensemble W $SEM_P(S) - SEM_P(W)$.

EPI ENSEMBLE W

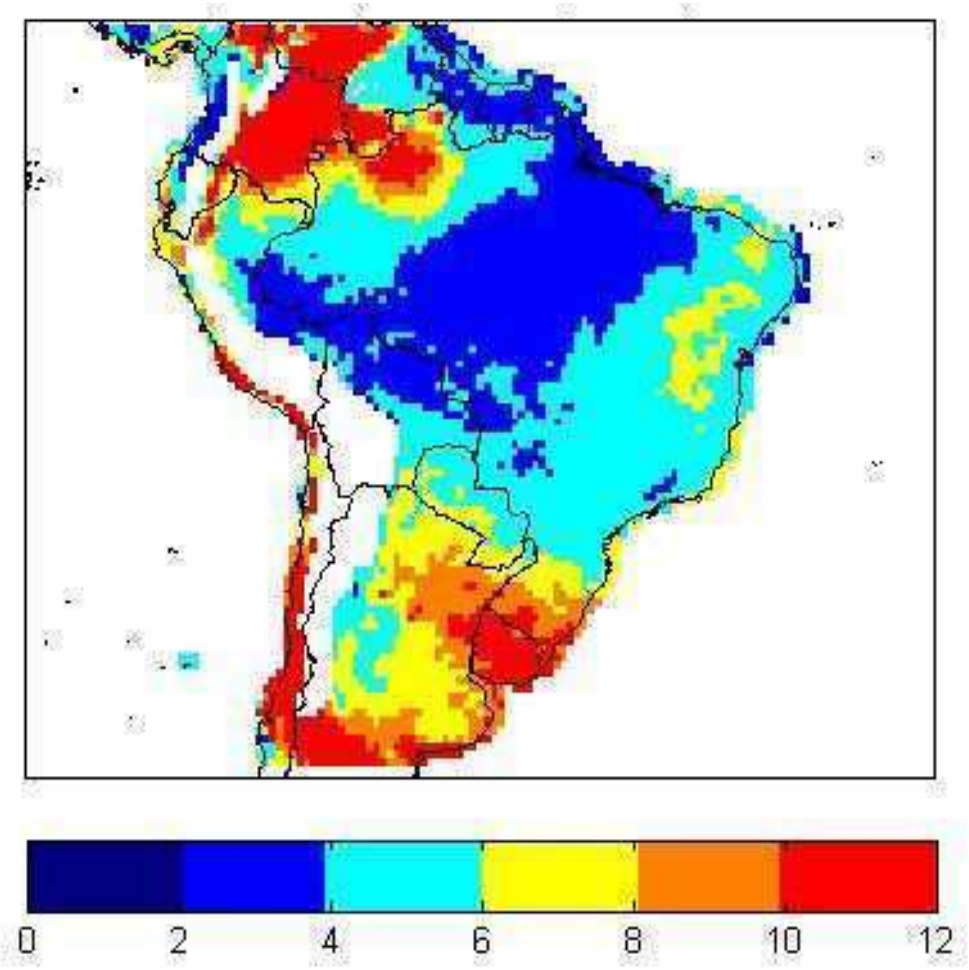

Figure 8.11: The extreme precipitation index (EPI) of the ensemble W (fraction of 95th percentile rainfall contribution to total rainfall in %) .

EPI ENSEMBLE S - EPI ENSEMBLE W

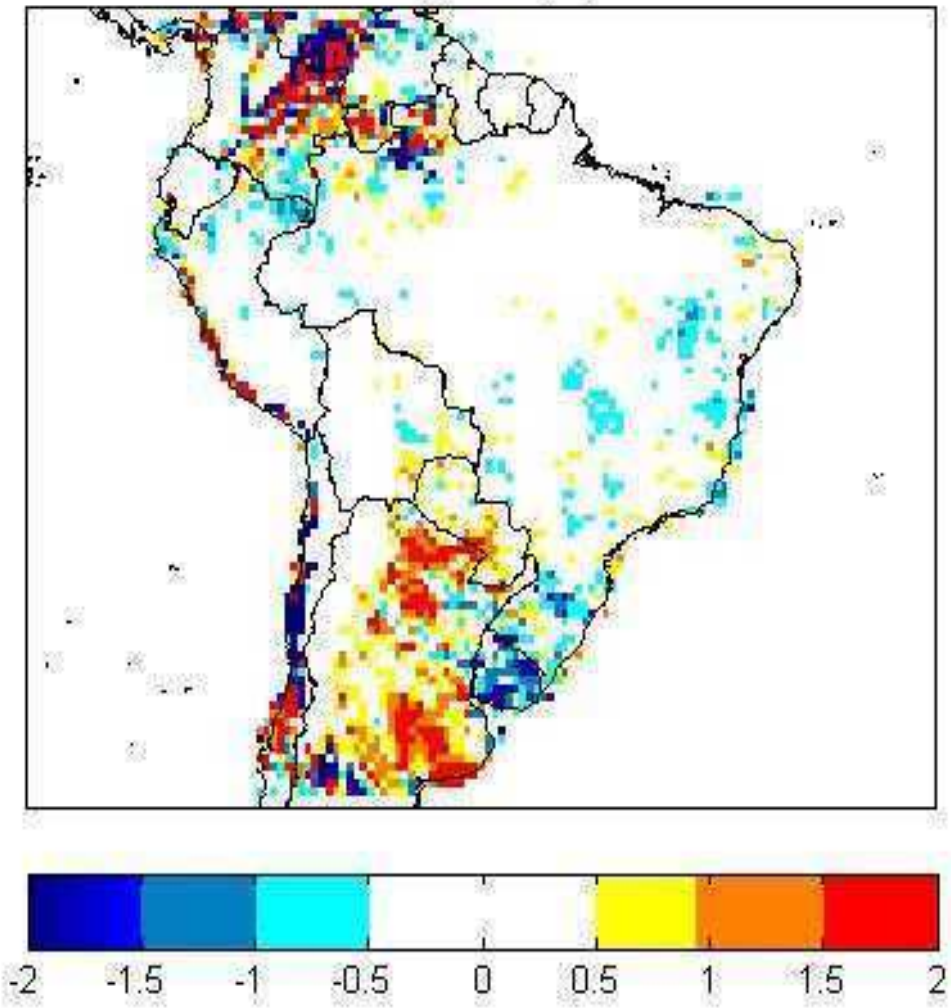

Figure 8.12: The difference between the ensembles (S-W) in extreme precipitation index (%).

RCA3-E DOMAINS

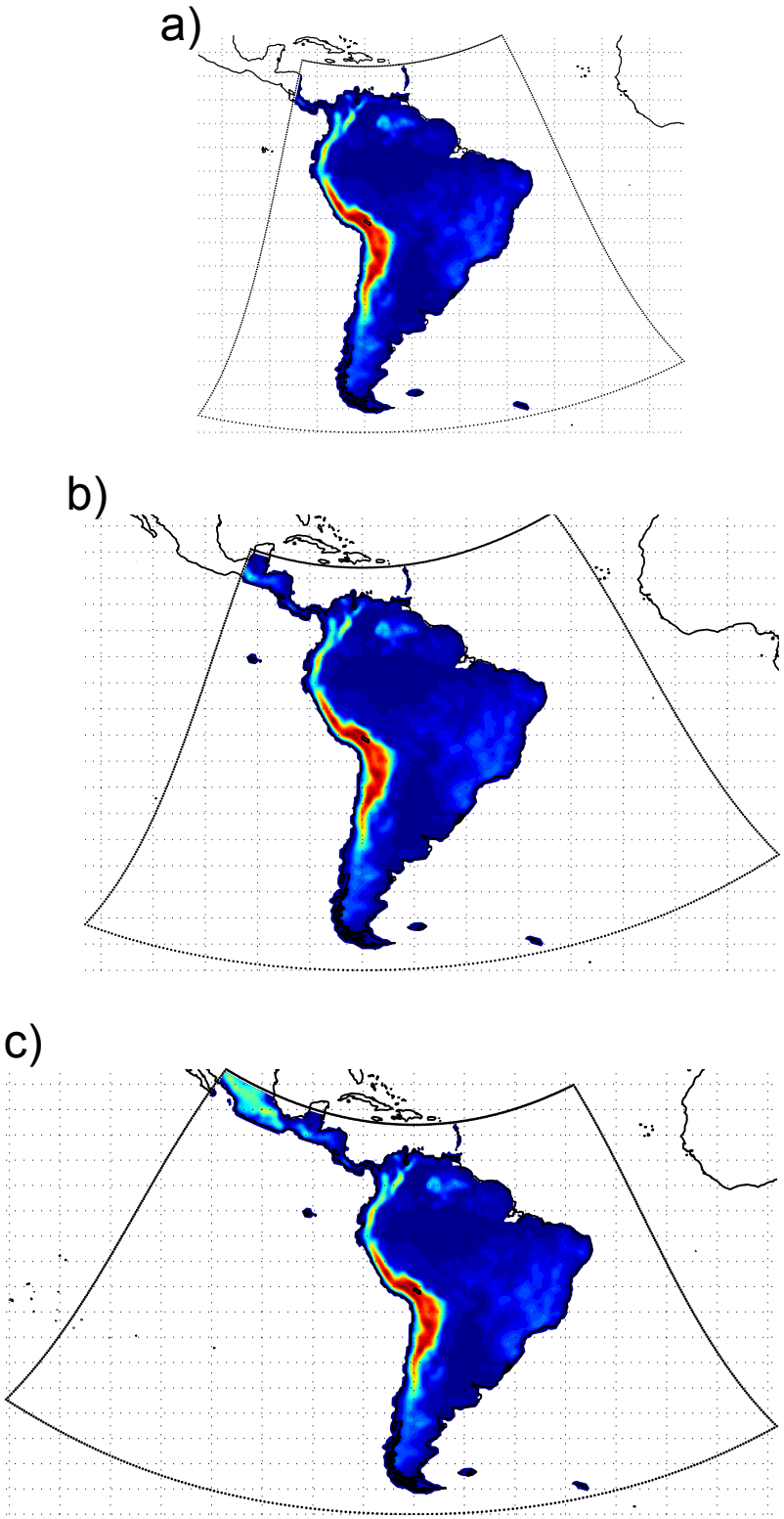

Figure 9.1: a) standard domain, b) Atlantic domain, c) Pacific domain.

TEMPERATURE ANNUAL CYCLES

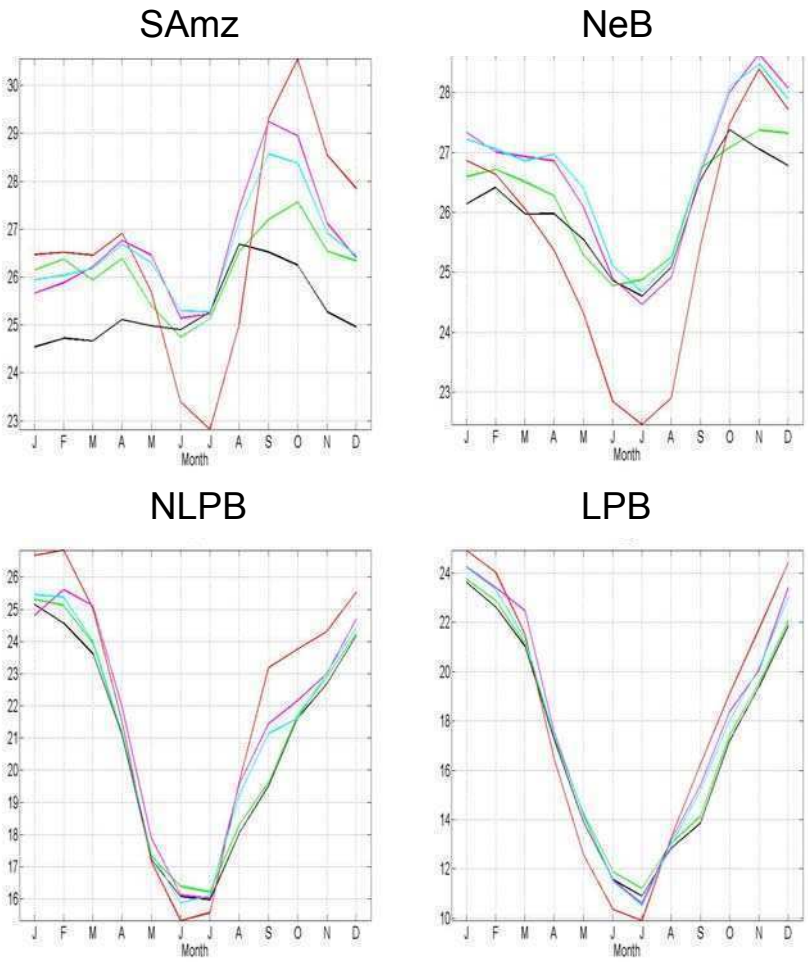

Figure 9.2: Open land t2m annual cycles (C°) for model versions RCA3-E, RCA3.5 with 24 vertical levels and RCA3.5 with 40 vertical levels as compared to CRU and the driving ERA-Interim reanalysis 1997-2001. Note different scales on y-axis.

SPRING TEMPERATURE BIASES

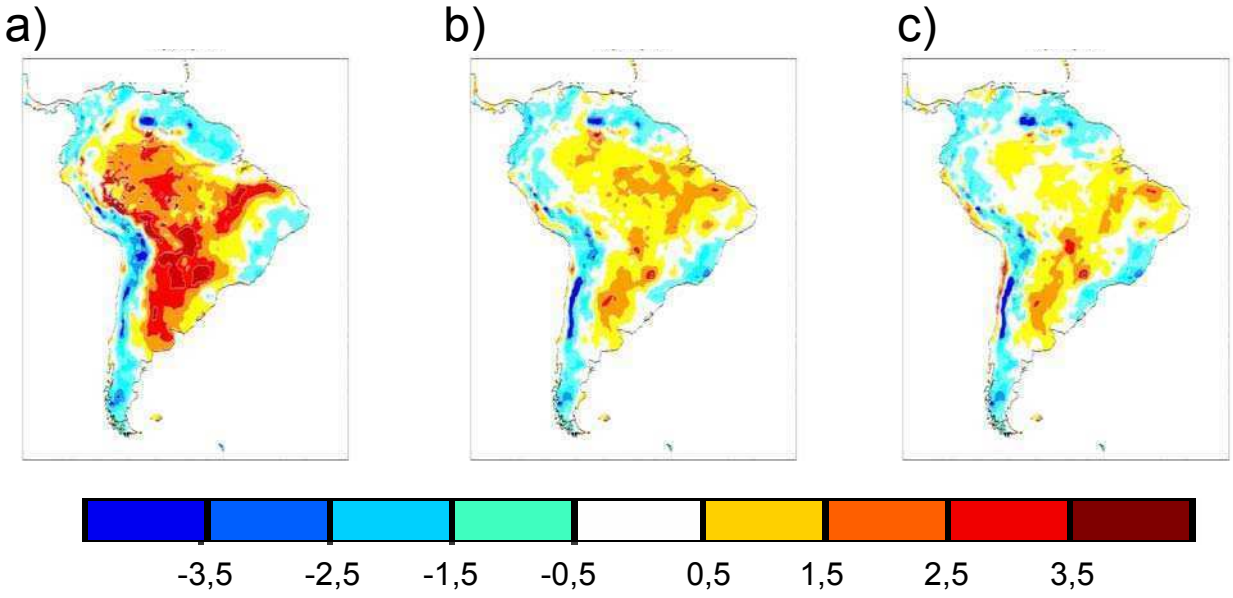

Figure 9.3:SON open land t2m bias (C°) relative to CRU for a) RCA3-E, b) RCA3.5 24, c) RCA3.5 40.

PRECIPITATION ANNUAL CYCLES

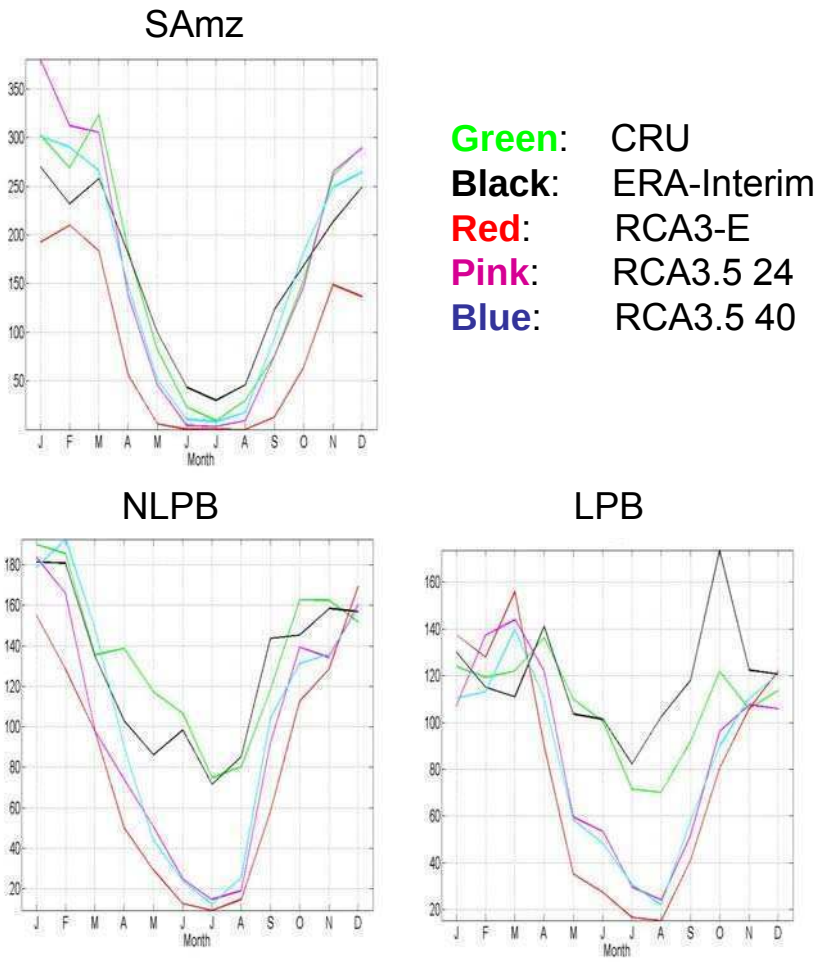

Figure 9.4: Precipitation annual cycles (mm/month) for model versions RCA3-E, RCA3.5 with 24 vertical levels and RCA3.5 with 40 vertical levels as compared to CRU and the driving ERA-interim reanalysis 1997-2001. Note different scales on y-axis.

NEAR SURFACE TEMPERATURE ANNUAL CYCLES

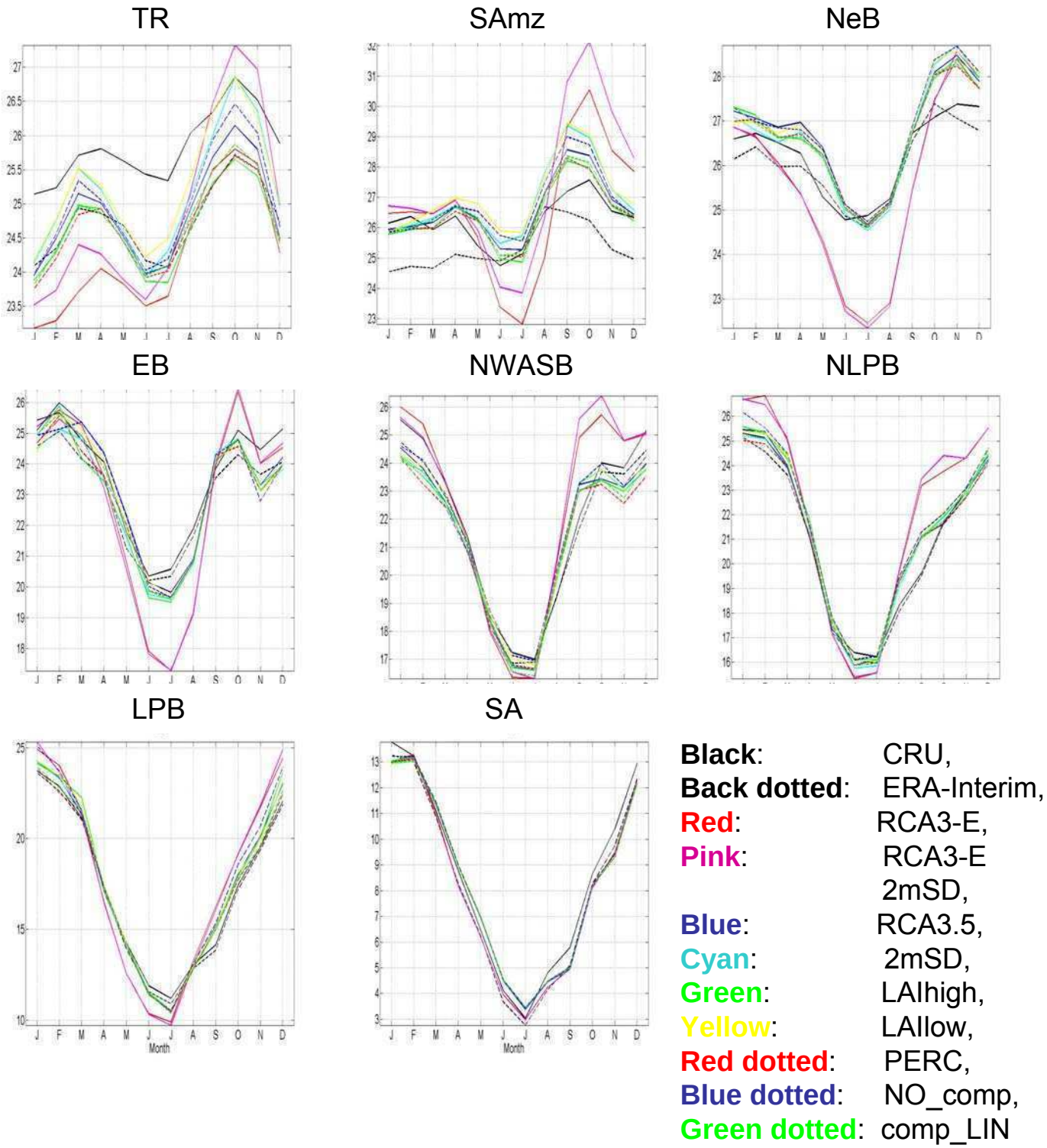

Figure 9.5: Annual cycles of open land temperature (C°) for the land surface parameterization ensemble, CRU and ERA-Interim. Note different scales on the y-axis.

SON NEAR SURFACE TEMPERATURE BIASES

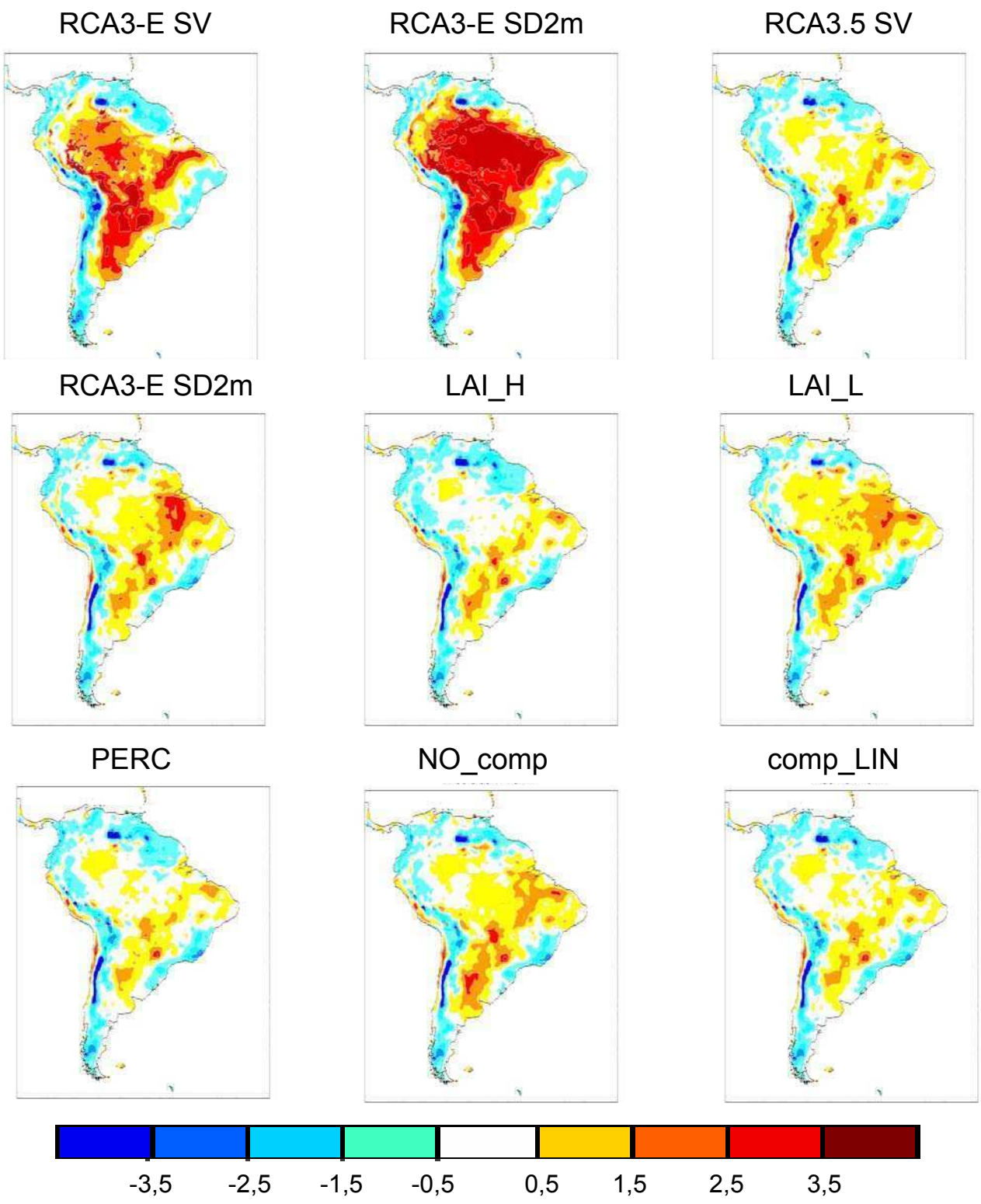

Figure 9.6: SON open land t2m bias (C°) relative to CRU for the ensemble members.

SAmz ANNUAL CYCLES OF SENSIBLE HEAT FLUX AND SOIL MOISTURE

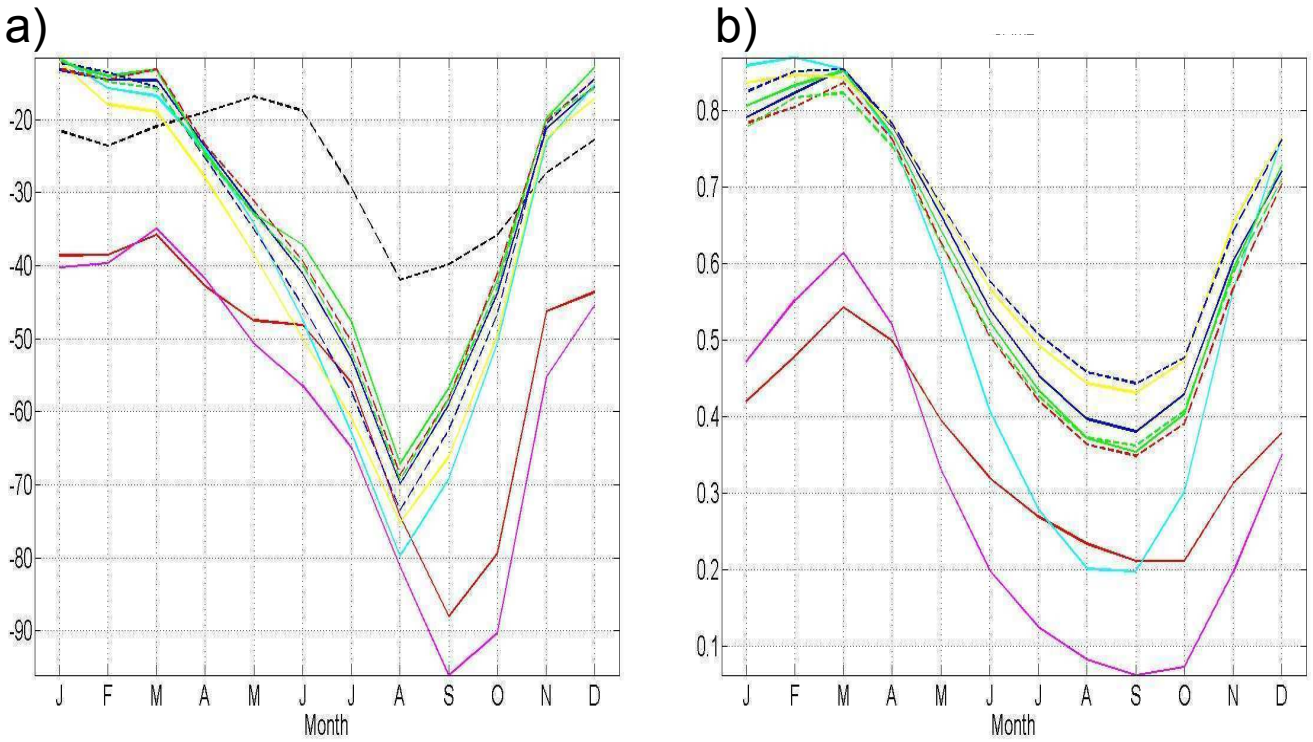

Black: CRU,
Back dotted: ERI,
Red: RCA3-E,
Pink: RCA3-E 2mSD,
Blue: RCA3.5,
Cyan: 2mSD,
Green: LAIhigh,
Yellow: LAIlow,
Red dotted: PERC,
Blue dotted: NO_comp,
Green dotted: comp_LIN

Figure 9.7: Annual cycles of a) sensible heat flux (W/m^2) and b) soil water availability (% of saturation) for the region Samz.

PRECIPITATION ANNUAL CYCLES

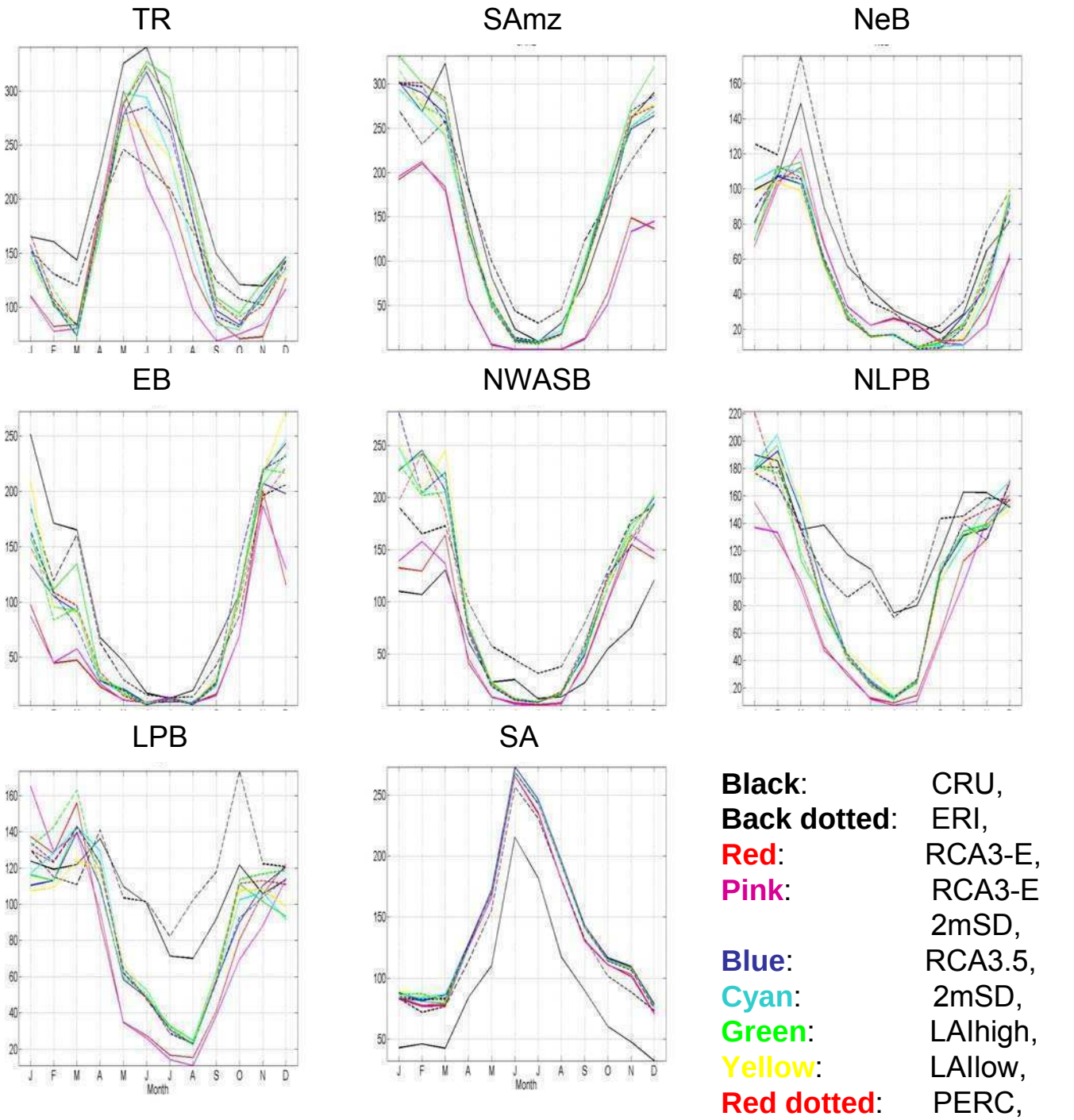

Figure 9.8: Annual cycles of precipitation (mm/month). Note different scales on the y-axis.

LPB AND NLPB ANNUAL CYCLES OF SOIL MOISTURE

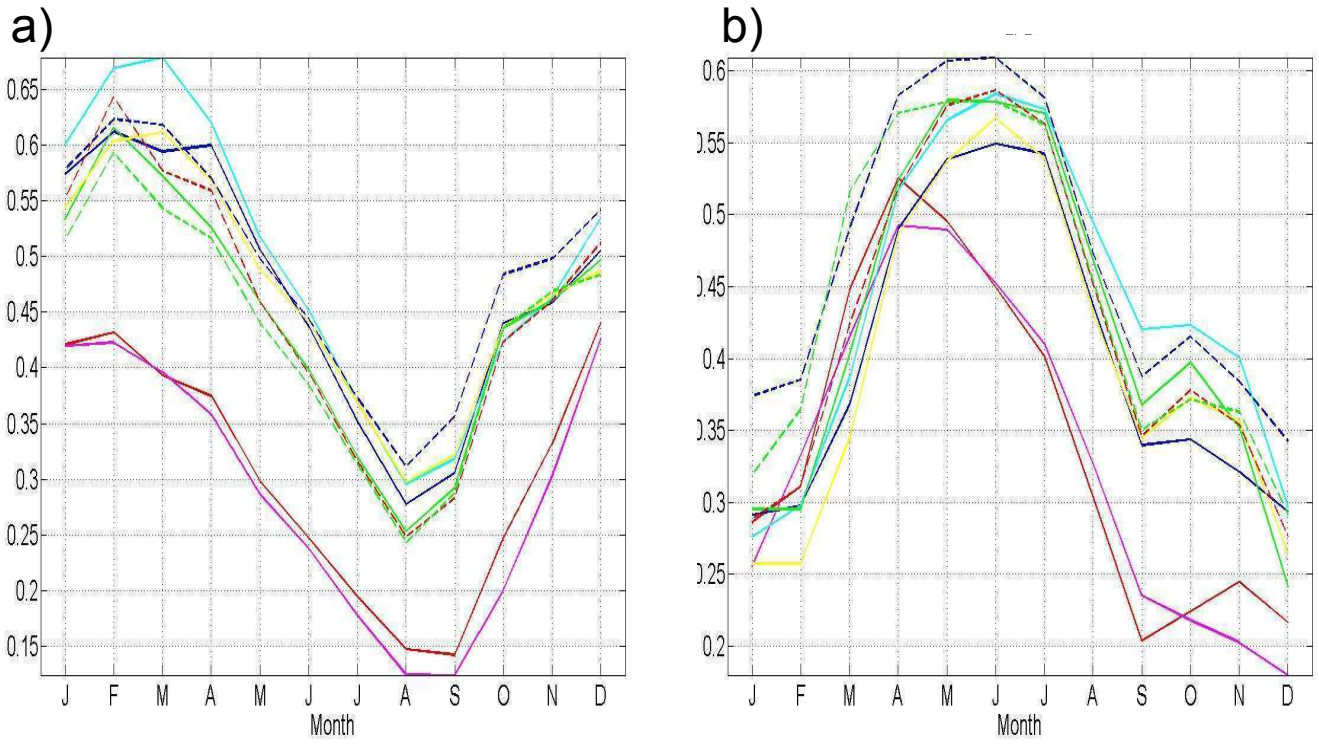

Black: CRU,
Back dotted: ERI,
Red: RCA3-E,
Pink: RCA3-E 2mSD,
Blue: RCA3.5,
Cyan: 2mSD,
Green: LAIhigh,
Yellow: LAIlow,
Red dotted: PERC,
Blue dotted: NO_comp,
Green dotted: comp_LIN

Figure 9.9: Annual cycles of soil water availability (% of saturation) for the regions a) LPB and b) NLPB.

LPB AND NLPB ANNUAL CYCLES OF EVAPOTRANSPIRATION

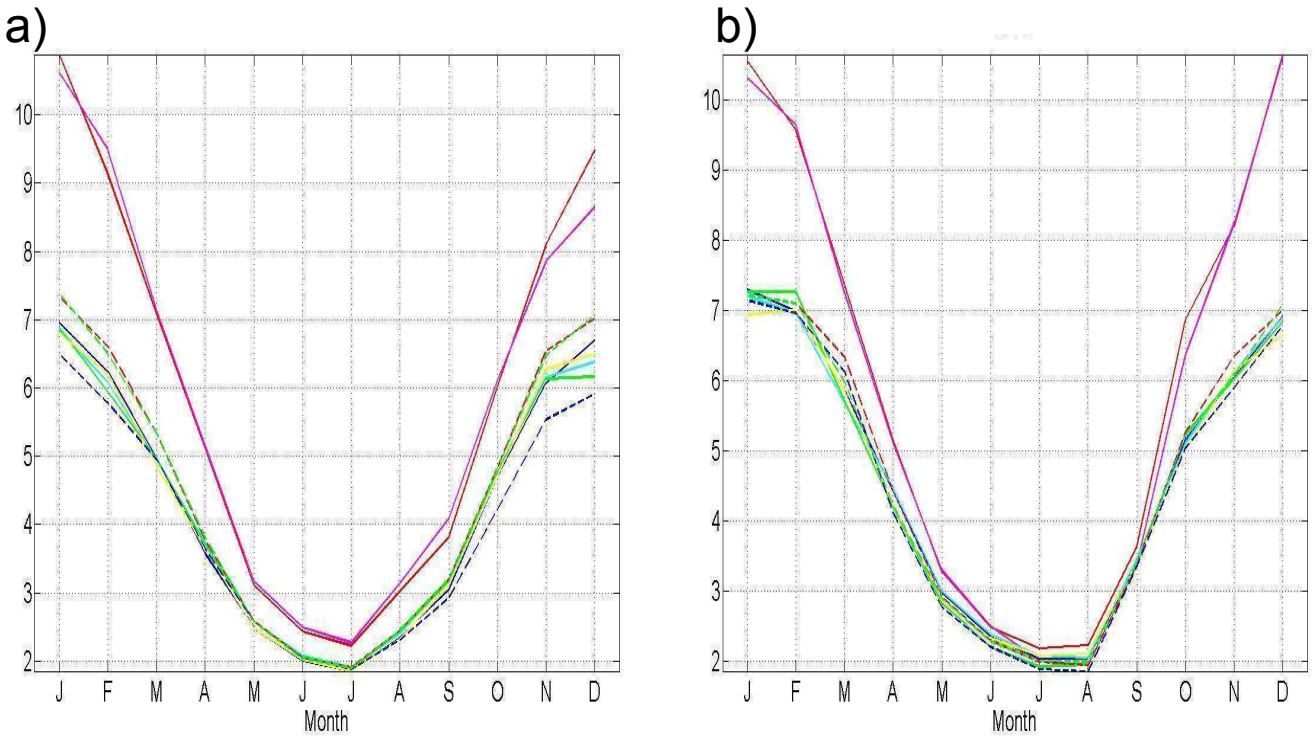

Black: CRU,
Back dotted: ERI,
Red: RCA3-E,
Pink: RCA3-E 2mSD,
Blue: RCA3.5,
Cyan: 2mSD,
Green: LAIhigh,
Yellow: LAIlow,
Red dotted: PERC,
Blue dotted: NO_comp,
Green dotted: comp_LIN

Figure 9.10: Annual cycles of evapotranspiration (mm/day) for the regions a) LPB and b) NLPB.

ANNUAL CLOUD COVER BIAS

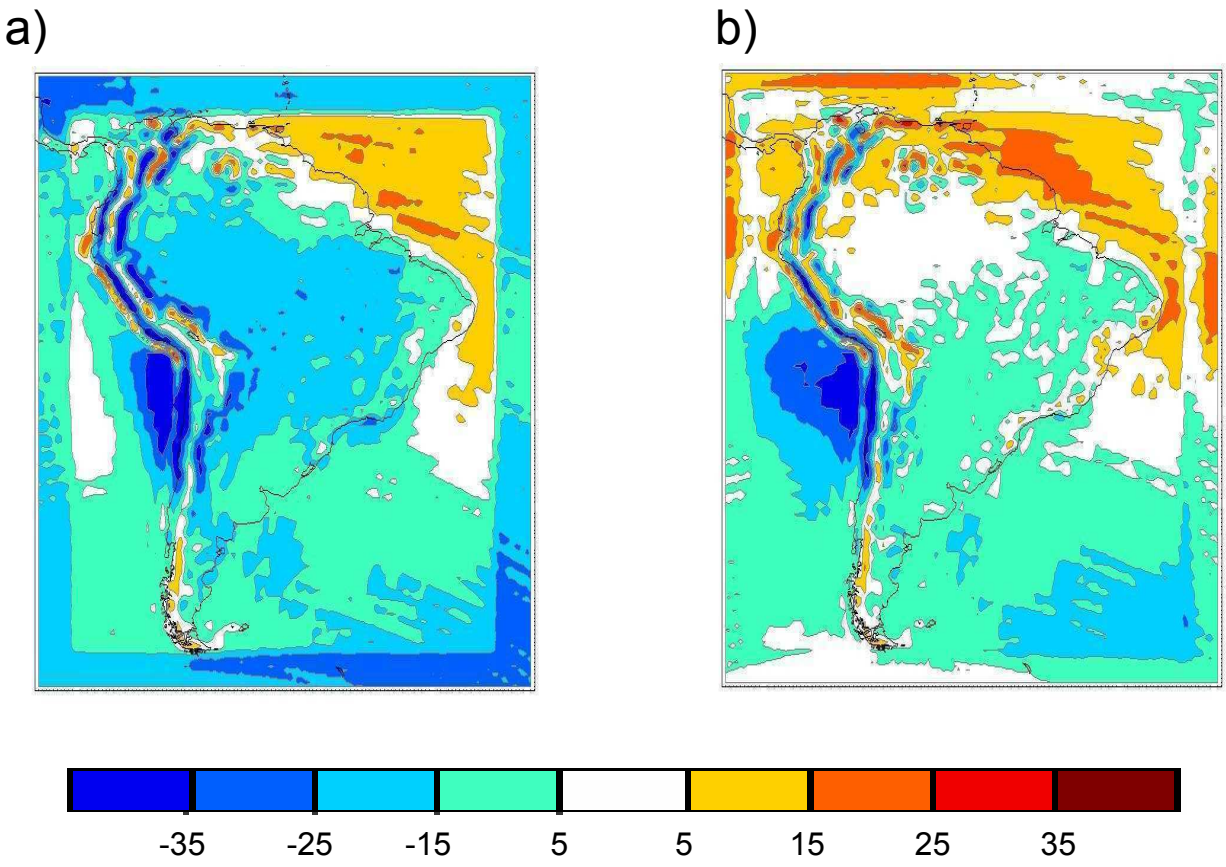

Figure 9.11

Figure 9.11: Annual cloud cover bias (percentage) relative to ISCCP for a) RCA3-E and b) RCA3.5.